論文 / 著書情報
Article / Book Information

題目(和文)	
Title(English)	Alternate transmission of different coded ultrasound for the extension of measurable distance in the pulse-echo method
著者(和文)	KHANISTHALEETANG
Author(English)	Leetang Khanistha
出典(和文)	学位:博士(学術), 学位授与機関:東京工業大学, 報告番号:甲第12128号, 授与年月日:2021年9月24日, 学位の種別:課程博士, 審査員:蜂屋 弘之,奥富 正敏,中尾 裕也,塚越 秀行,大山 真司,平田 慎之介
Citation(English)	Degree:Doctor (Academic), Conferring organization: Tokyo Institute of Technology, Report number:甲第12128号, Conferred date:2021/9/24, Degree Type:Course doctor, Examiner:,,,,,
学位種別(和文)	博士論文
Type(English)	Doctoral Thesis

Alternate transmission of different coded ultrasound for the extension of measurable distance in the pulse-echo method

東京工業大学
Tokyo Institute of Technology

Khanistha Leetang

Department of Systems and Control Engineering

Tokyo Institute of Technology

A thesis submitted for the degree of

Doctor of Philosophy

September 2021

ACADEMIC ADVISORS:

Supervisor: Prof. Hiroyuki Hachiya

Co-supervisor: Prof. Nakao Hiroya

Visiting-supervisor: Assoc. Prof. Shinnosuke Hirata

Abstract

The pulse-echo method is a typical method of ultrasonic distance measurement based on pulse transmission and time-of-flight (TOF) determination. The pulse width corresponds to the distance resolution. Therefore, a short pulse is applied to obtain the high distance resolution. Moreover, to improve the signal-to-noise ratio (SNR), pulse compression is often employed for the pulse-echo method. In pulse compression, a frequency-swept signal or a pseudo-random modulated signal is transmitted, then the received signal is correlated with the reference (transmitted) signal. When the received signal and the reference signal match, the high correlation value (compressed pulse) appears in the cross-correlation function. The temporal resolution of the distance measurement is the time required for a single measurement. The short pulse-repetition time in the pulse-echo method represents the high temporal resolution. In that case, however, the long-distance cannot be measured because the pulse-repetition time corresponds to the maximum limit of the measurable TOF (distance). Therefore, there is a trade-off relationship between the temporal resolution and the measurable distance in the pulse-echo method.

In this thesis, the alternate transmission of different coded signals in pulse compression is proposed to extend the measurable distance of the pulse-echo method without the degradation of the temporal resolution. In the proposed method, two different coded signals are alternatively and continually transmitted, then the received signal is correlated with each reference signal to obtain each cross-correlation function. In each cross-correlation function, the compressed pulses

alternatively appear, and the interval that corresponds to the pulse-repetition time is extended by double of that in the one-code transmission. Therefore, the measurable distance can be extended with the same temporal resolution as the one-code transmission by the alternate distance measurement from each cross-correlation function. However, the noise by interference between different coded signals occurs between the compressed pulses. If the noise, which is defined as the noise between peaks (NBP), is larger than the compressed pulses, actual distance cannot be measured, and the SNR can be degraded. Therefore, the combination of different coded signals with low NBP is searched, and the suitable combinations are determined. The linear-frequency-modulated (LFM) signal combination and M-sequence signal combination were studied in this thesis. In the case of the LFM signal, the combination of the up-chirp and the down-chirp can be employed to the alternate transmission. NBPs were estimated on the parameters, the center frequency of 35 kHz, the sweep bands from 10 kHz to 30 kHz, the signal lengths from 3.6 to 43.8 ms. In the case of M-sequence, a continuous signal is alternatively modulated by one cycle of each M-sequence to be transmitted signal. Then, the received signal is correlated with each reference signal, which corresponds to each M-sequence. There are several code combinations in the M-sequence. Therefore, the peak interval in each cross-correlation function can be extended many times. Since NBP differs greatly depending on the combination of M-sequence codes, a combination of codes that reduces NBP was examined.

In the typical modulation, a few sine waves or their inverse waves are assigned to 1 or -1 (integer modulation). The modulation in which the initial phase of sine waves is conjugately shifted by 1 or -1 is also investigated (complex modulation). In the proposed modulation, initial phases of different coded signals are shifted in the complex modulation. In the cross-correlation function, the alternate transmission of phase-shifted complex M-sequences can be applied to suppress NBP. Therefore, the initial phase of different coded signals is shifted in the

complex modulation. The variations of maximum and average amplitudes of truncation and truncated interference noises, acquired from the phase differences, are evaluated.

The maximum noise amplitude of NBP in the LFM signal is decreased at the long length of the signal. On the other hand, the maximum amplitude of NBP in the M-sequence signal is decreased in the high order M-sequences. NBP was compared for the combination of LFM and M sequence under the same signal length condition. By examining many combinations of M-sequence signals, we were able to understand the characteristics of the combinations in which the NBP increases and the combinations in which the NBP decreases. In addition to a combination with a small interference noise called a preferred pair, there is a combination that can realize the smallest NBP among symmetry pairs in which the order of the code sequences is reversed. The combination of LFM is advantageous when the system bandwidth is wide, but the expansion of the measurement distance is doubled. When the system bandwidth is not so wide, the combination of complex modulated M-sequence signals will enable lower NBP and more than double the measurement distance.

Experiments were conducted to confirm the results of the simulation. The experimental results agree well with the simulation results, and it was clarified that the measurement distance of the pulse-echo method can be expanded by the alternate transmission of different codes.

Acknowledgements

This thesis is the summary of my doctoral study at the Tokyo Institute of Technology, Tokyo, Japan. I am grateful to a large number of people who have helped me to accomplish this work.

First of all, I would like to express my sincere gratitude to my advisor, Professor Hiroyuki Hachiya, for his mentorship, guidance, and encouragement. By working under the supervision of Professor Hachiya, I received an invaluable experience that helped me to shape my academic and professional skills.

Second, I would like to thank Associate professor Shinnosuke Hirata for his encouragement and constant support since I came to Japan, who have been continuously teaching and encourage my research. I would never have been able to do my research without the guidance of your advice.

Third, I would also like to thank every member of the Hachiya laboratory for helping, supporting, comments, suggestions, and cooperation for all the year.

Lastly, I would like to thank all people who have contributed towards the completion of this research.

Contents

List of Figures

LIST OF FIGURES

LIST OF FIGURES

List of Tables

LIST OF TABLES

Chapter 1

Introduction

In this chapter, a research background is introduced. There is explained of the background for an ultrasonic sensor in the distance measurement. Moreover, objectives and the proposed method are described. There is explained about a problem of the conventional method and solving a problem. The objective of this research is the solving problem method. Furthermore, thesis organization is presented.

1.1 Background

Ultrasonic is an acoustic frequency higher than 20kHz. It is widely used to apply for measuring the distance of targets. The most popular method for ultrasound transducer in the distance measurement is the time of flight (TOF) determination. It is determined a distance measurement by TOF of acoustic-pulse transmission. In another method, the phase difference method is a typical method to measure the distance of objects by the phase difference between the transmitted signal and received signal. Range resolution is determined by the wavelength resolution and the transmission signal of the phase difference measurement. In this research, distance measurement by the TOF method is introduced. There are popular methods and simple techniques for ultrasonic distance measurement. The pulse-echo method is a simple technique for applying in distance measurement. This is a typical distance measurement method, which is applied in acoustic-pulse transmission and the determination of TOF. [1, 2, 3, 4].

Pulse compression has been introduced to the pulse-echo method to improve SNR and distance resolution. [5, 6, 7, 8, 9, 10]. The transmitted signal for pulse compression is a frequency-sweep-modulated burst wave or a pulse sequence coded by pseudo-random numbers. The received signal is then correlated with the reference signal, which corresponds to the transmitted signal. When the received signal and reference signal match, the high correlation value appears as a sharp peak in the cross-correlation function. Furthermore, environmental noise and non-correlative components can be suppressed by the cross-correlation process. Therefore, the TOF can be determined from a sharp peak with high resolution and high SNR. Pulse compression can improve SNR for ultrasound measurement.

1.2 Objective and the proposed method

In the general method, SNR is improved by pulse compression. However, there is a trade-off between temporal resolution and measurable distance. In some applications, researchers cannot measure very long distances with high accuracy for pulse compression. For example, we cannot measure the precise shape of land under very depth water. Therefore, the objective of this research is introduced to present an alternate transmission of different codes method to extend a measurable distance without the temporal resolution degradation. Thats means, in the cross-correlation function of the proposed method, each correlation signal can be alternately applied for the distance measurement in the same as the temporal resolution of the conventional transmission signals as indicated in Fig. 1.1.

In the proposed method, the alternate transmission of the LFM signal and the M-sequence signal is selected to apply in the pulse compression. The alternate transmission of LFM signals in the different In the proposed method, the alternate transmission of the LFM signal and the M-sequence signal is selected to apply in the pulse compression. The alternate transmission of LFM signals in the different signals as up-chirp and down-chirp are transmitted. Then, the received signal is correlated with each reference signal. The peak interval in each correlated signal is extended double times. On the other hand, a continuous signal is alternatively modulated by one cycle of each M-sequence to be transmitted signal.

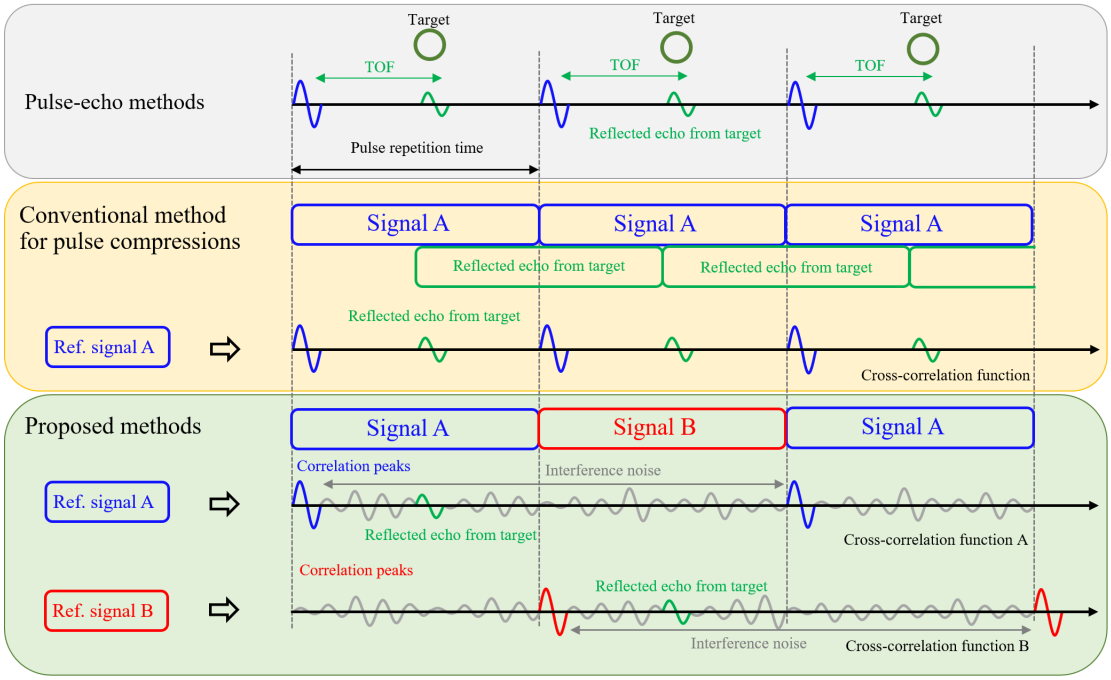

Figure 1.1: Proposed method

Then, the received signal is correlated with each reference signal, which corresponds to each M-sequence. Hence, the peak interval in each cross-correlation function is extended many times. In both signals, each cross-correlation function can be alternatively applied for distance measurement in the same as the original temporal resolution of the conventional M-sequence method. However, truncation noise and truncated interference noise are generated around sharp peaks of the cross-correlation signal in the proposed method. These noises correspond to SNR. In other words, the high amplitude, sharp peak, these noises affect the SNR improved by pulse compression, which is degraded SNR. Pattern differences of truncation and truncated interference noises are generated by the different alternate transmission of M-sequences. [11, 12]. Therefore, the suitable combination of M-sequences is studied and investigated from all patterns of combinations of M-sequences. [13].

1.3 Thesis organization

In this section, the layout of the thesis is explained. An organization of thesis as indicated in Fig. 1.2 is highlights the important points in each chapter. Chapter one is provided the research background, objectives, proposed method, and thesis organization of this research. In chapter two, the ultrasonic measurement is introduced. There is a method of the ultrasonic sensor for distance measurement and pulse compression methods. In chapter three, the alternate transmission of different codes method is described. There is a proposed method in this research to extend the measurable distance of the signal. In chapter four, all patterns of each signal are evaluated to investigate truncation and truncated interference noises for searching the best pattern in the proposed method. Chapter five is presented an experimental result. Three cycles for one digit of alternate transmission of the LFM signal and alternate transmission of the M-sequence signal is transmitted, that was selected from the lowest truncation and truncated interference noise in the simulation. Chapter six is the final chapter in this thesis that includes the conclusion and future work of the thesis.

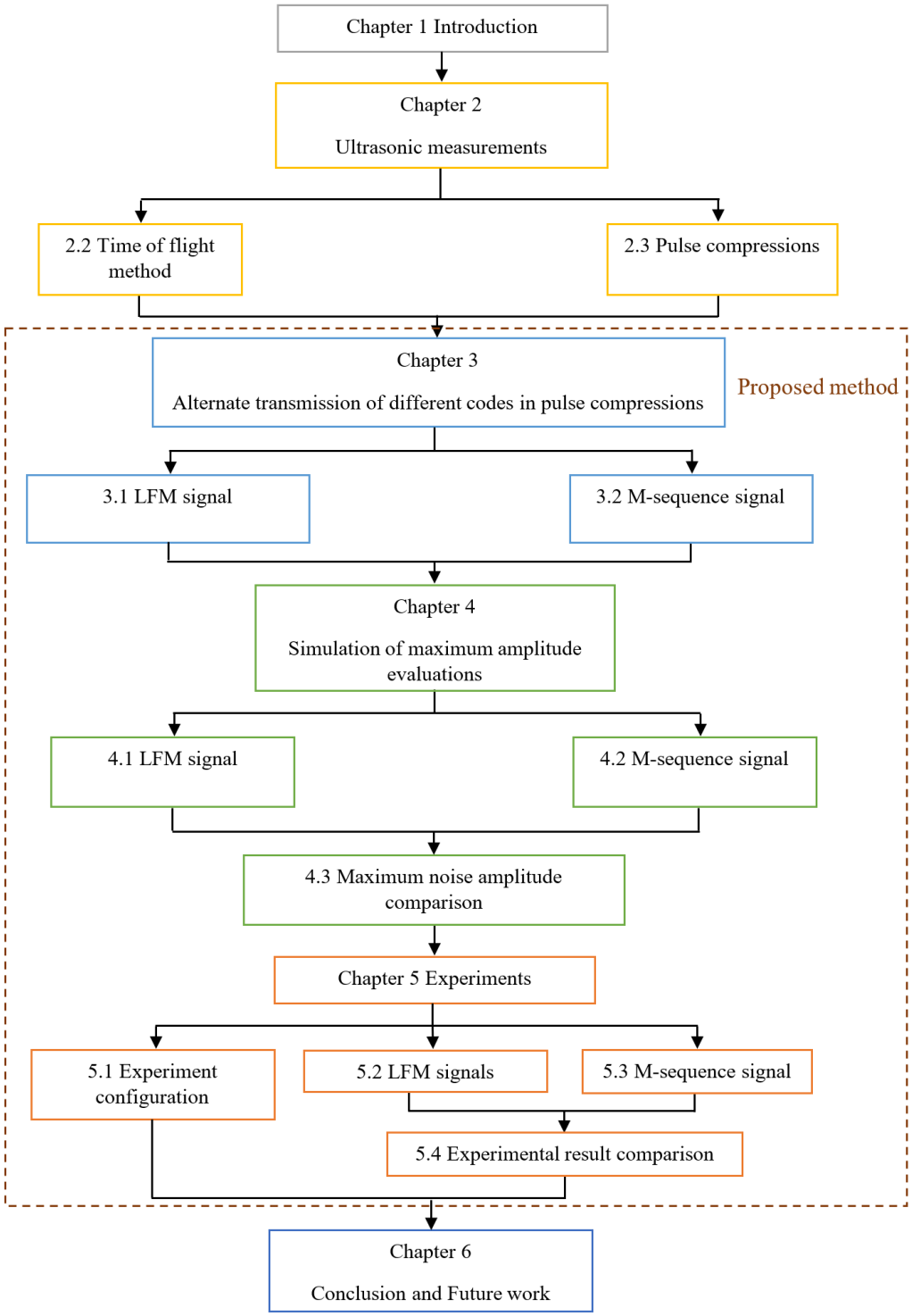

Figure 1.2: Organization of thesis

Chapter 2

Ultrasonic measurements

This chapter reviews related works of distance measurement. There is explained the phase difference method and the time of flight (TOF) method. The pulse-echo method is a method for ultrasonic measurement. Then, the basic concept of the phase difference method, time difference method, and pulse compression is explained. In this research, the alternate transmission of different codes method is proposed by the linear frequency modulation signal and the M-sequence signal method. There are popular to apply for pulse compression.

Generally, a distance measurement by the ultrasonic sensor is determined by TOF as indicated in Fig. 2.1. The distance (d) is calculated from the TOF measurement using the speed of sound (c) is given by [14]

$$d = \frac{c \cdot t_{travel}}{2} \tag{2.1}$$

Accuracy improvement of distance measurement by the speed of sound, the sound speed in the air is related with a temperature, humidity, and air pressure. However, the temperature is applied to consider the speed of sound as follow,

$$c = 20.06\sqrt{T + 273.15} \tag{2.2}$$

,where T is the temperature in Celsius.

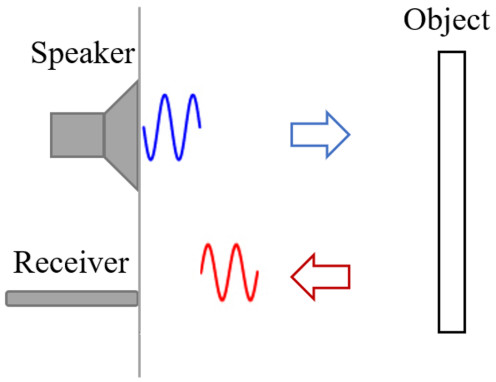

Figure 2.1: TOF determination by transmitted signal and received signal in the pulse-echo method.

2.1 Time of flight measurement

In most acoustic measurements, an ultrasonic sensor is used to apply for distance measurement of the target by using the pulse-echo method. The pulse-echo method is applied by the acoustic-pulse transmission to measure the pulse-propagation distance by determination of TOF as indicated in Fig. 2.2. The pulse width of the transmitted signal is related to the distance resolution as indicated in Fig. 2.3. In the moving object measurement, many pulse-echo methods are transmitted and received a reflected signal from objects. The temporal resolution of the measurement is the times required for a single measurement. There is identified by the pulse repetition time. The minimum pulse repetition time corresponds to the time duration of the transmitted signal in pulse compression. Moreover, the pulse repetition time is used to identify the maximum limit of measurable TOF. However, if the measurable TOF limit is extended, the temporal resolution is decreased. There is a meaning of trade-off between the temporal resolution and the measurable distance. Nevertheless, the SNR of this method is degraded because environment noise are detected.

In the research of an acoustic method, a conventional method is possible to be applied for fast and accurate measurement on the distance of targets. The distance measurement is calculated by TOF determination. The TOF is a delay

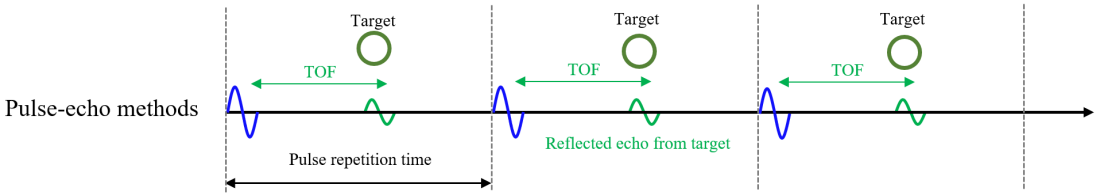

Figure 2.2: The acoustic-pulse transmission to measure the pulse-propagation distance by determination of the time of flight (TOF).

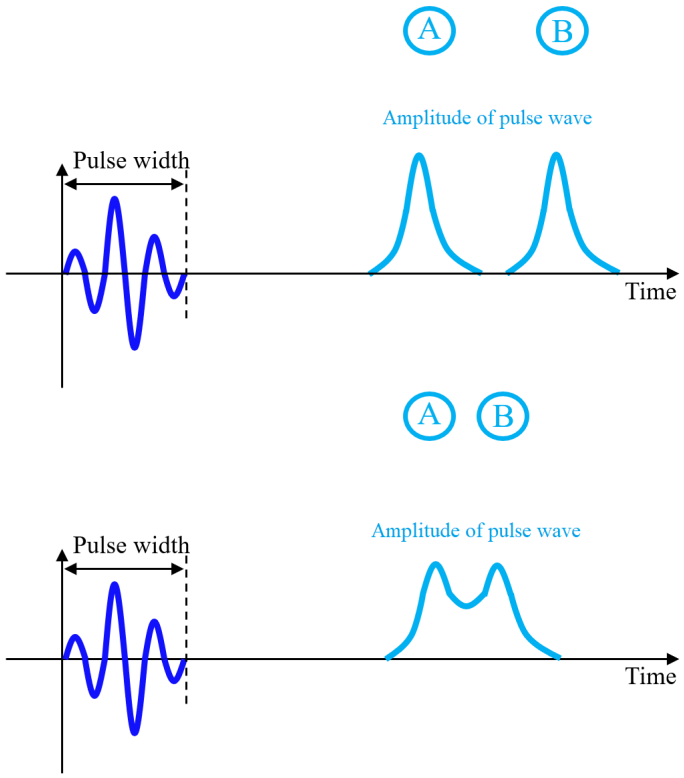

Figure 2.3: Distance resolution of a short pulse.

time of transmission signal and received signal of echo reflection from the target [13, 15]. It is not easy to identify the acoustic signal. A received signal can detect reverberation components because the SNR of a conventional method is lower. Moreover, environmental noises and the scattering of signals on the target surface are detected [16].

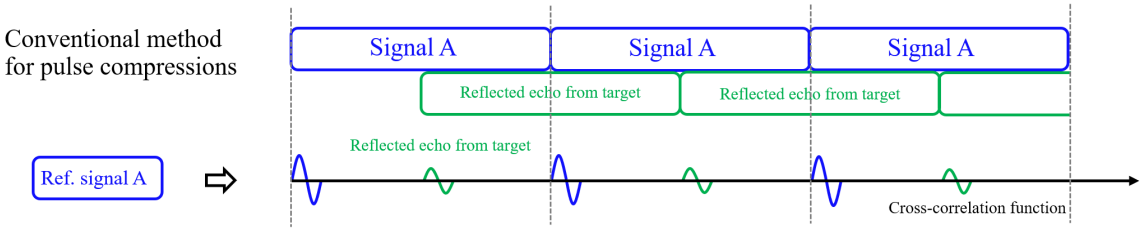

Figure 2.4: Pulse compression methods.

2.2 Pulse compressions

In the pulse-echo method, a short pulse is a low SNR because it is detected environment noise in the received signal. However, we can improve the SNR of the pulse-echo method by pulse compressions. Pulse compression has been introduced as the method for improving SNR and distance resolution as indicated in Fig. 2.4. The frequency-sweep-modulated burst signal or pulse sequence coded is applied to be transmitted signal. Then, the received signal is correlated with the reference signal, that is one cycle of the transmitted signal. If those signals match, the large sharp peak is indicated in the cross-correlation function. Moreover, the background noises and environmental noise can be suppressed by the cross-correlation process. Therefore, the TOF of targets can be identified from a sharp peak with high resolution and high SNR. In this research, LFM signals and M-sequence signals are selected to study in the proposed method. There are simple techniques and most popular for applying in pulse compression.

2.2.1 LFM signal

In a linear-frequency-modulated (LFM) signal, the received signal is correlated by a reference signal, which is one cycle of the transmitted signal. The TOF of the LFM signal is evaluated from the maximum time in the cross-correlation function between the received signal and the reference signal. The cross-correlation method can be used to improve the accuracy of distance in environmental noise[17]. LFM is modulated increased linearly during the time duration of the signal. There is popular to select for pulse compression. LFM signal has modulated the frequency of long pulse during transmission. When increase bandwidth that is

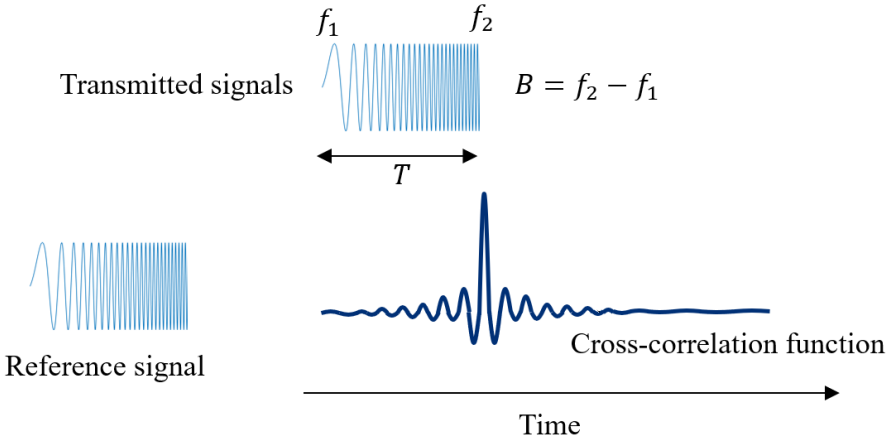

Figure 2.5: LFM pulse compressions.

improved the maximum operating distance and range resolution of the signal. Moreover, increase bandwidth that is improved the maximum operating distance and range resolution of the signal.[18, 19]. The LFM can classify as up chirp and down chirp as given by, [20]

$$s(t) = A\sin 2\pi \left(f_1 + \frac{f_2 - f_1}{2T} t \right) t \tag{2.3}$$

Where A is the amplitude of signals, T is the periodicity, f_1 and f_2 are the starting and the ending frequency. Generally, in the LFM pulse compression, the highest temporal resolution is obtained by the cross-correlation of one-chirp transmission. Then, correlated with the reference signal is indicated in Fig. 2.5. The transmission signal is including with the LFM signal and Gaussian noise. In the correlation function, correlation of LFM signal and signal with noise in the cross-correlation function appears. It is improved SNR by pulse compressions, $SNR_{db} = \sqrt{TB}$.

In the cross-correlation method for the special case of LFM signals, the time resolution of TOF in the received signal is improved by interpolating the cross-correlation function. Moreover, TOF can estimate the maximum peak time in this method. One-chirp transmission of LFM signal to correlate with reference

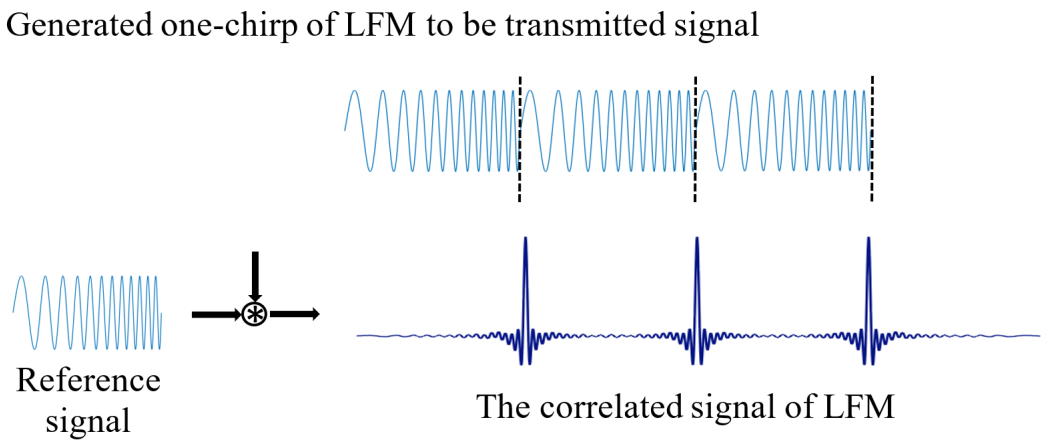

Figure 2.6: Cross-correlation function obtain by the one-chirp transmission of LFM compression

signal is indicated in Fig. 2.6. Three cycles of the up-chirp signal are modulated to apply for transmitting signal. Then the received signal is correlated with the reference signal. The large correlation value appears as a sharp peak in the cross-correlation function. The measurable distance of the correlated signal is the same as the length of the LFM signal. It can improve SNR by pulse compression and improved accuracy of distance in the environment noise. Moreover, the increased bandwidth and length of the LFM signal is improved the maximum operating distance and range resolution of the signal.

2.2.2 M-sequence signal

An M-sequence is one of the pseudorandom sequences, which is generated from the linear feedback shift register (LFSR). There is a good autocorrelation property in the sequential transmission. The n-th order of M-sequence is modulated using a shift register with n parts and XOR, $\bigoplus$ gate as indicated in Fig. 2.7. This is an example of generating 3rd order M-sequence. The length N of n-th order M-sequence is $2^n - 1$ [21]. In the cross-correlation, an M-sequence signal can be applied for improving the SNR and measuring a stable manner of the reflected wave, which is not able to detect by using a conventional impulse [22, 23]. Moreover, SNR is the most important to improve in the measurement system be-

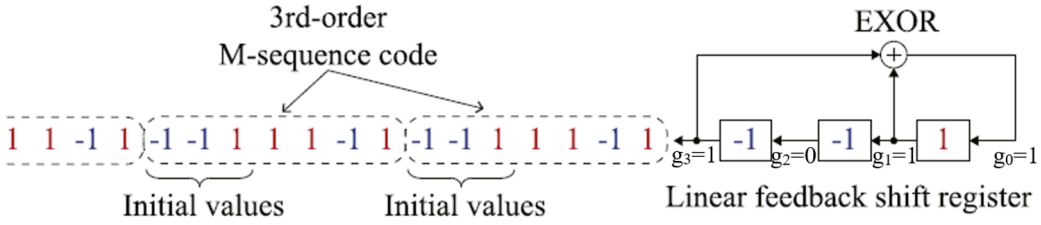

Figure 2.7: LFSR for generating 3rd order M-sequence

cause it is one of the factors to determine the accuracy of measurement. A Gold sequence is a set of gold codes, which can generate with a preferred pair of M-sequences [24, 25]. It is one of the combinations to investigate. The M-sequence is represented as a polynomial equation and given by

$$G(x) = g_n x^n + g_{n-1} x^{n-1} + g_{n-2} x^{n-2} + ... + g_1 x + g_0 \tag{2.4}$$

Where n is n-th order of M-sequence, x is an initial value of LFSR (-1 or 1). The modulated M-sequence is applied to be transmitted signal for simulating in binary condition. In general, the integer and complex m-sequence is given by

$$m_k = u + v b_k = \begin{cases} u + v, b_k = +1 \\ u - v, b_k = -1 \end{cases} \tag{2.5}$$

The complex m-sequence is able to make in polar form to evaluate such as $e^{(\theta \pm \theta_L)} = \cos(\theta \pm \theta_L) + j\sin(\theta \pm \theta_L), \theta_L = \tan^{-1}\sqrt{L}$ and $L = 2^n - 1$. In the periodic pseudorandom binary sequence, the n-th order M-sequence signal in sinuous waveform is given by

$$s(t) = A\sin\left(\omega t + \theta_k\left(t\right)\right) \tag{2.6}$$

Where A is the amplitude of carrier signal and θ_k is the phase of signal. The modulated M-sequence signal is applied to be transmitted signal in the experiment.

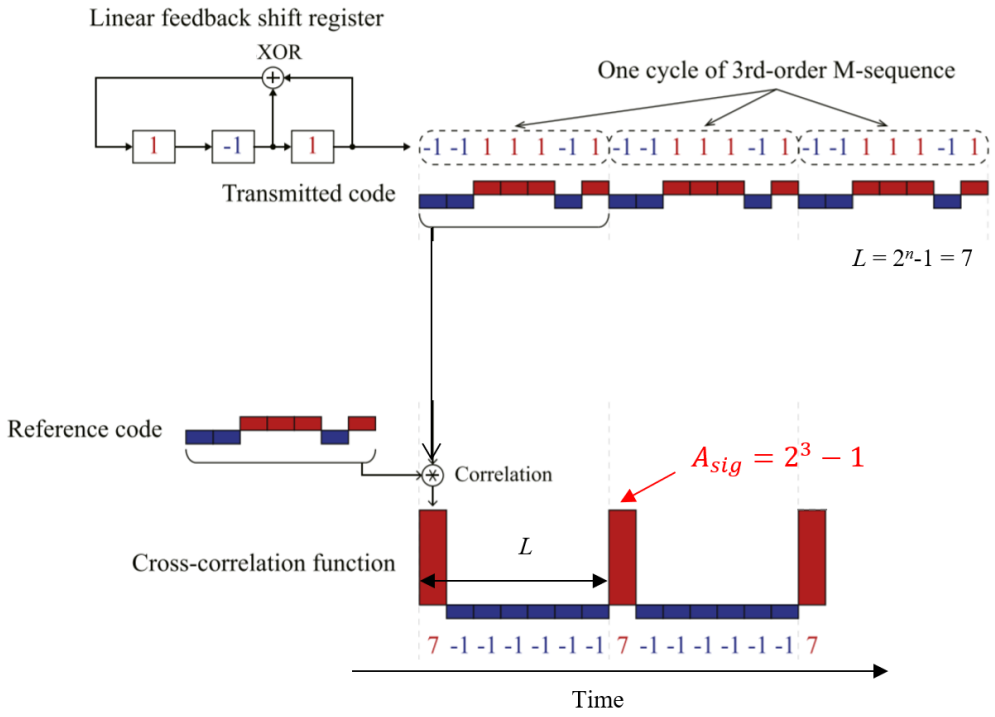

Figure 2.8: Cross-correlation function obtain by the one-code transmissions in M-sequence pulse compression

If the integer or complex m-sequence is m_k, the cross-correlation function of mk sequence is given by

$$R_m[s] = \frac{1}{L}\sum_{L}^{k=1} m_k m_*^{k+s} \tag{2.7}$$

$$R_m[s] = \frac{1}{L}\sum_{L}^{k=1}(uu^* + uv^* b_{k+s} + vb_k u^* + vb_k v^* b_{k+s}) \tag{2.8}$$

Where b_k and $b_{(k+s)}$ are ± 1, which depends on the M-sequence characters. In the complex m-sequence, a condition of complex form is $|v|^2 = L|v|^2$.

In this method for M-sequence codes, a continuous signal is generated by binary characters such as 1 and -1 in the cyclic M-sequence for applying to be

the transmitted signal. Then, the received signal is correlated with the reference signal, which is one cycle of the transmitted signal. When the received signal and reference signal match, the large correlation value indicates a sharp peak in the cross-correlation function as indicated in Fig. 2.8. An M-sequence is a pseudo-random binary sequence to be regularly applied for pulse compression [6, 16, 22, 24, 26, 27, 28, 29, 30, 31, 32, 33, 34, 35, 36, 37, 38, 39, 40, 41, 42, 43]. In the M-sequence pulse compression, a continuous signal is generated by binary characters for applying to be the transmitted signal. Then, one cycle of the M-sequence is applied to the reference signal. Sharp peaks appear at an interval of the cycle length, which is a time duration of the M-sequence-coded signal. In the correlation signal, the large interval is the effect on the limit of measurable distance. However, an increased limit of measurable distance is the effect on the decreased resolution of the measurement. Moreover, non-correlative components and environmental noise can be suppressed by the cross-correlation process. Furthermore, white Gaussian noise including in the M-sequence modulated signal is also increased $\sqrt{L}$ times by the cross-correlation function. Therefore, the SNR of the received signal is improved $\sqrt{7}$ times[26].

In the typical M-sequence pulse compression, amplitudes of transmitted sinusoid waves are modified by binary characters of the M-sequence. That means the initial phases of sinusoid waves are assigned to 0 and -π radian. In the integer alternate transmission method, the transmitted signal is alternately coded by M-sequences A and B in the same way. On the other hand, in the complex alternate transmission method, the initial phases of sinusoid waves correspond to the M-sequence A are assigned to 0 and -π radian, those in the M-sequence B are assigned to 0+α and -π + α radian respectively. In the phase-shift modulation of M-sequence, magnitudes of truncation noise A, truncation noise B and truncated interference noise between A and B are not changed. However, absolute amplitudes in summation of those noises are changed by the phase shift . In this research, the variation of these absolute amplitudes by the phase shift in the alternate transmission of different M-sequences is estimated. All combinations of M-sequences are employed to the research. The phase shift is changed from 0 to 2π radian. The suitable combination of M-sequences and the phase shift can

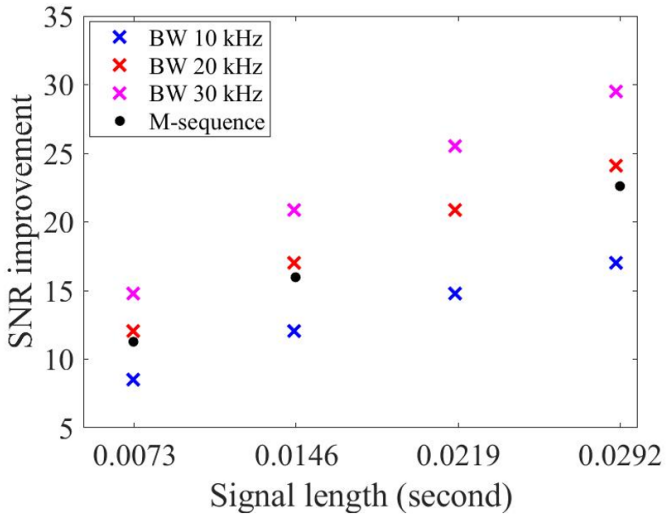

Figure 2.9: SNR improvement comparison between LFM signal and M-sequence signal.

be determined from absolute amplitudes of truncation and truncated interference noises. Furthermore, SNR improvement is indicated in Fig. 2.9. There is an SNR improvement comparison between the LFM signal and the 7th to 9th order M-sequence signal. SNR improvement of LFM signal and M-sequence signal are calculated by $\sqrt{L \times BW}$ and $\sqrt{L}$, respectively. In the M-sequence signal, high SNR improvement is indicated at the high order M-sequence. In the LFM signal, SNR improvement is more improved by increased bandwidth and length of the LFM signal.

Chapter 3

Alternate transmission of different codes in pulse compressions

In the alternate transmission of different signals, a method for the extension of the measurable distance in pulse compression without degradation of the temporal resolution is described for a proposed method. In the proposed method, a continuous signal alternately modulated by two or more different signals is transmitted. Then, the received signal is correlated with each reference signal, which corresponds to each transmitted signal. In each cross-correlation function, the peak interval is extended two or more times. Furthermore, peaks in different cross-correlation functions alternately arise. Therefore, distance measurement can be performed with the same temporal resolution by alternately using each cross-correlation function.

In the proposed method, the alternate transmission of two different signals is extended a measurable distance in double times as indicated in Fig. 3.1. Alternate transmission of the different signals is transmitted. Then, it is correlated with each reference signal. In the cross-correlation function, truncation noise and truncated interference noise are generated around the correlation peaks. Truncation noise denotes the fluctuating correlation values except for the peak in the auto-correlation function. Moreover, if these noises are larger than the reduced

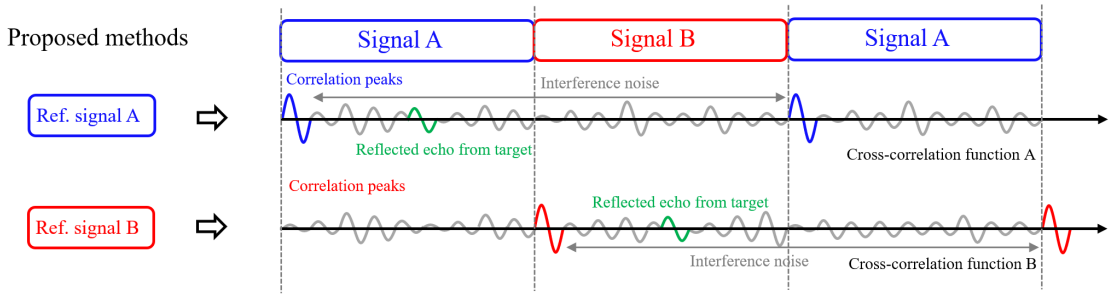

Figure 3.1: Alternate transmission of two different and obtained cross-correlation functions comparisons.

noise component, SNRs are degraded.

3.1 LFM signal

Linear frequency modulation (LFM) is modulated increased linearly during the time duration of the signal. There is the modulated frequency of long pulses during transmission. An LFM signal is a signal with a certain time width while changing the frequency, and then the SNR is improved by correlation processing. The term chirp signal has almost the same meaning as LFM. If the bandwidth of the LFM signal is change, the degree of improvement in the signal-to-noise ratio is changed. The larger bandwidth is greater to improve the SNR. In the alternate transmission method of LFM as indicated in Fig. 3.2 to compare with one-code transmission signal. In the case of one-code transmission, many cycles of an up-chirp signal are transmitted. Then, it is correlated with a one-cycle of LFM signal to obtain the cross-correlation functions. Measurable distance length, L is the same as the one-chip signal length. In the case of two-codes transmission, there is a proposed method. Up-chirp and down-chirp of LFM signal is modulated to be transmitted signal. Then, a received signal is correlated by one cycle of LFM signal A and B, which are called reference signal A and reference signal B respectively. In each cross-correlation function, the compressed pulses arise at double intervals and extend the measurable distance in double times, without degraded temporal resolution by using two cross-correlation functions. Moreover, SNR alternate transmission LFM signal is improved by the correlation function.

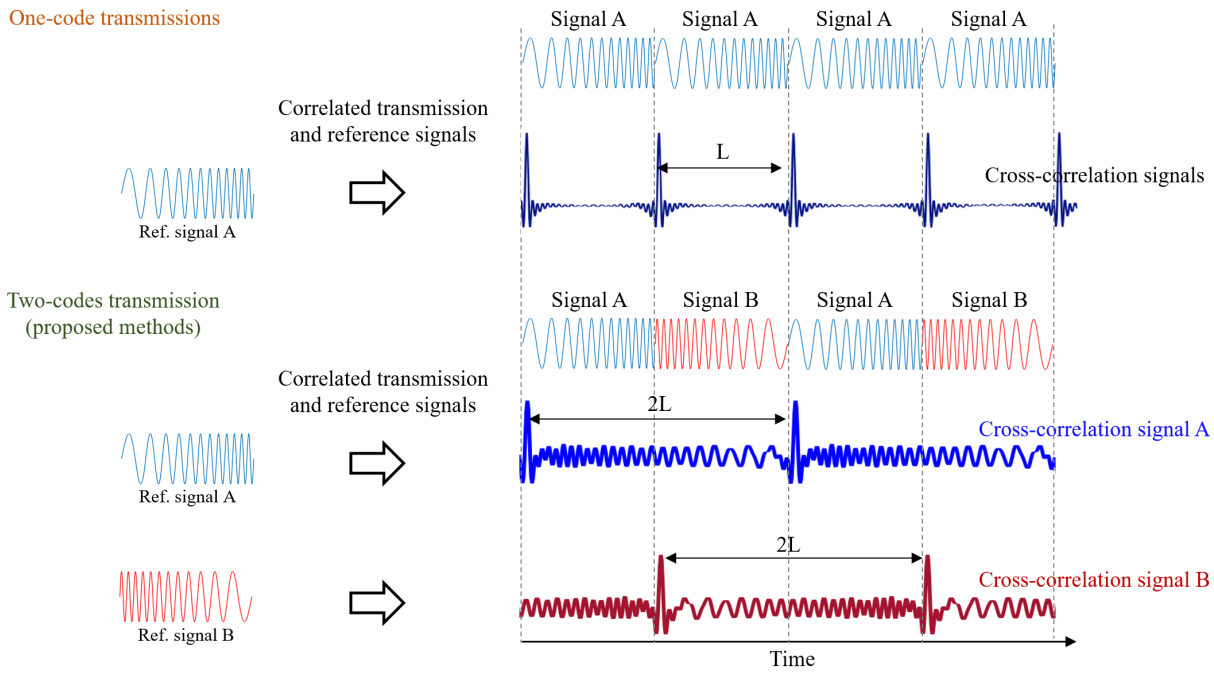

Figure 3.2: One-code and two-codes transmission of LFM signals.

However, noise characteristics of alternate are changed by different bandwidth and lengths of LFM signal. The large bandwidth and long length of the LFM signal are improved SNR.

Sweep frequency to modulated LFM signal is 20 kHz to 80 kHz and 80 kHz to 20 kHz for 60kHz of bandwidth, 30 kHz to 70 kHz and 70 kHz to 30 kHz for 40kHz of bandwidth and 40 kHz to 60 kHz and 60 kHz to 40 kHz for 20kHz of bandwidth. In the transmitted signal, three sequences of up-chirp and down-chirp are transmitted to be correlated with each reference signal. The length of each sweep frequency to modulated for comparing with center frequency 25kHz of M-sequence signal from 8th to 9th order is 10.22 ms and 20.44 ms respectively. The amplitudes are normalized by the correlation peak. Maximum noise amplitude of correlated signal and spectrum of noise is indicated. The correlated signal of alternate transmission in the LFM signal is indicated in Fig. 3.3. Noise characteristics are changed by different bandwidth and lengths of LFM signal. LFM signal is a signal with a certain time width while changing the frequency, and then

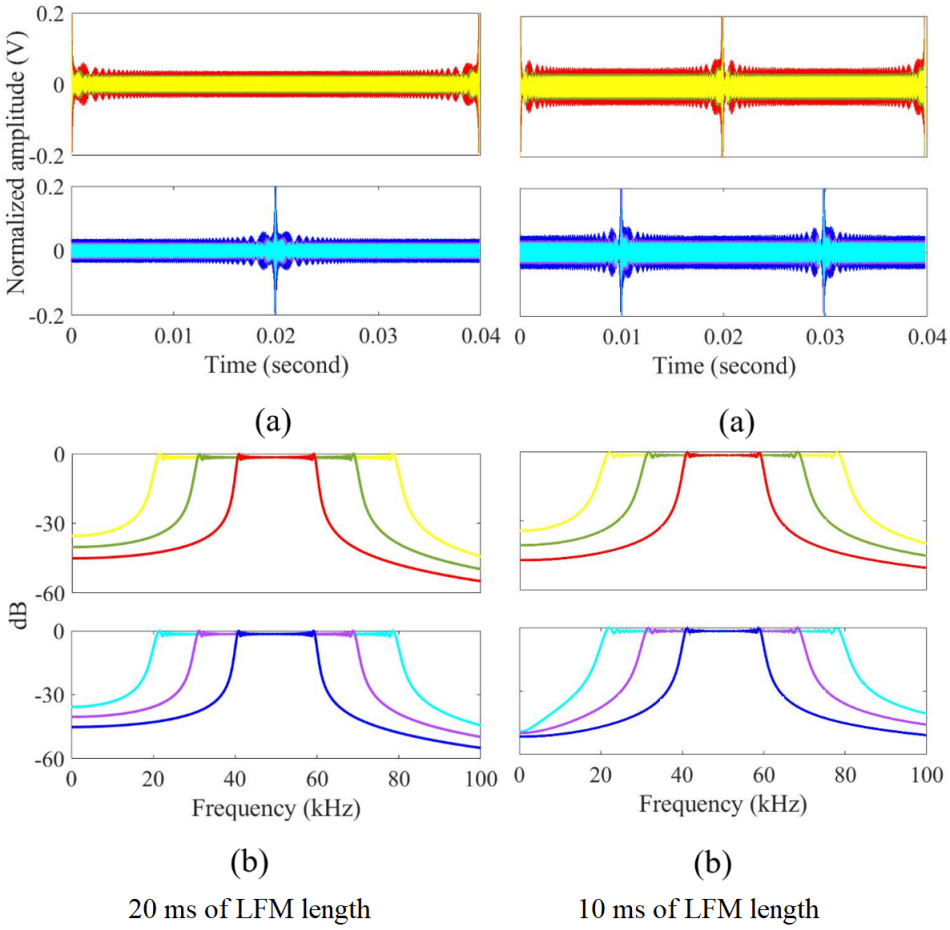

Figure 3.3: Correlation signal of different length for alternate LFM transmissions.

the SNR is improved by the correlation processing. Changing the bandwidth is changes the degree of improvement in the SNR. Therefore, the larger bandwidth width is greater to improve the SNR.

3.2 M-sequence signal

The M-sequence is generated from a linear feedback shift register (LFSR), which is modulated by a periodic pseudorandom binary signal (0 or 1). The length n of the LFSR is the order of the M-sequence. In the n-th order M-sequence, the

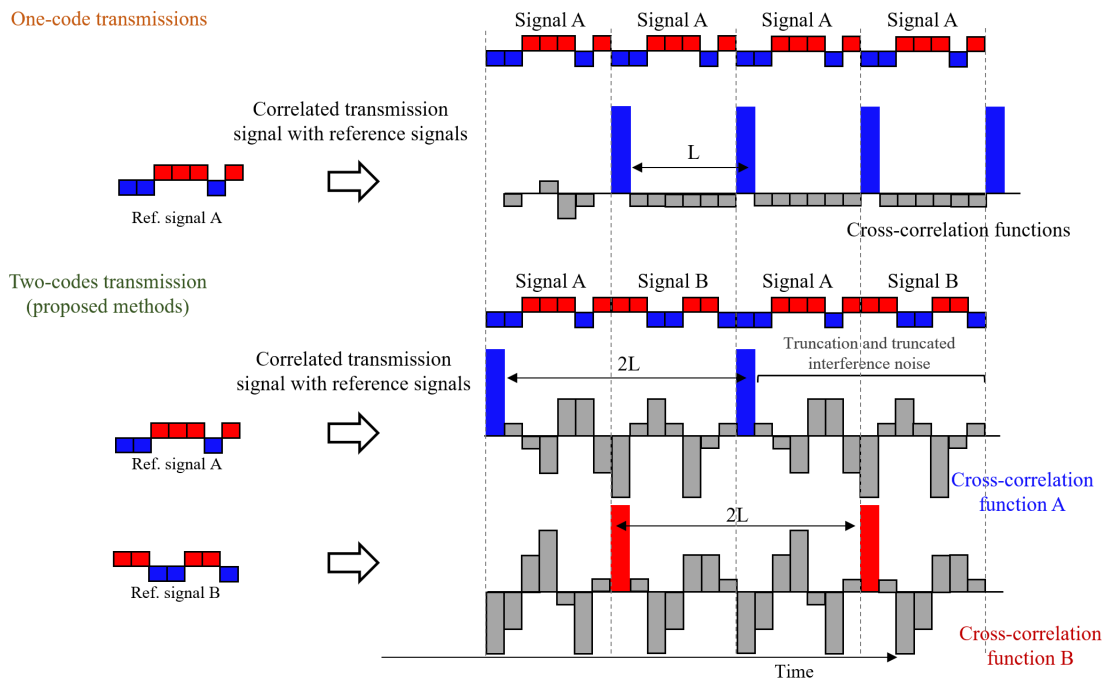

Figure 3.4: One-code and two-codes transmission of LFM signals.

number L of binary characters in one cycle is $2^n - 1$. The number of one cycle of the M-sequence is also L. The conventional M-sequence and the proposed method of M-sequence is indicated in Fig. 3.4. The different M-sequence codes are modulated from different numbers and different feedback taps position of LFSR. In the case of one-code for M-sequence transmission, continuous of the same M-sequence code is transmitted signal. Then, correlated with the reference signal to obtain the cross-correlation functions. The values of the amplitudes and interval of compressed pulses are L. In the case of two codes for M-sequence transmission, the continuous signal is alternately modulated by one cycle of each M-sequence to be transmitted signal. Then, a received signal is correlated with each reference signal, which corresponds to each M-sequence code. In the cross-correlation function, each correlation function can be alternately applied for distance measurement in the same as the one-code temporal resolution. However, the peak interval in each correlation function is extended double times. Nevertheless, truncation and truncated interference noise are generated around the sharp peak of the cross-correlation functions. Moreover, different M-sequence combinations are

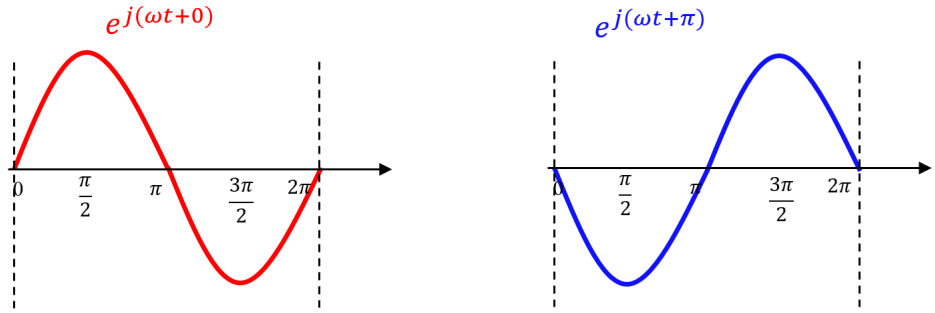

Figure 3.5: Integer M-sequence modulation

an effect with these noises. In the white Gaussian noise including with the received signal, the amplitude of the correlated signal is increased $\sqrt{L}$ times by the cross-correlation. Therefore, the SNR of the received signal is improved $\sqrt{L}$ times by the M-sequence pulse compression because of increased pulse amplitude L times. The pulse-repetition time or the pulse interval is determined by the cycle length of M-sequence, the product of L, and the time duration of the signal is assigned to each character.

3.2.1 Integer M-sequence modulation signals

M-sequence modulation is made from binary characters 1 and -1 of M-sequence codes as indicated in Fig. 3.5. There are modulated by sinewave as $e^{j(0)}$ and $e^{j(\pi)}$, respectively. The alternate M-sequence of two different codes is transmitted to extend the pulse-repetition time with the original temporal resolution. Moreover, in the cross-correlation method, the received signal is correlated with each M-sequence, as illustrated in Fig. 3.6. In the typical M-sequence pulse compression, a sinusoid wave and the inverse sinusoid wave are assigned to binary characters 1 and -1, which means that the initial phases of sinusoid waves are assigned to 0 and -π radian, respectively. The cross-correlation functions A and B are obtained by correlations with the discrete reference signal A and B, respectively. In each cross-correlation function, the compressed pulses arise at double intervals and the measurable distance is extended in double times. Nevertheless, the original temporal resolution can be maintained by using two cross-correlation functions. However, in both cross-correlation functions, truncation

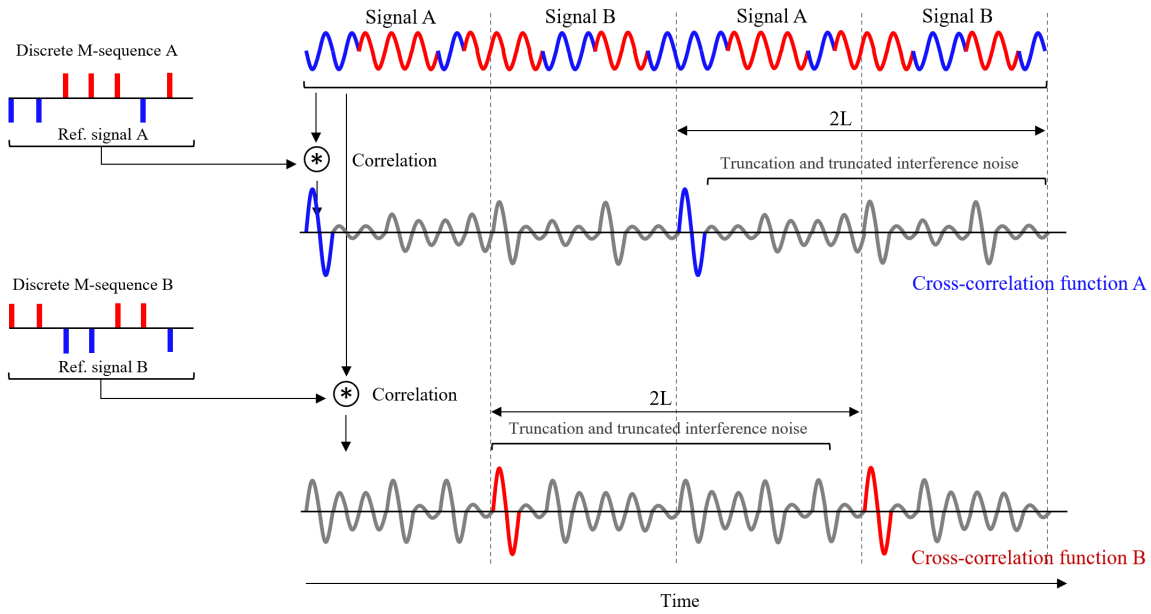

Figure 3.6: Alternate transmission of different signal on pulse compression for integer M-sequence modulations

noise and truncated interference noise is appeared except for compressed pulses. The truncation noise is the autocorrelation values of one cycle of M-sequence A or B except the center pulse of the correlated signal. The truncated interference noise is the cross-correlation function of one cycle of different M-sequence. In the case of these noises, amplitudes are large, the TOF of the correlated signal is not accurate when determined from the compressed pulse. The amplitudes of truncation and truncated interference noises are varied by combinations of M-sequences. Therefore, the suitable combinations of M-sequences are studied and searched in this research.

3.2.2 Complex M-sequence modulation signal

The modulation method in the alternate transmission of different M-sequences is alternated to suppress truncation and truncated interference noises better than the integer M-sequence signals. The transmitted signal in the originally M-sequence pulse compression is given by

3. ALTERNATE TRANSMISSION OF DIFFERENT CODES IN PULSE COMPRESSIONS

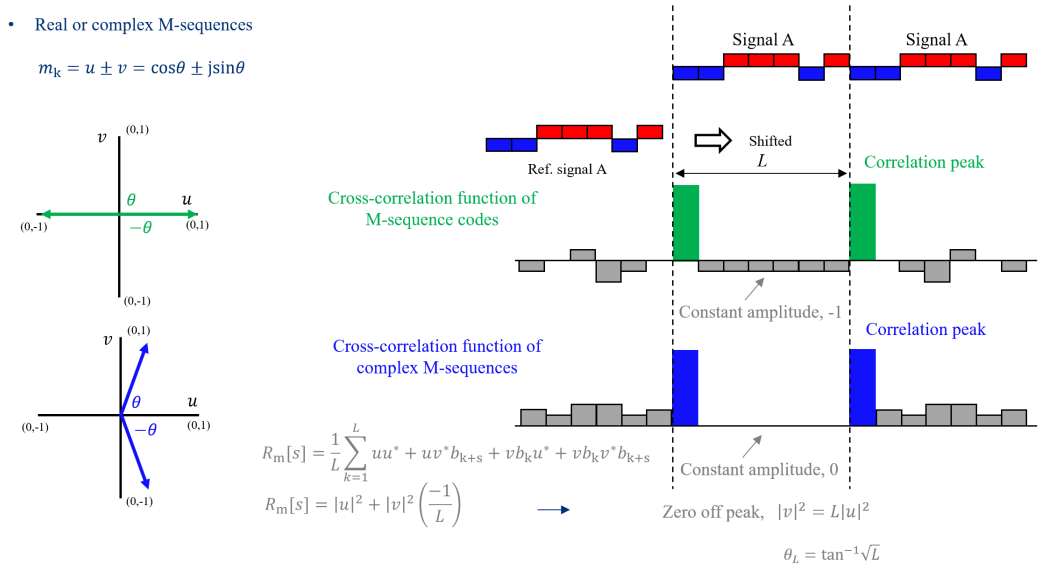

Figure 3.7: Integer and complex M-sequence in the cross-correlation function comparision

$$m_k = \begin{cases} e^{j(\omega t+\theta_p)} = \cos(\omega t+\theta_p) + j\sin(\omega t+\theta_p), b_k = 1 \\ e^{j(\omega t-\theta_n)} = \cos(\omega t+\theta_n) - j\sin(\omega t+\theta_n), b_k = -1 \end{cases} \tag{3.1}$$

Where b_k is the binary character of M-sequence, m_k is the transmission signal associated with each binary character, ω is angular frequency of carrier wave and θ_p and θ_n are the initial phases of carrier waves. In the complex M-sequence pulse compression, initial phases of complex numbers $e^{j(\omega t+\theta)}$ are assigned to $\tan^{-1}\sqrt{L}$ and -$\tan^{-1}\sqrt{L}$ radian. The real parts of $e^{j(\omega t+\tan^{-1}(\sqrt{L})}$ and $e^{j(\omega t-\tan^{-1}(\sqrt{L})}$ are assigned to binary characters 1 and -1. It is used to transmit wave forms of M-sequence pulse compression. Then, the received signal is converted to the complex signal by the Hilbert transform and correlated with the reference signal, which is the complex M-sequence. The TOF of correlated signal is determined from absolute values of cross-correlation function. The amplitudes of compressed pulses and other correlation values except compressed pulses are l and 0. Modulation function of integer and M-sequence is same idea. However, in the complex M-sequence modulation is focus on phased-shift of M-sequence combinations. In

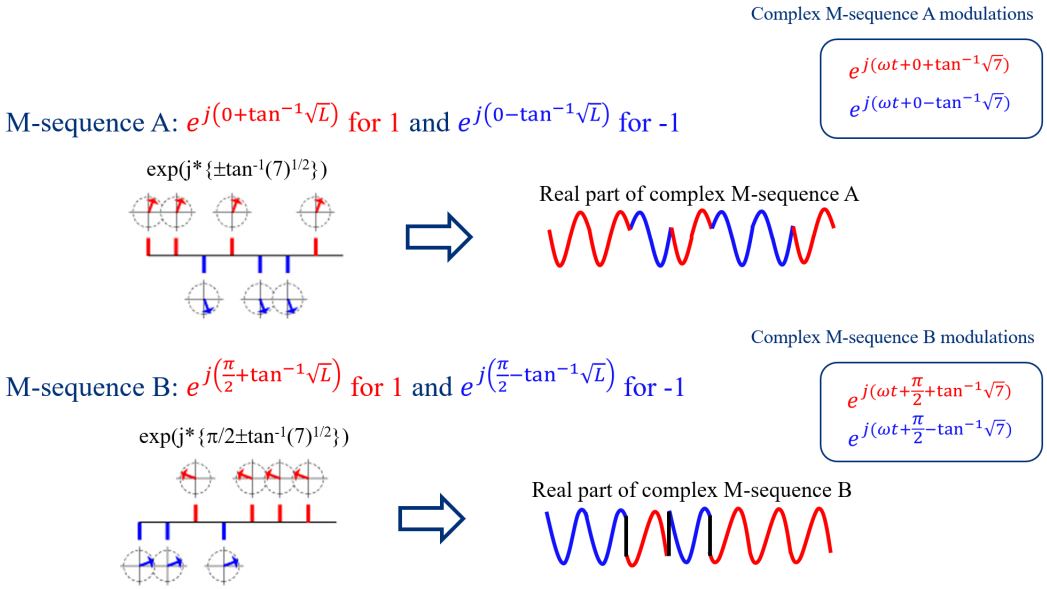

Figure 3.8: Complex M-sequence modulation A (above) and B (below).

the cross-correlation function, there is modulated by conjugated between transmitted signal and reference signal. Moreover, constant amplitude of integer and complex M-sequence is difference as indicated in Fig. 3.7. Constant amplitude of integer M-sequence is -1. However, in case of the complex M-sequence, constant amplitude is zero. In the proposed method of this research, the phases of M-sequence B are shifted from those of M-sequence A by α radian. Complex M-sequence modulation A and B is indicated in Fig. 3.8. Therefore, $e^{j(\omega t+\tan^{-1}(\sqrt{L})}$ and $e^{j(\omega t-\tan^{-1}(\sqrt{L})}$ are assigned to binary characters of 1 and -1 in M-sequences A. Moreover, $e^{j(\omega t+\tan^{-1}(\sqrt{L}+\alpha)}$ and $e^{j(\omega t-\tan^{-1}(\sqrt{L}+\alpha)}$ are assigned to binary characters of 1 and -1 in M-sequences B. Alternate transmission of two different complex M-sequences and obtained absolute cross-correlation functions is illustrated in Fig. 3.9. The real component of the carrier wave is transmitted, and the received signal is converted to a complex signal by the Hilbert transform. The reference signals are discrete complex signals composed of $e^{j\theta_L}$ and $e^{-j\theta_L}$, $e^{j\theta_L+\alpha}$ and $e^{-j\theta_L+\alpha}$, respectively. The TOFs are determined from absolute cross-correlation functions between the received signal and each reference signal. Amplitudes of truncation and truncated interference noises are varied by combinations of M-sequences. Therefore, absolute amplitudes of truncation and truncated interference noises

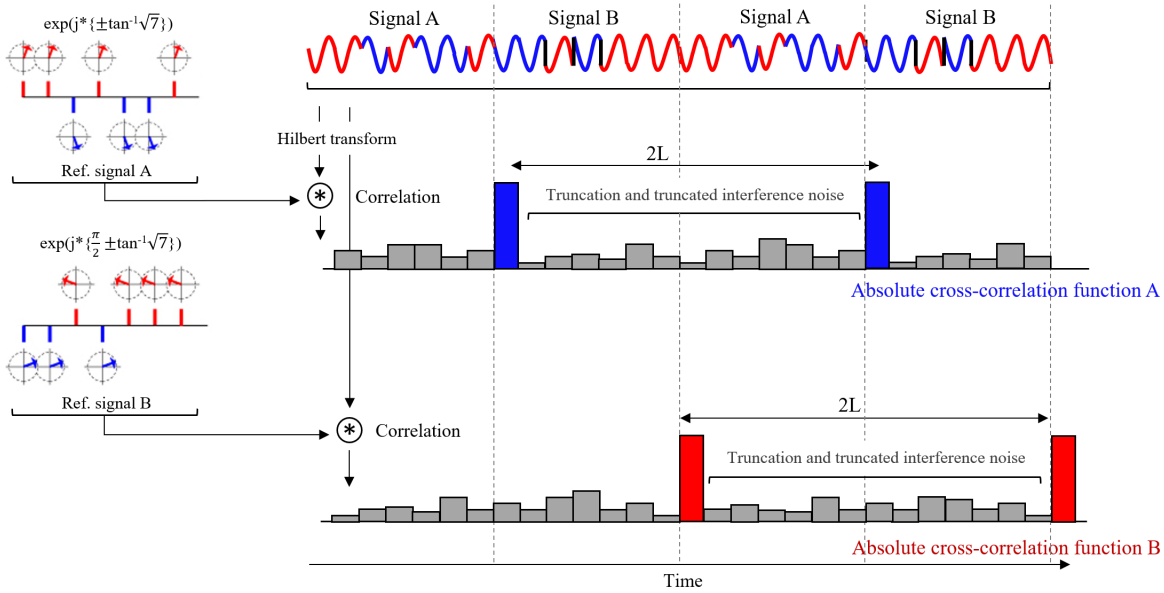

Figure 3.9: Alternate transmission of different signal on pulse compression for integer M-sequence modulations and absolute cross-correlation functions

seem to be also varied by the phase shift and combination of M-sequences.

Chapter 4

Simulation of noise amplitude evaluations

In the proposed method, truncation noise and truncated interference noise are generated around the correlation peaks. Truncation noise denotes the fluctuating correlation values except for the peak in the auto-correlation function of an M-sequence code. Truncated interference noise is the cross-correlation function between different signals. In the case of alternate LFM signals, difference bandwidth and length are effect by truncation and truncated interference noise. In the case of transmission of a single M-sequence code and two or more different codes, SNRs of correlation peaks are equally improved because the effect of SNR improvement depends on the length of the reference M-sequence code. However, if these noises are larger than the reduced noise component, SNRs are degraded. On the other hand, different patterns of truncation noise and truncated interference noise in the alternate M-sequence signal are generated from different combinations of M-sequence codes. Therefore, all patterns of truncation noise and truncated interference noise are quantitatively evaluated. By selecting suitable M-sequence codes, the SNR degradation of the proposed method can be suppressed. This chapter presents a simulation of maximum noise amplitude evaluation in the alternate LFM and alternate M-sequence signal.

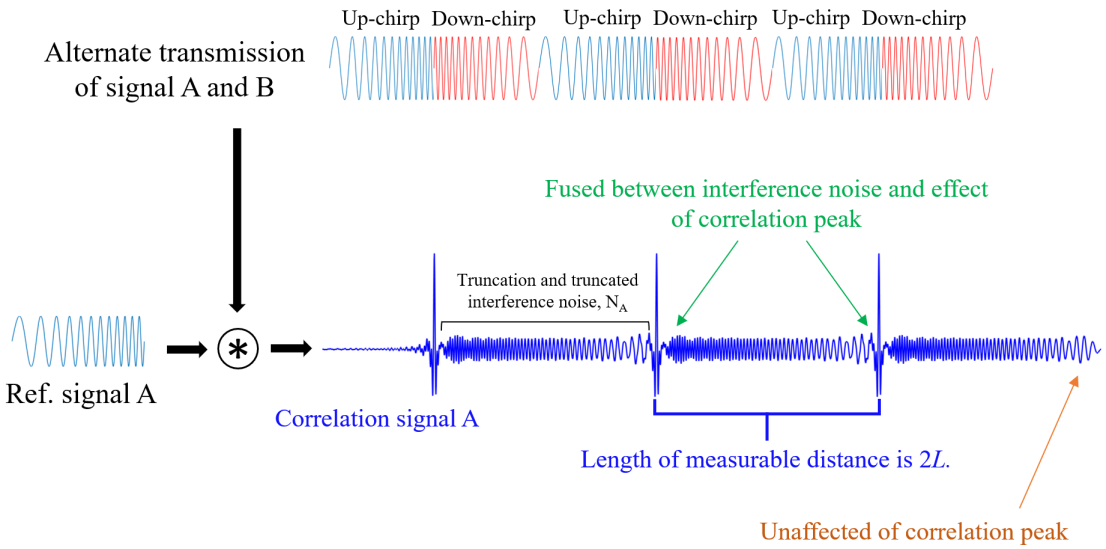

Figure 4.1: Noise characteristic of alternate transmission in the LFM signal.

4.1 LFM signal

LFM signal is a signal with a certain time width while changing the frequency, and then SNR is improved by correlation processing. In this research, different bandwidths of alternate transmission in LFM signals are evaluated with respect to their amplitude. In the conventional method of LFM signal, the autocorrelation function is applied to study a noise characteristic of the LFM signal. Noise amplitude of correlation signal is lower when the length of the LFM signal is longer. In the alternate transmission of the LFM signal, noise from auto-correlation function and interference noise is appeared by cross-correlation function. There are fused and difficult for separating them as indicated in Fig. 4.1. In this research, the loudspeaker is generated 10kHz of 30 kHz to 40 kHz in the LFM signals. Moreover, the simulation to evaluate maximum noise amplitude, 30 kHz to 40 kHz and 40 kHz to 30 kHz of LFM signal are transmitted signal. Then, the transmitted signal is correlated by each reference signal. The noise from autocorrelation and interference noise is appeared by the cross-correlation function. Noise by autocorrelation function is not separated. In this simulation, the length of the alternate LFM signal for generating be transmitted signal is 7.3 ms, 14.57 ms, and 29.2 ms, respectively. There is generated to compare with 35 kHz of 7th order to 9th order

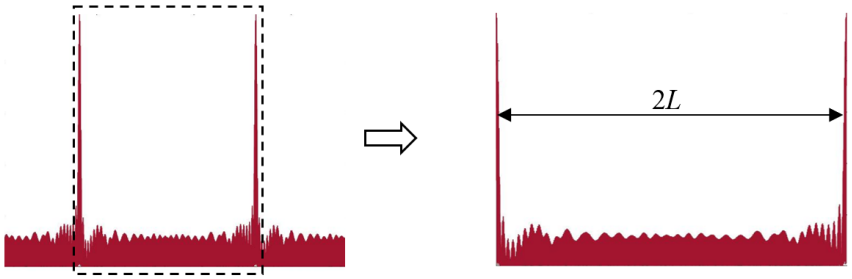

(a) Absolute values of cross-correlation signal in the alternate transmission method

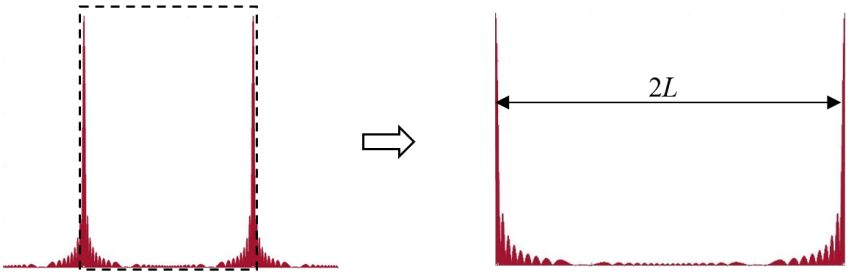

(b) Two repeated signals of absolute values in the autocorrelation signal

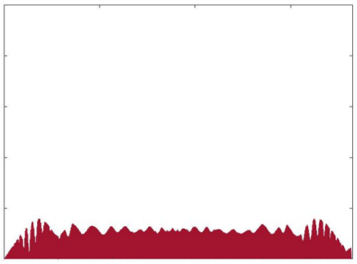

(c) Subtraction signal (interference noise)

Figure 4.2: Absolute signal for subtracting mehod.

M-sequence signals. However, only interference noise of correlation signal is investigated. In the evaluation method, noise from the auto-correlation function is removed by subtracting method as indicated in Fig. 4.2. Two repeated signals of the auto-correlation function are applied to subtract with cross-correlation signal of alternate transmission method. The subtraction method is applied to evaluate the interference noise of alternate transmission of LFM signal.

The absolute value of interference noise to compare with 35 kHz of 7th order

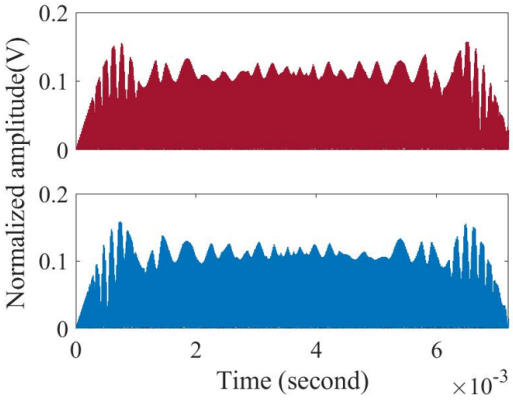

(a) 7.3 ms of alternate LFM signal length

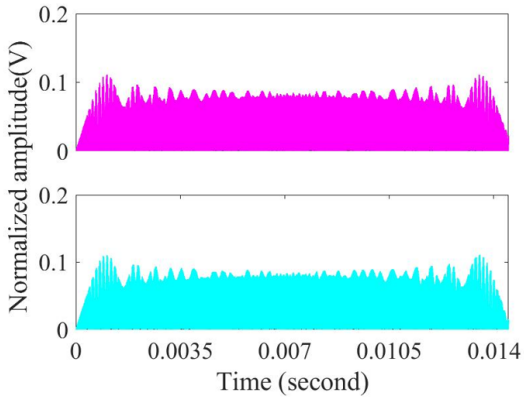

(b) 14.57 ms of alternate LFM signal length

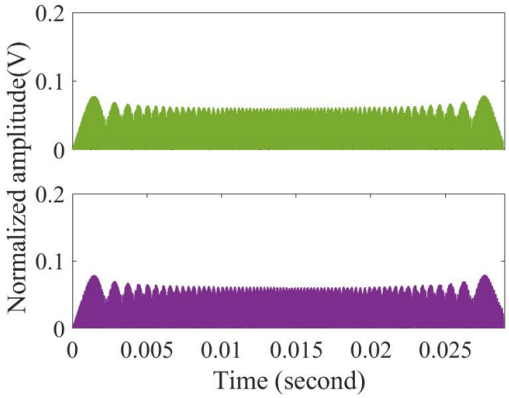

(c) 29.2 ms of alternate LFM signal length

Figure 4.3: Interference noise of alternate LFM signal with different alternate LFM signal length

Table 4.1: Maximum amplitude of alternate transmission of LFM signal to compare with 35 kHz of carrier frequency in 7th, 8th and 9th order M-sequence signal.

LFM length	Max. of N_A/Mean	Max. of N_B/Mean	Max. of $N_A + N_B$/Mean
7.30 ms	0.1575/0.0650	0.1582/0.0655	0.3156/0.1304
14.57 ms	0.1116/0.0470	0.1111/0.0471	0.2218/0.0941
29.20 ms	0.0790/0.0349	0.0796/0.0350	0.1580/0.0699

Table 4.2: Highest SNRs in the alternative transmission of LFM signal.

LFM length	SNR_A	SNR_B
7.30 ms	16.05 dB	16.02 dB
14.57 ms	19.02 dB	19.08 dB
29.20 ms	22.99 dB	22.99 dB

to 9th order is illustrated in Fig. 4.3. The above and below in each figure are subtraction signals of correlation signal with reference signal A and B, respectively. Maximum noise amplitude is indicated in Table 4.1. The maximum amplitude of the noise is lower when the length of the LFM signal is longer. SNR improvement is depending on the length of LFM signals. In this research, the SNR for truncation noise and truncated interference noise is defined to evaluate combinations as given by

$$\mathrm{SNR} = 20\log\frac{1}{MA} \tag{4.1}$$

MA is the maximum amplitude of truncation noise and truncated interference noise when the correlation peak is normalized to 1. The highest SNRs in the alternate transmission of the LFM signal are indicated in Table 4.2. In the long length of the LFM signal, the highest SNR appears. The highest SNRs improved from 6.94 dB to 6.97 dB when compared with 7.30 ms of LFM signal length. Lastly, 30 kHz to 40 kHz and 40 kHz to 30 kHz of alternate LFM signal to compare with 7th order to 9th order M-sequences are indicated in Fig. 4.4.

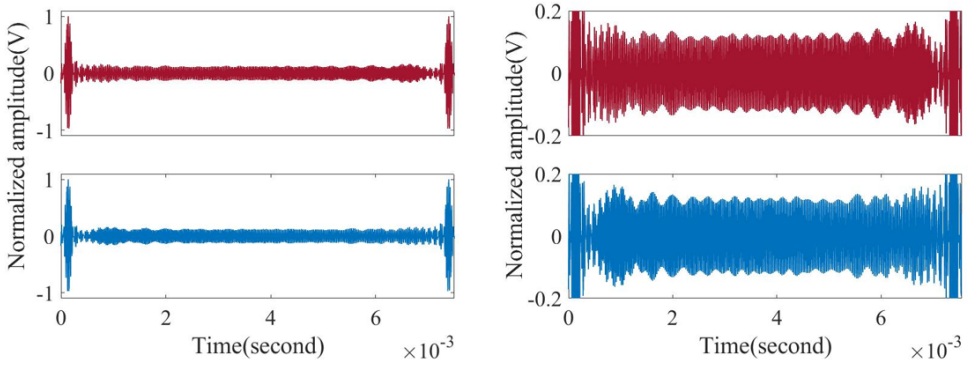

(a) 7.30 ms of alternate LFM signal length

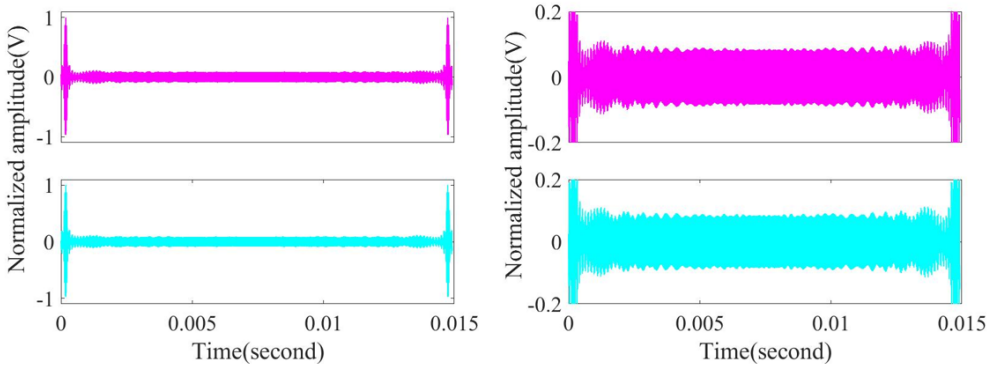

(b) 14.57 ms of alternate LFM signal length

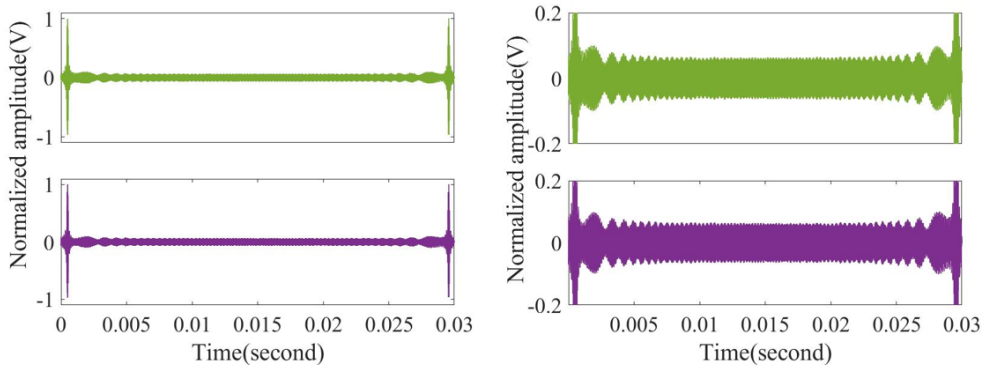

(c) 14.57 ms of alternate LFM signal length

Figure 4.4: Different length of alternate LFM signal in the cross-correlation function comparisons.

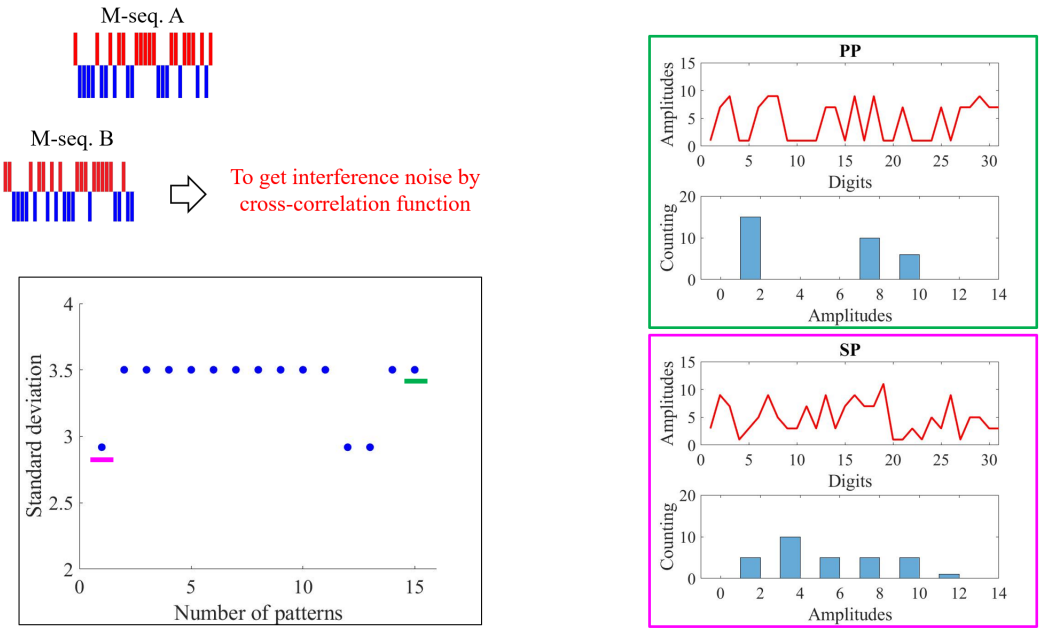

Figure 4.5: M-sequence combination of 5th order M-sequences

4.2 M-sequence signal

In this research, truncation and truncated interference noises in the alternate transmission of different M-sequences appears. Incidentally, particularly for orders greater than the 6th order, several different distributions appear to be included in their distributions. There are several types of combinations of M-sequences. Therefore, the differences of truncation noise and truncated interference noise with respect to the types of combinations of M-sequences are focused on. The noise characteristic of each combination in the 5th order M-sequence is indicated in Fig. 4.5. It is calculated from interference noise of M-sequence combination. There is indicated standard deviation of interference noise and interference noise characteristic of 5th order M-sequence as an example. The symmetry pair (SP) is the combination of M-sequences generated from symmetry LFSRs. M-sequences in the SP is also symmetry sequences themselves. Moreover, the standard deviation of the interference noise in the SP is the lowest value. The preferred pair (PP) is the combination of M-sequences that has lower interference noise composed of three correlation values. Moreover, the lowest value of

Table 4.3: Numbers of all patterns for the truncation noise and truncated interference noise in the alternative transmission of integer M-sequences from the 4th to 9th order

Order of M-sequence	Binary character, l	Combination of M-sequence, c	Patterns of noise $c \times l \times l$
4	15	SP: 1	225
5	31	SP: 3	2,883
		PP: 12	11,532
6	63	SP: 3	22,907
		PP: 6	23,814
		OP: 6	23,814
7	127	SP: 9	1,741,932
		PP: 90	1,451,610
		OP: 54	870,966
8	255	SP: 8	520,200
		qPP: 16	1,040,400
		HIP: 8	520,200
		OP: 88	5,722,200
9	511	SP: 24	6,266,904
		PP: 288	75,202,848
		OP: 816	213,074,736

the interference noise appears in PP. In the case of the 8thorder (a multiple of 4th order) M-sequences, there is no PP but quasi preferred pairs (qPP) that have lower interference noise composed of four correlation values. Furthermore, there are high interference pairs (HIP) for which two-thirds or more binary characters in their M-sequences are the same in the 8th order. Therefore, the orders of M-sequences are investigated from 4th to 9th. Noise patterns of one combination are varied by the initial values, l in each M-sequence. Therefore, all patterns of truncation and truncated interference noises in each-order M-sequence is $c \times l \times l$. The numbers of noise patterns in the alternative transmission of two different codes in the M-sequences from 4th to 9th order are illustrated in Table 4.3. In

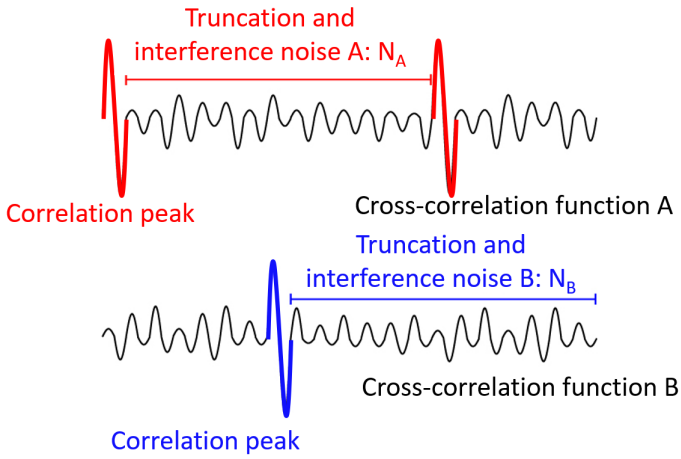

Figure 4.6: Truncation and truncated interference noise evaluations

this research, other pairs of 9th order M-sequence are not evaluated because a memory of the personal computer is not enough for calculating.

In the simulation, the binary sequence of the M-sequence A, $e^{j\left(\omega t+\tan^{-1}\sqrt{L}\right)}$ or $e^{j\left(\omega t-\tan^{-1}\sqrt{L}\right)}$ and the M-sequence B, $e^{j\left(\omega t+\tan^{-1}\sqrt{L}+\alpha\right)}$ or $e^{j\left(\omega t-\tan^{-1}\sqrt{L}+\alpha\right)}$ are alternately to be transmit signal, which is defined as the correlated signal. Each reference signal is the M-sequence A or B, which is one cycle of M-sequence A or B. The cross-correlation function A or B is obtained from the correlated signal of the M-sequence A or B. The correlation peaks of absolute cross-correlation function A and B are normalized to 1. The truncation and truncated interference noises in absolute cross-correlation functions A and B are defined as N_A and N_B, which are absolute correlation values of $2L-1$ between correlation peaks as indicated in Fig. 4.6. In this research, maximum amplitudes and standard deviation in N_A and N_B are estimated for the integer M-sequence. Nevertheless, maximum amplitude and average values in N_A and N_B are evaluated for the complex M-sequence. Hence, the summation of each maximum amplitude and each average value in N_A and N_B are investigated in all patterns of truncation and truncated interference noises.

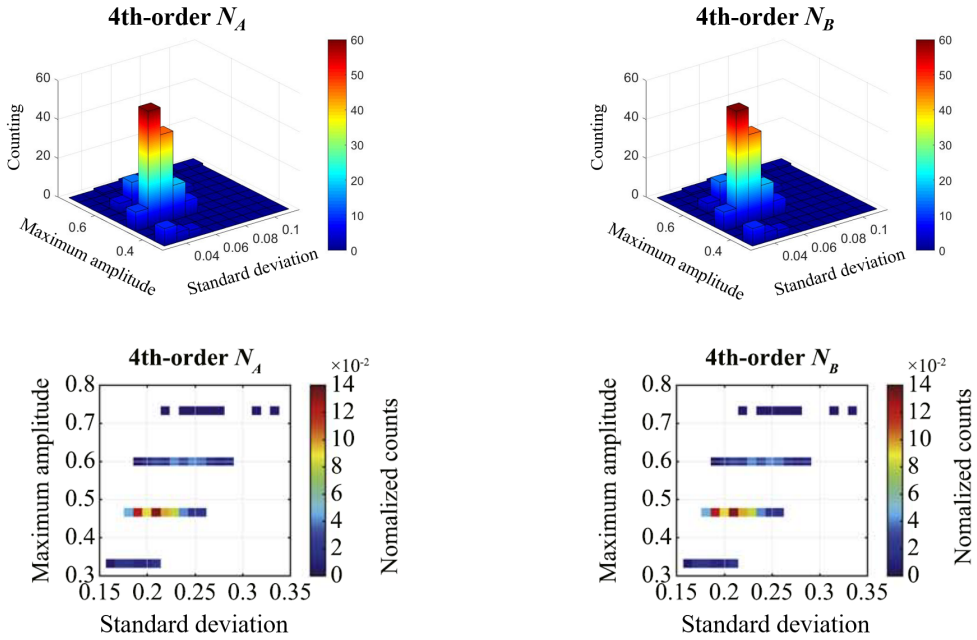

Figure 4.7: 3D and 2D distribution of maximum amplitude and standard deviation of truncation and truncated interference noise of 4th order M-sequences

4.2.1 Integer M-sequence signal

All patterns of truncation noise and truncated interference noise in the alternate transmission of two different M-sequence codes are evaluated with respect to their amplitudes. Their amplitudes are normalized by the correlation peak. Distributions of maximum amplitudes and standard deviations of N_A and N_B in each M-sequence order are indicated. Moreover, the maximum amplitude and the standard deviation are obtained from each of the N_A and N_B as indicated in Fig. 4.7. 3D figure as indicated in above figure is distribution of maximum noise amplitude and standard deviation. Moreover, z-axis is indicated counting points. In 2D figure as indicated in below figure is illustrated distribition of maximum amplitude of truncation and truncated interference noise as well There are a topview of 3D figures. Difference color is normalized counts, which corresponds with color bar. In alternate transmission, all values are desirable to be lower. Therefore, summations of both maximum amplitudes and those of both standard deviation values are also evaluated. Distributions of summations of maximum

amplitudes and those of standard deviations are indicated as $N_A + N_B$. Distributions from 4th order to 9th order M-sequences are illustrated in Fig. 4.8. The maximum amplitude is shown on the ordinate; the standard deviations are shown on the abscissa. Colors denote the count of patterns divided by the total number. Furthermore, the highest and lowest values of maximum amplitudes and standard deviations of $N_A + N_B$ are illustrated in Fig. 4.9. Both values decrease as the order of the M-sequence increases. The lowest maximum amplitudes are less than half of the highest values. In the case of orders greater than the 7th order, the lowest values are less than one-third of the highest values. However, differences between the lowest and highest standard deviations decrease as the order of the M-sequence increases. Selecting M-sequence codes, in which maximum amplitudes of truncation noise and truncated interference noise are lowest, is effective in the identification of actual correlation peaks in the alternate transmission of different M-sequence codes.

The distributions of maximum amplitudes and standard deviation of $N_A + N_B$ in each type of combination are indicated. Distributions from 4th to 9th order M-sequences are illustrated in Fig. 4.10. Particularly, lower maximum amplitudes principally consist of SP, PP, and qPP. The lowest values of maximum amplitudes in SP, PP, and qPP and lowest average values of their noise are given in Table 4.5. The lowest maximum amplitudes in SP and PP are the same and smaller than those in qPP. Furthermore, the lowest average values in SP are smaller than those in PP or qPP except for the 5th order. Interference noises in PP and qPP are lower than those in OP or HIP. Therefore, it is understandable that their maximum amplitudes are lower. Meanwhile, it is not known why maximum amplitudes of SP are lower in this study. However, in the case of alternate transmission of two different integers M-sequence codes, M-sequence codes should be selected from symmetry pairs of M-sequences.

In M-sequence pulse compression, sharp peaks in the cross-correlation function are recognized as TOFs of targets. Therefore, maximum amplitudes of $N_A + N_B$ should be as lower as possible. Consequently, the suitable combination is a combination, in which the maximum amplitude is the lowest and the standard

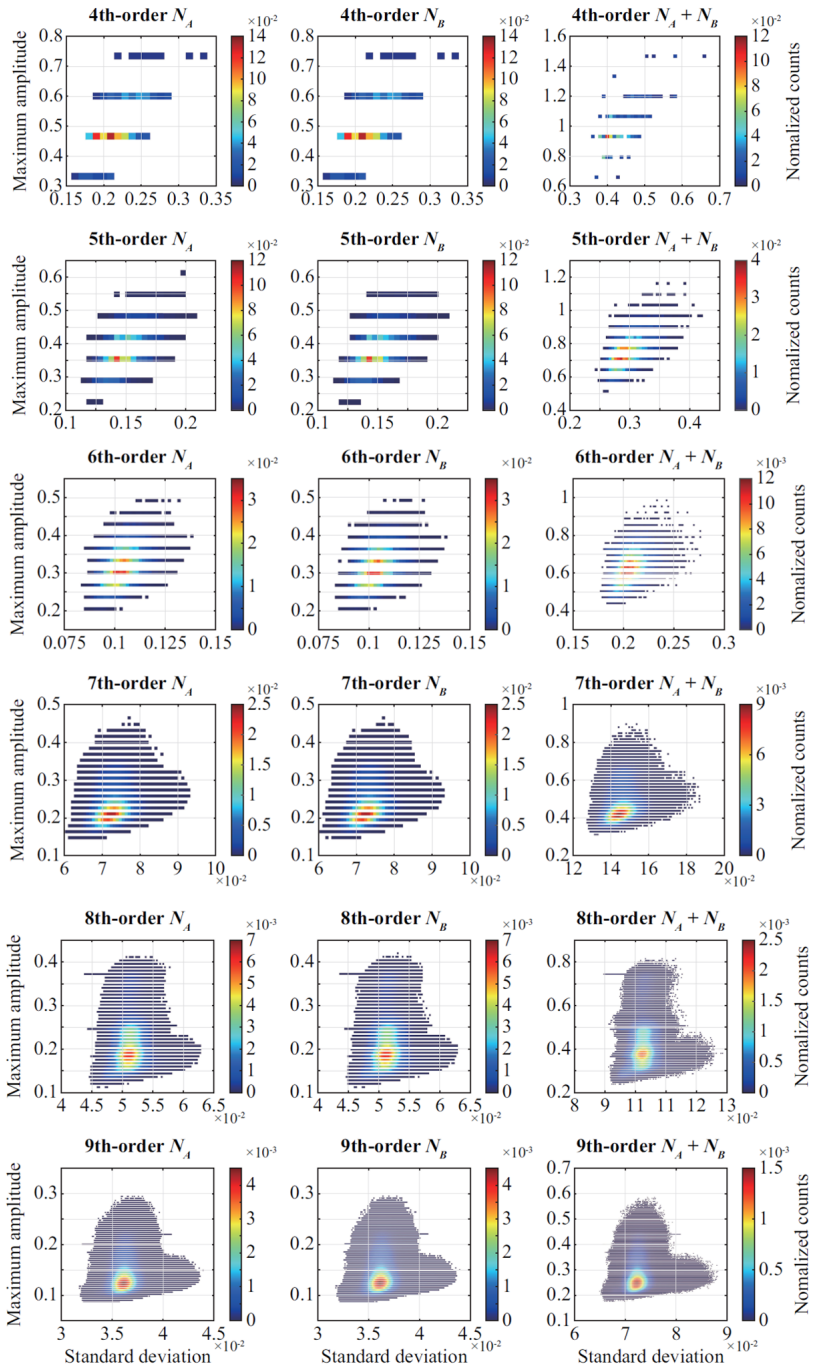

Figure 4.8: Distributions of maximum amplitudes and standard deviation of truncation noise and truncated interference noise from 4th to 9th order M-sequences.

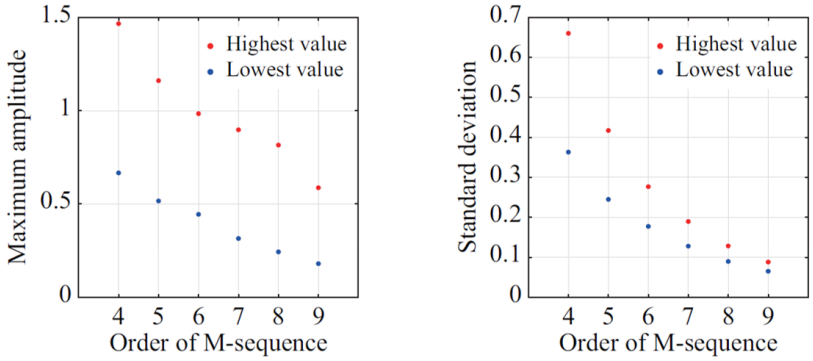

Figure 4.9: Highest and lowest values of maximum amplitudes and standard deviation of $N_A + N_B$ from 4th to 9th order M-sequences.

Table 4.4: Lowest values of maximum amplitudes of $N_A + N_B$ and lowest standard deviation of $N_A + N_B$ with lowest maximum amplitudes

Order	SP	PP (qPP)
4	0.667/0.180	-
5	0.516/0.218	0.516/0.211
6	0.444/0.147	0.444/0.152
7	0.315/0.105	0.315/0.105
8	0.243/0.074	0.259/0.075
9	0.180/0.052	0.180/0.054

deviation with the lowest maximum amplitude is also the lowest. In the 4th to 9th order M-sequence, there are two suitable combinations which are the same values of $N_A + N_B$.

SNRs of suitable M-sequence codes A and B are illustrated in Fig. 4.11. For comparison, the average SNR of all patterns of cross-correlation functions in each order is also indicated. SNRs could be improved from approximately 2.3 to 5.2 dB than averages of all patterns of codes in 4th order to 9th order M-sequence. Therefore, the selection of suitable combinations can suppress the SNR degradation of the proposed method in M-sequence pulse compression. The actual SNR of the proposed method is the smaller of this SNR for truncation noise and truncated interference noise and the typical SNR for environmental noise or

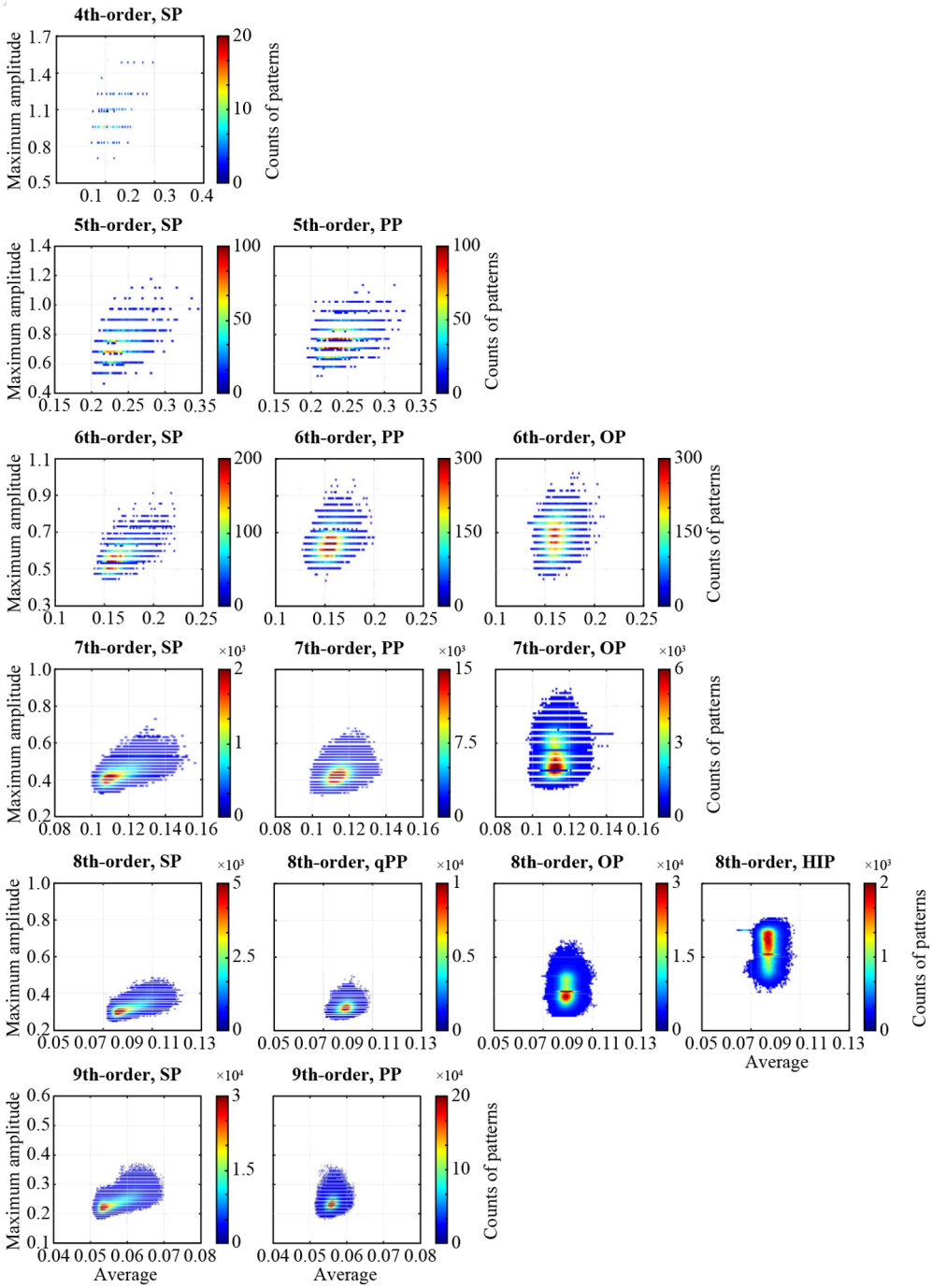

Figure 4.10: Distributions of maximum amplitudes and average values of N_A+N_B in each type of combination of M-sequences from 4th to 9th order M-sequence.

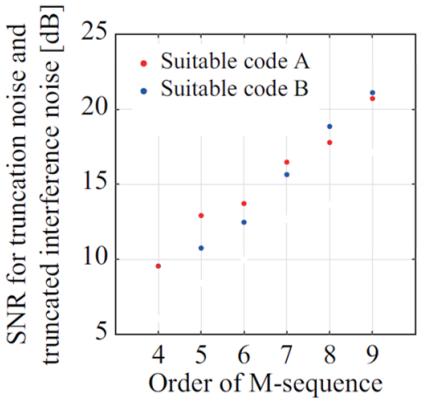

Figure 4.11: SNRs for truncation noise and truncated interference noise in suitable M-sequence codes A and B.

read-out noise. Finally, examples of the most suitable combinations of two M-sequence codes are presented. Suitable combinations are defined such that the maximum amplitude of $N_A + N_B$ is the lowest in all patterns and the standard deviation is the lowest in patterns with the lowest maximum amplitude. LFSRs to generate M-sequence codes and cross-correlation functions with each code in the 7th, 8th and 9th order are illustrated in Figs. 4.12 to 4.14.

4.2.2 Complex M-sequence signal

All patterns of truncation noise and truncated interference noise in the alternative transmission of phase-shifted complex M-sequences from 7th to 9th order were evaluated concerning their amplitudes of absolute cross-correlation functions. Absolute amplitudes were normalized by the correlation peak. Maximum amplitudes and average amplitudes of truncation and truncated interference noises are varied by combinations of M-sequences and their initial values. Furthermore, they are also varied by phase differences between complex M-sequences. In the proposed method, maximum amplitudes of absolute cross-correlation function A and B are both desirable to be lower. Therefore, the summation of maximum amplitudes (MA) and that of averages (AV) in both cross-correlation functions are investigated. The orders of M-sequences are investigated from 7th to 9th. The initial phases between both M-sequences are shifted from 0 to $11/6\pi$ by $1/6\pi$. There-

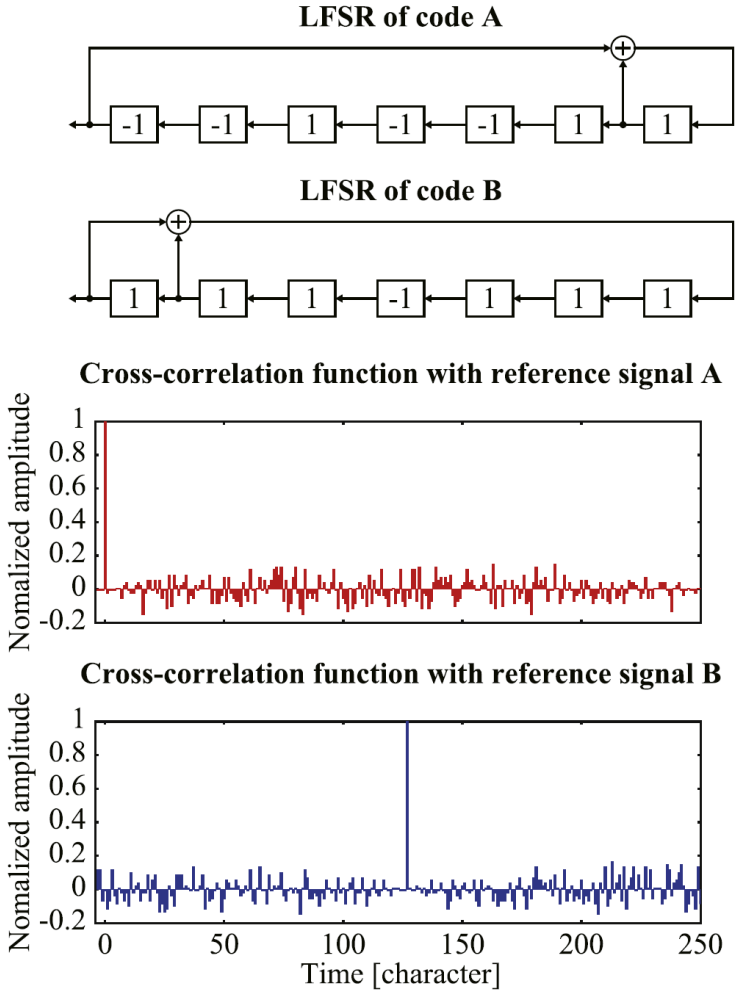

Figure 4.12: LFSRs to generate suitable combination of M-sequence codes and cross-correlation functions with each code in the 7th order.

fore, the number p of phase shifts is 12. In the combinations of preferred-pair M-sequences, there are cases both preferred-pair M-sequences are symmetric each other in two combinations. In the case of the noise patterns of M-sequence, each phase shift is also symmetrical. For example, noise patterns of one M-sequence combination in phase shift of $1/6\pi$ are the same as those of other M-sequence combinations in phase shift of $11/6\pi$. Therefore, the number, c of investigated combinations is half of all combinations of preferred-pair M-sequences. Noise patterns of one combination are varied by the initial values, l in each M-sequence. Therefore, all patterns of truncation and truncated interference noises in each-

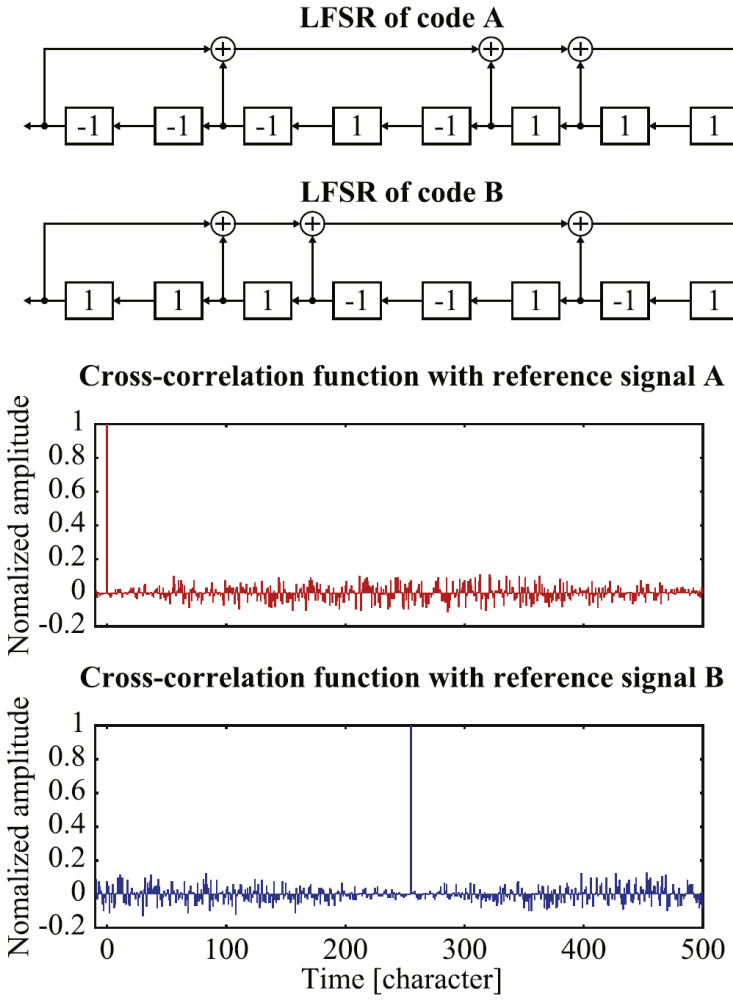

Figure 4.13: LFSRs to generate suitable combination of M-sequence codes and cross-correlation functions with each code in the 8th order.

order M-sequence is $p \times c \times l \times l$. The numbers of noise patterns in the alternative transmission of two different codes in phase-shifted complex M-sequences from 7th to 9th order are illustrated in Table 4.6. Distributions of MAs and AVs in each phase difference are illustrated in Fig. 4.15 to 4.17. Combinations of M-sequences are the symmetry-pair and preferred-pair in 7th to 9th order. The MA is shown on the ordinate; the AV is shown on the abscissa. Colors denote the count of patterns.

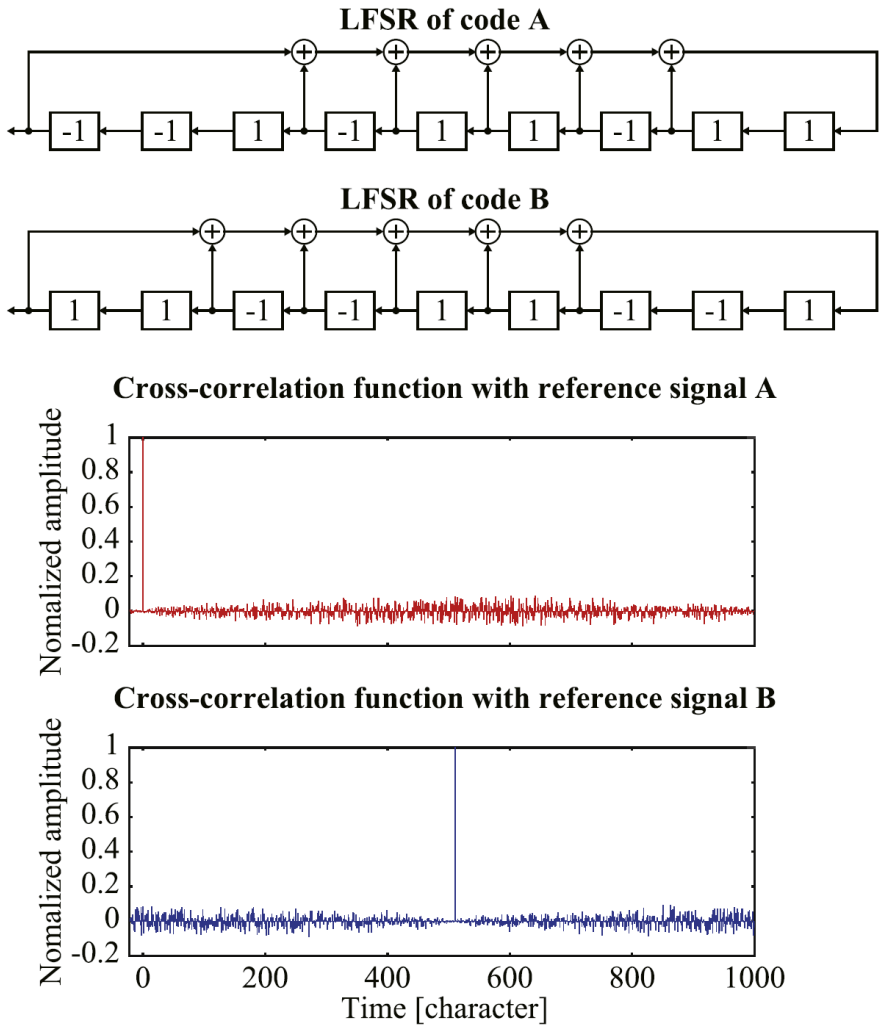

Figure 4.14: LFSRs to generate suitable combination of M-sequence codes and cross-correlation functions with each code in the 9th order.

In the M-sequence pulse compression, correlation peaks in the cross-correlation function are recognized as TOFs of targets. Therefore, the MA should be as lower as possible. Consequently, the suitable combination is a combination, in which the MA is the lowest and the AV with the lowest MA is also the lowest. Then, the lowest MAs, lowest AVs, and phase difference with each lowest MA are indicated in Table 4.7. Like those of the previous method, the MA and the AV of absolute cross-correlation functions in the integer M-sequence pulse compression are also

Table 4.5: Numbers of all patterns of the truncation noise and truncated interference noise in the alternative transmission of phase-shifted complex M-sequences from the 7th to 9th order

Order of M-sequence	Binary character, l	Combination of M-sequence	Analyzed combinations of M-sequence, c	Patterns of noise $p \times c \times l \times l$
7	127	SP: 9	SP: 9	1,741,932
		PP: 90	PP: 45	8,709,660
8	255	SP: 8	SP: 8	6,242,400
		PP: 16	qPP: 8	6,242,400
9	511	SP: 24	SP: 24	75,202,848
		PP: 288	PP: 144	451,217,088

Table 4.6: Lowest MAs, lowest AVs and phase differences with each lowest MA in truncation noise and truncated interference noise of complex M-sequences from 7th to 9th order

Order	SP			PP (qPP)			Integer M-seq.	
	MA	AV	α	MA	AV	α	MA	AV
7	0.2827	0.1187	90°/270°	0.2804	0.1224	270°	0.3150	0.1046
8	0.2109	0.0821	90°/270°	0.2362	0.0848	270°	0.2431	0.0735
9	0.1570	0.0584	90°/270°	0.1588	0.0617	270°	0.1800	0.0520

indicated. In the 7th order M-sequence, the lowest MA in PP was lower than that in SP. In the 8th and 9th order M-sequence, those in SP were lower than those in PP (qPP). In all cases, MAs are lowest when phase differences are 90° or 270°. In contrast, MAs are higher when phase differences are 0° or 180°. Furthermore, all MAs are lower than those of the previous method.

Hence, the SNR, the ratio of the correlation peak to the maximum amplitude of truncation noise and truncated interference noise, is defined to evaluate the noise suppression. The highest SNRs of cross-correlation functions A and B in 7th order to 9th order M-sequence are indicated in Table 4.8. SNRs were improved from 0.6 dB to 1.3 dB compared with the previous method. Therefore, selecting

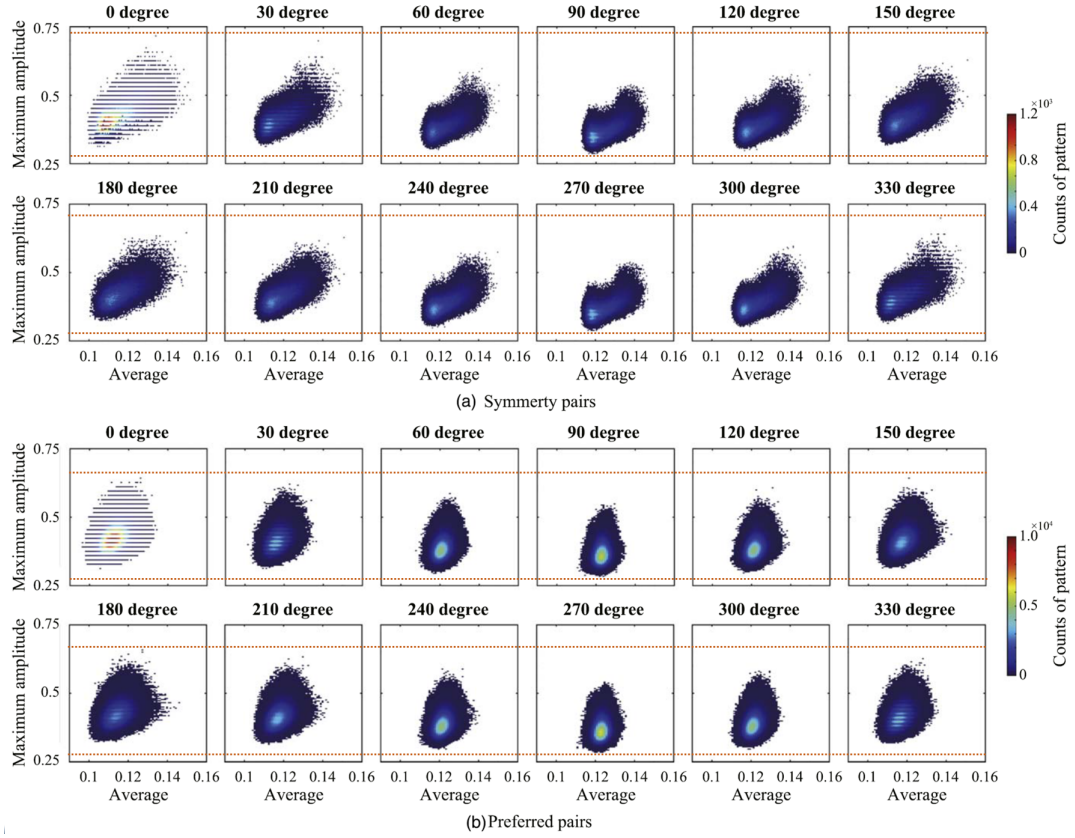

Figure 4.15: Distributions of MAs and AVs in truncation noise and truncated interference noise of 7th order complex M-sequences.

Table 4.7: Highest SNRs in the alternative transmission of phase-shifted complex M-sequences from 7th to 9th order

Order	Complex M-seq.				Integer M-seq.	
	Types	α	SNR_A	SNR_B	SNR_A	SNR_B
7	PP	270°	16.98 dB	17.75 dB	15.63 dB	16.50 dB
8	SP	90°/270°	19.70 dB	19.38 dB	18.86 dB	17.79 dB
9	SP	90°/270°	22.10 dB	22.09 dB	21.50 dB	21.50 dB

a suitable combination of complex M-sequences and phase differences could suppress truncation and truncated interference noises in the alternate transmission method. Truncation noise and truncated interference noise in the alternative transmission of phase-shifted complex M-sequences could be suppressed by se-

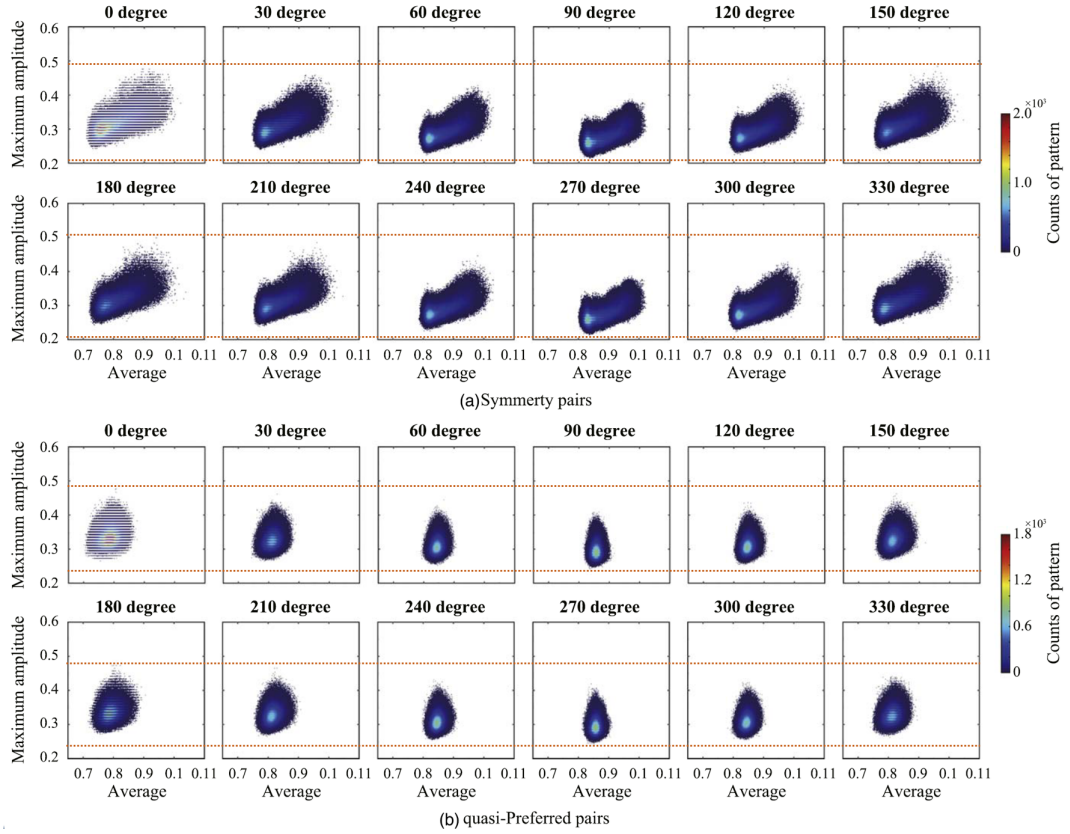

Figure 4.16: Distributions of MAs and AVs in truncation noise and truncated interference noise of 8th order complex M-sequences.

lecting a suitable combination and phase difference. In this section, how noise characteristics change by the phase difference and why the phase difference of 90° or 270° is better are discussed.

The variation of maximum amplitudes in truncation and truncated interference noises are investigated. Therefore, combinations whose MA in the phase difference of 0° are lowest, highest, and mean values are focused. Then, variations of their MA and AV by phase differences are illustrated in Fig. 4.18. Combinations of M-sequences are 7th order PP. Amounts of variation of MA are smaller or similar to differences of MA between lowest and mean values or mean and highest values in cases of the phase difference of 0°. Therefore, the selection of the M-sequences combination is also important to suppress truncation and

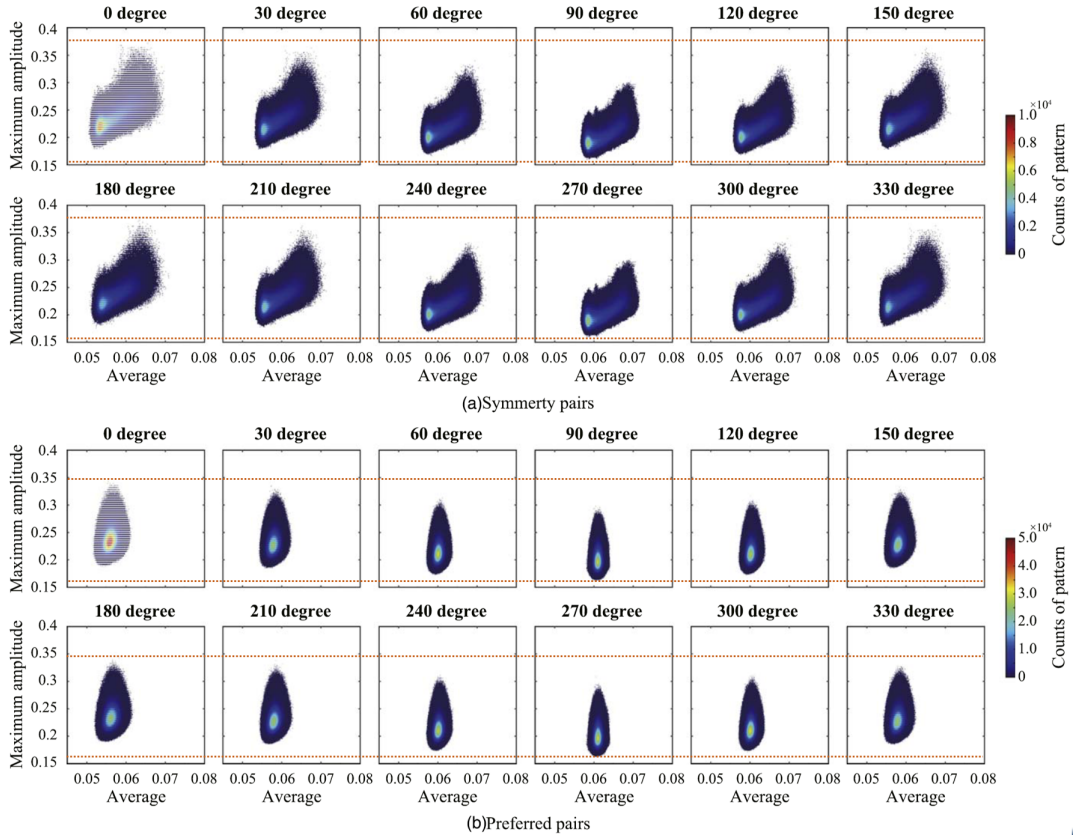

Figure 4.17: Distributions of MAs and AVs in truncation noise and truncated interference noise of 9th order complex M-sequences.

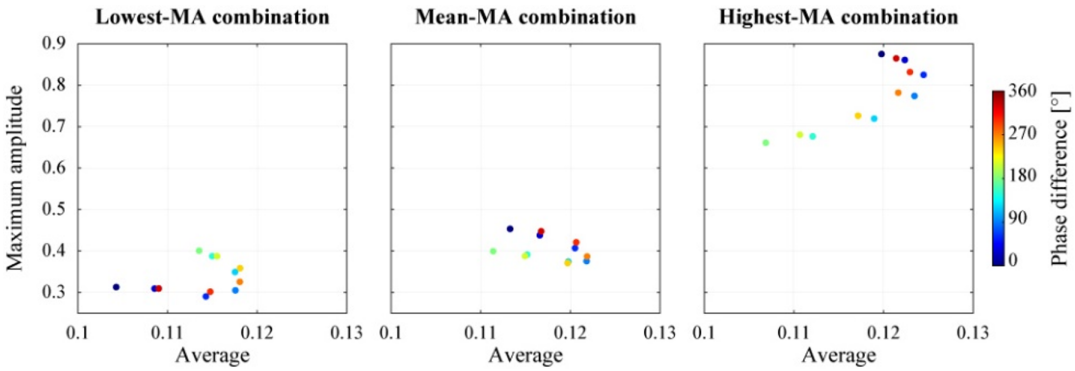

Figure 4.18: Variations of MA and AV in truncation and truncated interference noises by phase differences of PP combinations in 7th order M-sequence with lowest, mean and highest values of MA in the phase difference of 0°.

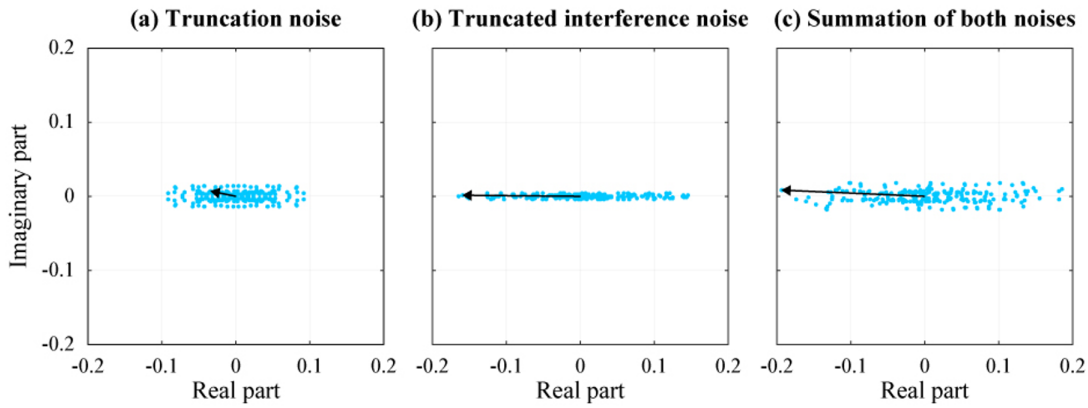

Figure 4.19: All data samples of the truncation noise of M-sequence B, the truncated interference noise of M-sequence A and B, the cross-correlation function B which is summed both noises in the phase difference of 0°.

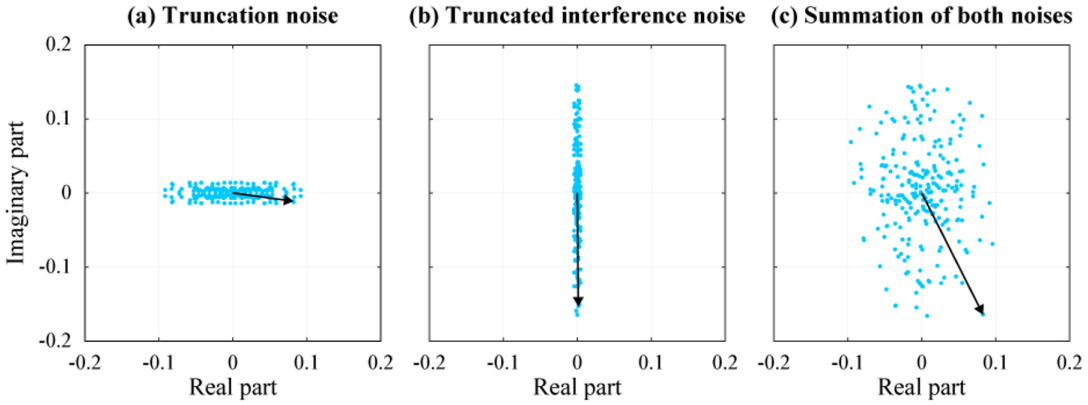

Figure 4.20: All data samples of the truncation noise of M-sequence B, the truncated interference noise of M-sequence A and B, the cross-correlation function B which is summed both noises in the phase difference of 90°.

truncated interference noises. However, MA of the lowest-MA combination in the phase difference of 90°, the lowest value in Fig. 4.18, is not the lowest MA in all combinations.

Then, reasons for noise-amplitude variation by the phase difference are investigated. In the alternative transmission method, truncation noise and truncated interference noise are fused. However, their noises are separately investigated in

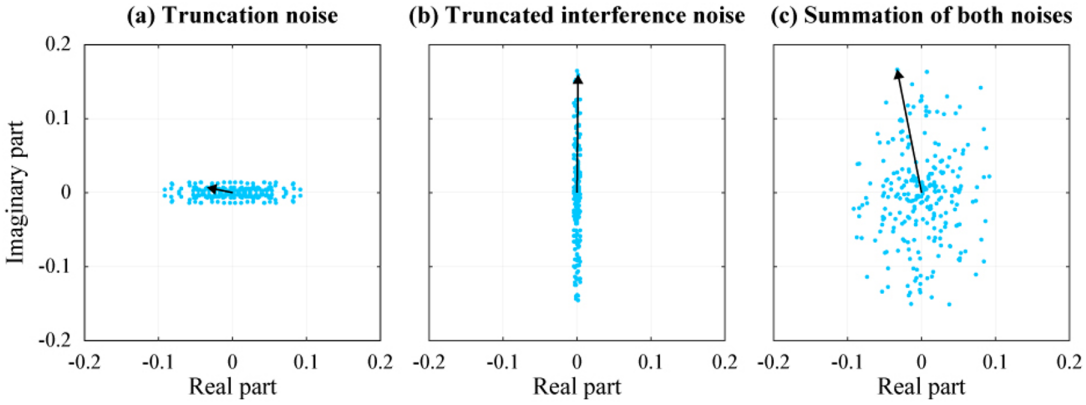

Figure 4.21: All data samples of the truncation noise of M-sequence B, the truncated interference noise of M-sequence A and B, the cross-correlation function B which is summed both noises in the phase difference of 270°.

this section. All data samples in the complex plane of the truncation noise of M-sequence B, the truncated interference noise of M-sequence A and B, the cross-correlation function B which is summed both noises in the phase difference of 0° of Fig. 4.18 are illustrated in Fig. 4.19. The sample of the maximum amplitude of the absolute cross-correlation function and samples in the truncation noise and the truncated interference noise, which constitute the maximum-amplitude sample, are also indicated. All samples are horizontally distributed. In cases matched characters are much than unmatched characters in the cross-correlation, samples are distributed on the right side in the truncation noise or truncated interference noise. In opposite cases, samples are distributed on the left side. Moreover, all data samples of the truncation noise, the truncated interference noise, the cross-correlation function in the phase difference of 90° and 270° of Fig. 4.18 are also illustrated in Fig 4.20 and 4.21. Even if the phase of the M-sequence B was shifted, samples in the truncation noise do not vary because the cross-correlation is complex conjugation. In the case of the truncated interference noise, the absolute amplitude of each sample also does not vary as well. However, the distribution rotates by the phase difference. Therefore, the distribution of the cross-correlation function varies and the phase difference around 90° or 270° can effectively suppress truncation and truncated interference noises.

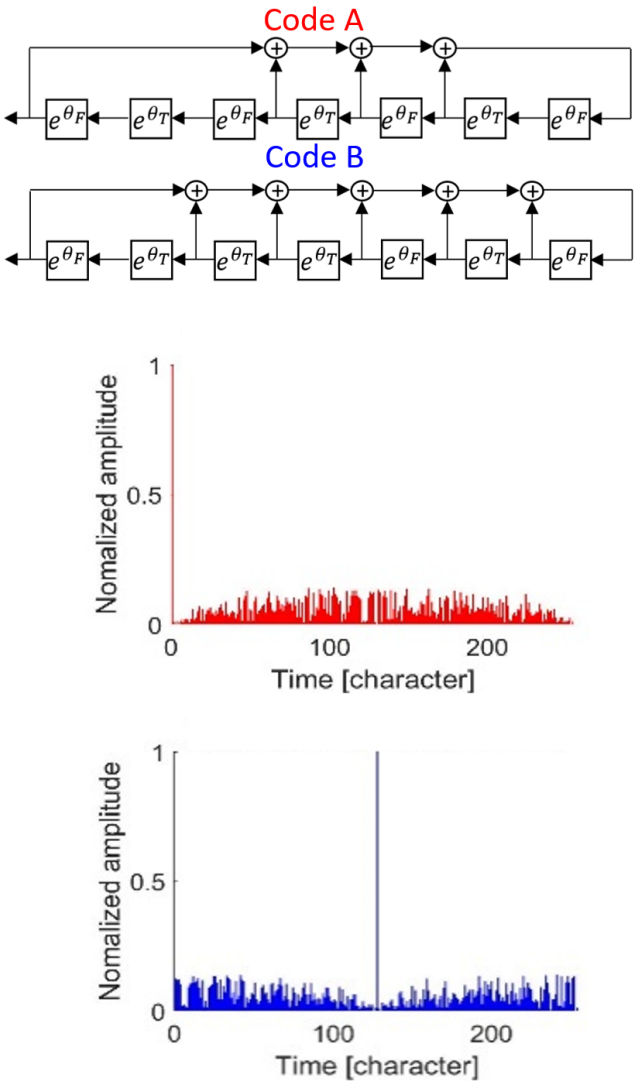

Figure 4.22: LFSRs to generate suitable combination of complex M-sequence codes and cross-correlation functions with each code in the 7th order and phase difference of 90°.

Lastly, the suitable combination of two different codes in the complex M-sequence is indicated as an example. LFSRs to generated complex M-sequence and absolute of the cross-correlation functions with each reference signal in the 7th order to 9th order are indicated in Fig. 4.22 to 4.24.

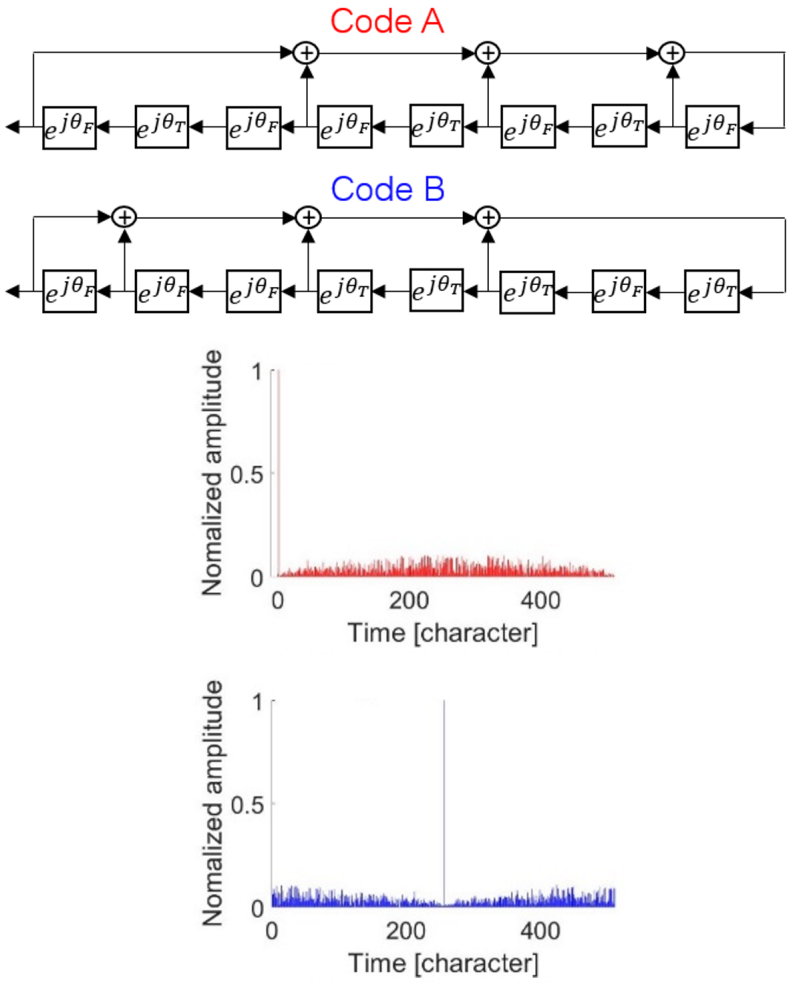

Figure 4.23: LFSRs to generate suitable combination of complex M-sequence codes and cross-correlation functions with each code in the 8th order and phase difference of 90°.

4.3 Maximum noise amplitude comparison

In the LFM and M-sequence simulation of the proposed method, truncation and truncated interference noises are evaluated. The length of LFM to evaluate is the same as the length of 35 kHz of 7th order, 8th order, and 9th order M-sequence signal for comparing noise characteristics. In the comparison results, the maximum amplitude and average value of the noise are indicated in Fig. 4.25. 30 kHz to 40 kHz and 40 kHz to 30 kHz of LFM signal are simulated

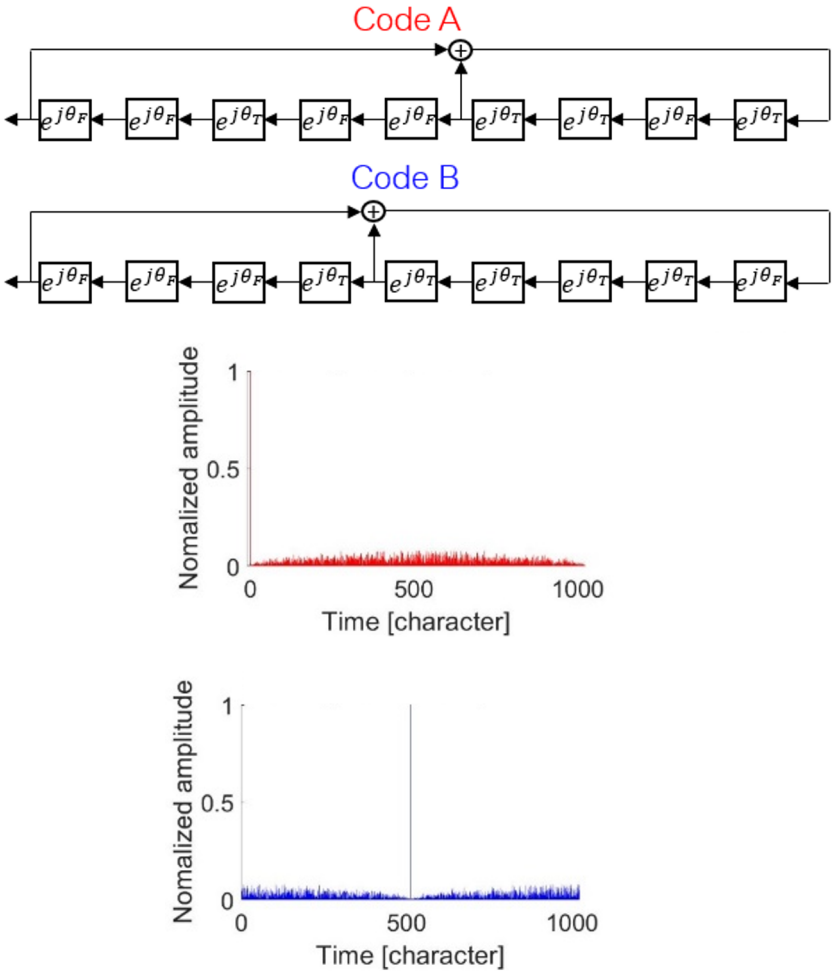

Figure 4.24: LFSRs to generate suitable combination of complex M-sequence codes and cross-correlation functions with each code in the 9th order and phase difference of 90°.

in the alternate transmission method to compare maximum amplitude with M-sequence signal. As a result, the lowest value of the maximum amplitude of noise is selected from a complex M-sequence signal. However, in the LFM signal, the larger bandwidth is more improved SNR in the correlation processing. There is depending on the performance of the loudspeaker to generate the LFM signals. Moreover, SNR of LFM signal and M-sequence signal is indicated in Fig. 4.26. In 29.20 ms of signal length, the highest SNR of the complex M-sequence is selected. Lastly, truncation and truncated interference noise characteristics in the cross-

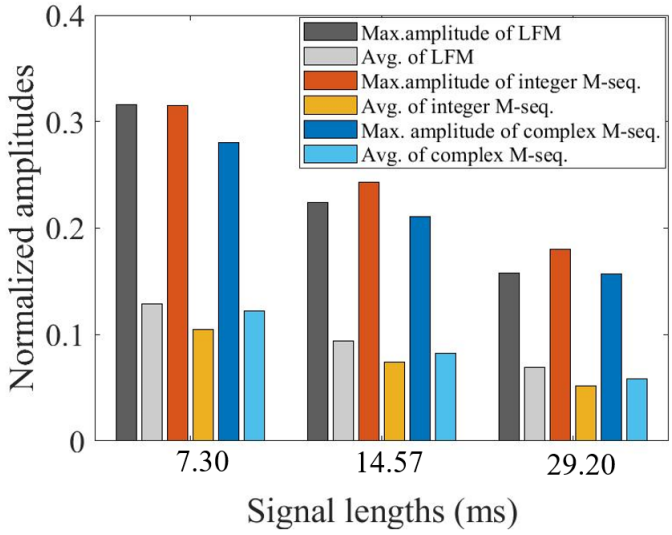

Figure 4.25: Lowest MA, N_A+N_B and average value in truncation and truncated interference noise comparison between LFM signal and M-sequence signal.

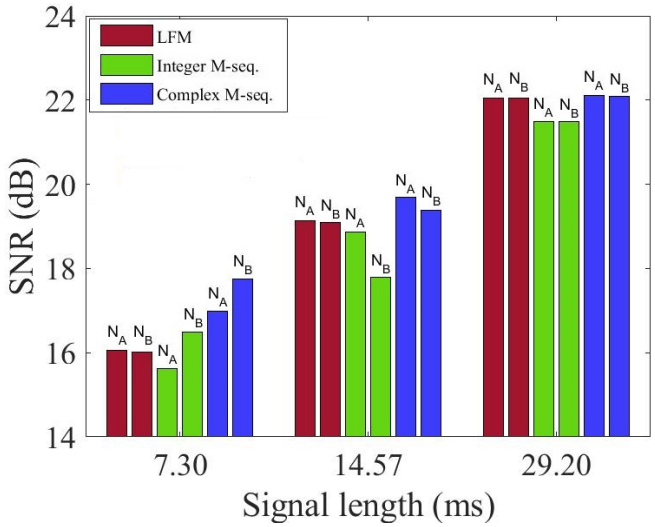

Figure 4.26: SNR in truncation and truncated interference noise comparison between LFM signal and M-sequence signal.

correlation function among alternate LFM signal (30 kHz to 40 kHz and 40 kHz to 30 kHz), alternate integer M-sequence and alternate complex M-sequence is compared as indicated in Fig. 4.27.

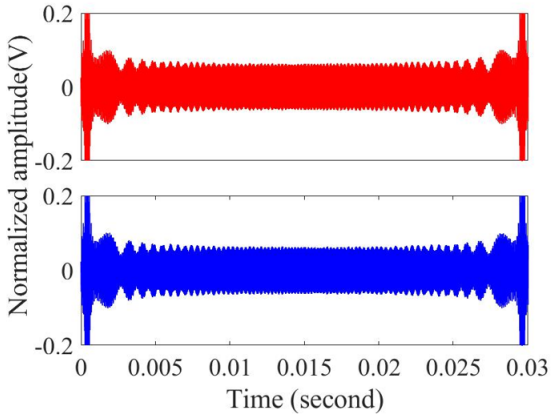

(a) Alternate LFM signal, 30 kHz to 40 kHz and 40 kHz and 30 kHz

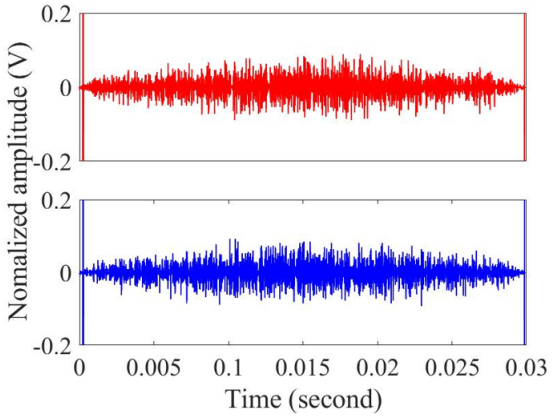

(b) Alternate integer M-sequence signal

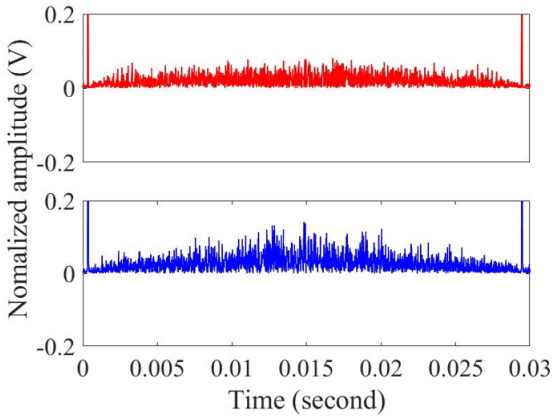

(c) Alternate complex M-sequence signal

Figure 4.27: Truncation and truncated noise characteristic comparison.

Chapter 5

Experiment of noise amplitude evaluations

In the simulation of alternate transmission signals, a suitable combination of M-sequence and 14.6 ms of LFM length are selected for generating. However, three cycles for one digit of M-sequence signal and 43.8 ms of LFM length are selected to be transmitted signal in the experiment. It has been the lowest noise amplitude by the cross-correlation functions. 30 kHz to 40 kHz and 40 kHz to 30 kHz of LFM signal are generated to evaluate maximum noise amplitude by the cross-correlation functions. Moreover, 35 kHz of carrier frequency in the conventional M-sequence method and the alternate transmission of M-sequence signal are generated in the experiment as an example.

5.1 Experiment configuration

In the experiments, the proposed method is verified based on distance measurement. The received signal is anticipated that the reflected signal of the target includes the background noises and reverberation components. However, the environmental noise can reduce by using cross-correlation functions. The suppression of the truncation and truncated interference noises in alternate transmission was verified based on distance measurement experiments. The limit of distance measurement depends on a measurable distance, which is related to the transmission signal length to be transmitted. The experimental setup is used

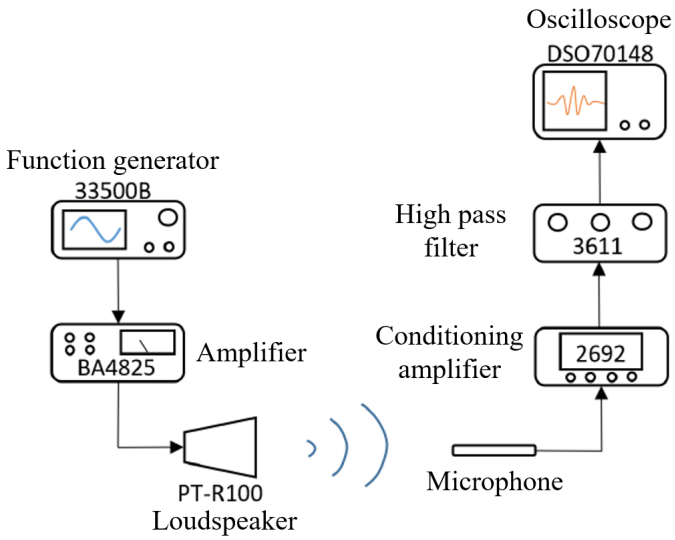

Figure 5.1: Setup of electronic devices in the experiment.

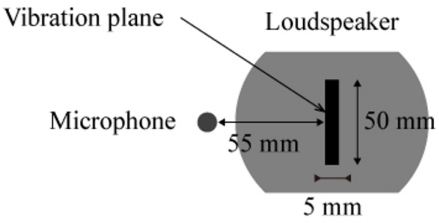

Figure 5.2: Front view of loudspeaker and microphone.

one loudspeaker (Pioneer, PT-R100) and one microphone (B&K, Type 4939 and 2670) were placed 1.00 m above the floor. The installation of an electronic device in the experiment is indicated in Fig. 5.1. Function generator (33500B) is used to generated transmitted signals to amplifiers (BA4825). The impedance of the amplifier is 50 Ohm. The output of the amplifier is connected to a loudspeaker (PT-R100). This section is a transmission signal part. Then, a microphone is used to receive an echo signal. There is connected to a conditioning amplifier (2692), high pass filter (3611), and oscilloscope (DSO70148), respectively. The experimental setup is used one loudspeaker and one microphone were placed 1.00 m above the floor. Loudspeaker and microphone installation is indicated in Fig. 5.2.

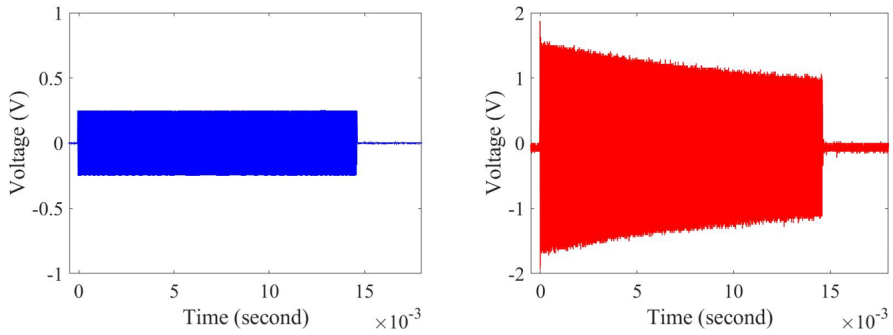

(a) (b)

Figure 5.3: Transmitted signal (a) and input voltage signal of loudspeaker (b).

5.2 LFM signal

In the case of the LFM transmission signal, the larger bandwidth of the LFM signal cannot be transmitted by our loudspeaker because of loudspeaker performance limitations. Therefore, the researcher has to check the performance of the loudspeaker first. In this experiment, 30 kHz to 40 kHz and 40 kHz to 30 kHz are selected to transmit in the alternate LFM signal. LFM length for one-code transmission is 14.6 milliseconds and 0.5 Vpp of LFM signal was transmitted to the amplifier. The gain and impedance of the amplifier were 10 times and 50 Ohm respectively. The output of the conditioning amplifier was 1 V/Pa. The received signals were received through a high-pass filter of 1 kHz and recorded at a sampling frequency of 5 MHz. The transmitted signal and input voltage signal from the loudspeaker in the experiment are indicated in Fig. 5.2. The stable amplitude of the transmitted signal is applied by the function generator. However, the amplitude of the input voltage signal by the loudspeaker is unstable. Therefore, a new LFM signal is generated to be transmitted signal. The new LFM signal is made from the inverse amplitude of the input voltage signal by MATLAB as indicated in Fig. 5.4. The sampling point for one sinewave is 57. The sweep frequency of the new LFM signal is 30 kHz to 40 kHz.

In the alternate transmission of the LFM signal, the center frequency of the ultrasound was 35 kHz and transmitted signal was 30 kHz to 40 kHz and 40 kHz

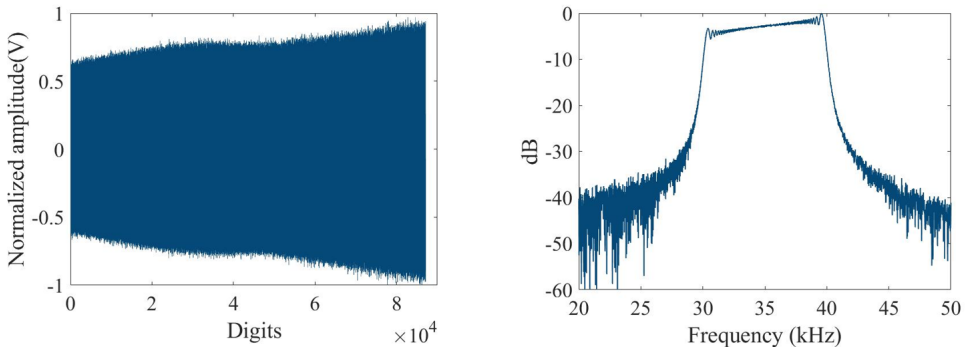

Figure 5.4: New LFM signal in time domain and frequency domain.

to 30 kHz of alternate LFM signals are transmitted signals. The length of linear frequency modulation was 43.8 millisecond to compare with three cycles for one digit of 35 kHz of 9th order M-sequence signal. The transmitted signals of 0.5 Vpp were applied by the function generator. The gain and impedance of the amplifier were 10 times and 50 Ohm respectively. The output of the conditioning amplifier is 1 V/Pa. The received signals were received through a high-pass filter of 1 kHz, AC mode, and the gain of HPF was 0 dB. Moreover, recorded data at a sampling frequency was 2 MHz. Transmitted signal, input voltage signal, and received signal in the experiment are indicated in Fig. 5.5. In the cross-correlation function of alternate transmission of LFM signal, three sequences of alternate transmission in a new LFM signal (up-chirp and down-chirp) are applied by the function generator to get a stable amplitude of the input voltage signal. Then, a received signal is correlated with the constant amplitude of LFM signal A and B, respectively. The cross-correlation signal with reference signals A and B in the time domain and the frequency domain are indicated in Fig. 5.6. In the proposed method, a measurable distance by the cross-correlation function is extended. However, the reflected echo of some targets appears in the correlation signals. It is fused with truncation and truncated interference noise. Moreover, noise characteristics by cross-correlation function between the experimental result and the simulation result are compared as indicated in Fig. 5.7.

As a result, the maximum amplitude of the noise is investigated by the ab-

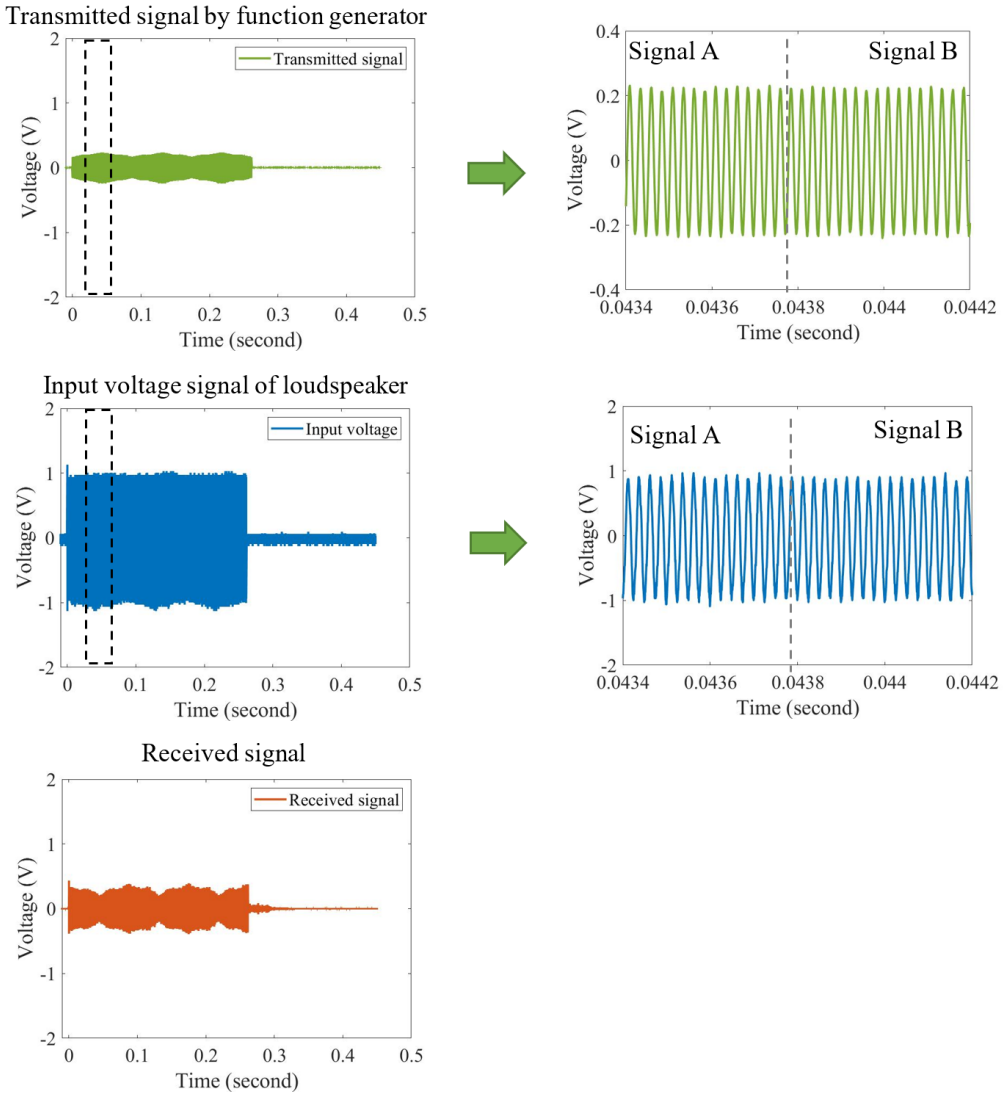

Figure 5.5: Alternate transmission of LFM signal from the experiment.

solute value of the cross-correlation function. The maximum amplitude of noise comparison between the simulation and experiment is indicated in Table 5.1. N_A + N_B of the experiment is more than the simulation. In the experimental results, both correlation signals are included background noise, reverberation noise, etc. Moreover, SNR evaluation from each correlation signal is indicated in Table 5.2. SNR_A in the experiment is a little better than SNR_B about 0.04 dB.

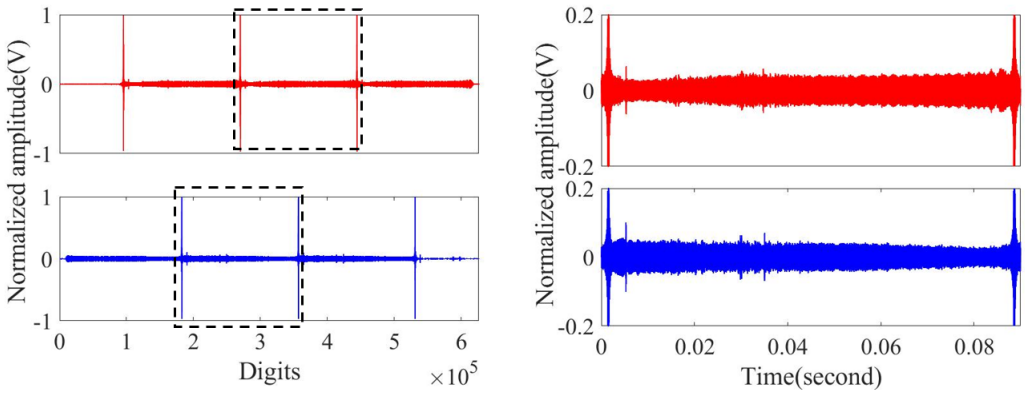

(a) Cross-correlation function with reference signal A (above) and B (below)

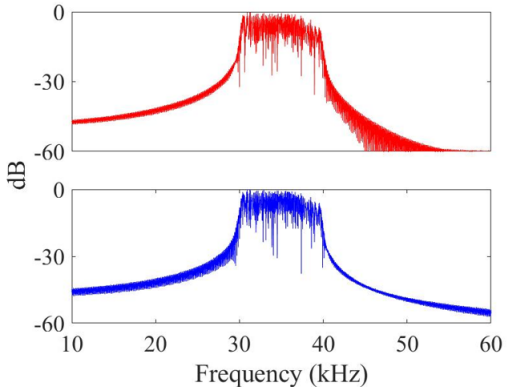

(b) Spectrum of correlation signal

Figure 5.6: Obtain cross-correlation function in time domain (a) and frequency domain (b).

Table 5.1: Maximum amplitude of noise comparison between the simulation and the experiment.

Truncation and truncated interference noise	Simulation			Experiment		
	N_A	N_B	$N_A + N_B$	N_A	N_B	$N_A + N_B$
N_B	$N_A + N_B$					
Maximum amplitudes	0.0461	0.0461	0.0922	0.0579	0.0576	0.1155
Average	0.0206	0.0206	0.0412	0.0242	0.0204	0.0446

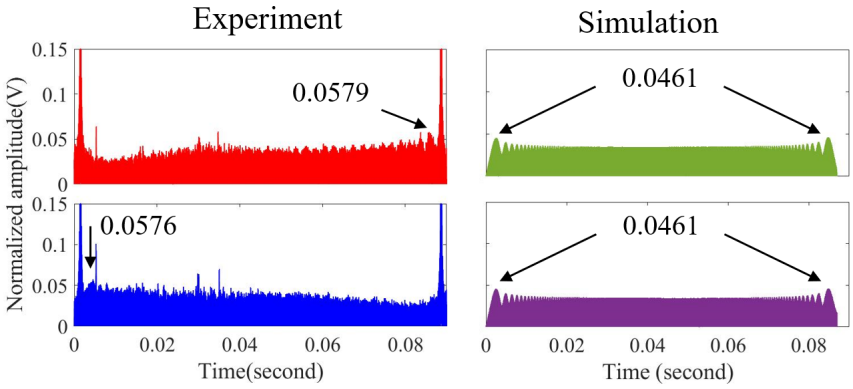

Figure 5.7: Maximum noise amplitude comparison between the experimental result and the simulation result of LFM signal.

Table 5.2: SNRs comparison of alternate transmission of LFM signal between the simulation and the experiment.

Signals	SNR_A	SNR_B
Experiments	24.75 dB	24.79 dB
Simulations	26.73 dB	26.73 dB

5.3 M-sequence signal

5.3.1 Integer M-sequence signal

In this experiment of M-sequence, the suitable combination of 9th order M-sequence is generated to be transmitted signal. Carrier frequency is 35kHz. The gain and impedance of the amplifier were 10 times and 50 Ohm respectively. The output of the conditioning amplifier was 1 V/Pa. The received signals were received through a high-pass filter of 1 kHz, AC mode of HPF, and 0 dB for the gain of HPF. Moreover, recorded data at a sampling frequency was 2 MHz.

In the integer M-sequence modulation, the sinusoid waves are modified by the binary character of M-sequence codes. The initial phase of sinusoid waves is assigned to 0 and -π. Three cycles of alternate transmission of signal A and signal B with 0.45 of Tukey window as indicated in Fig.5.8 is transmitted signal in the experiment. The integer M-sequence signal is generated by the function

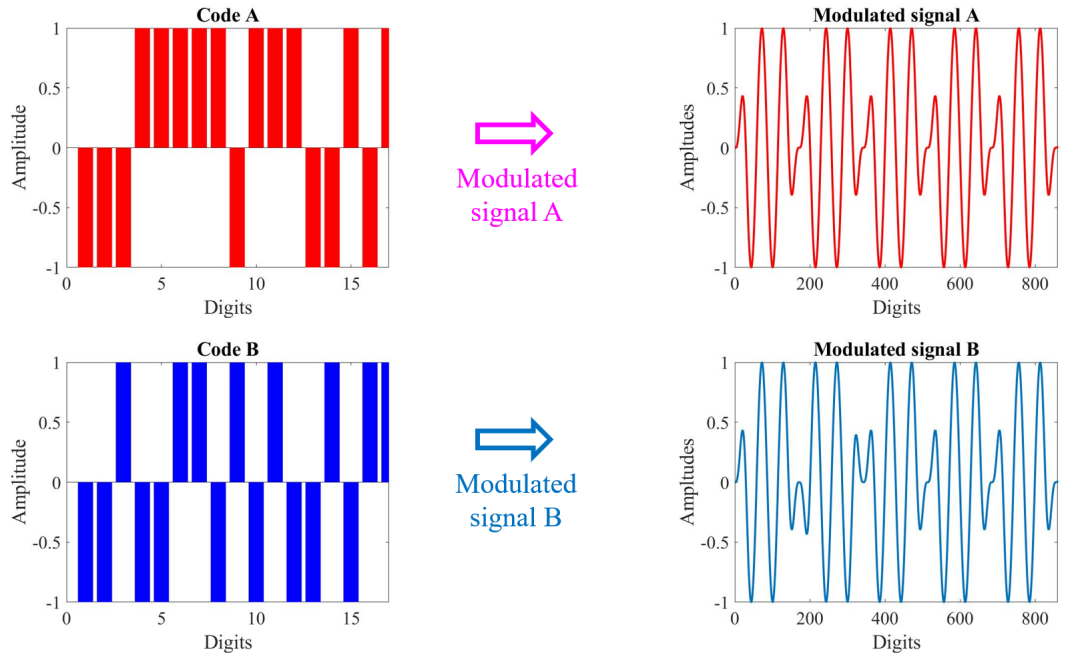

Figure 5.8: Modulated integer M-sequence signal A and B in three cycles for one digit with 0.45 of Tukey window.

generator and transmitted by the loudspeaker. The transmitted signal, input voltage signal, and received signal of integer M-sequence are indicated in Fig. 5.9. The number of characters in the alternate transmission of the 9th order M-sequence code is 1022. Therefore, the length of three cycles for one digit of 9th order M-sequence is 43.8 ms. In the cross-correlation function, the received signal is correlated with each reference signal to be obtained the correlation signal A and B as indicated in Fig. 5.10. In the proposed method, a measurable distance by the cross-correlation function is extended without degraded temporal resolution. One window of the cross-correlation function is focused on. Truncation and truncated interference noise appear. Therefore, the maximum amplitude of these noises is investigated by the absolute value of the correlation signal. Moreover, the average of these noises is calculated from the absolute values of the Hilbert transform. Moreover, noise characteristics from the experiment and the simulation are compared as indicated in Fig. 5.11. The maximum amplitude of noise and average values comparison is indicated in Table. 5.3. Furthermore, SNR val-

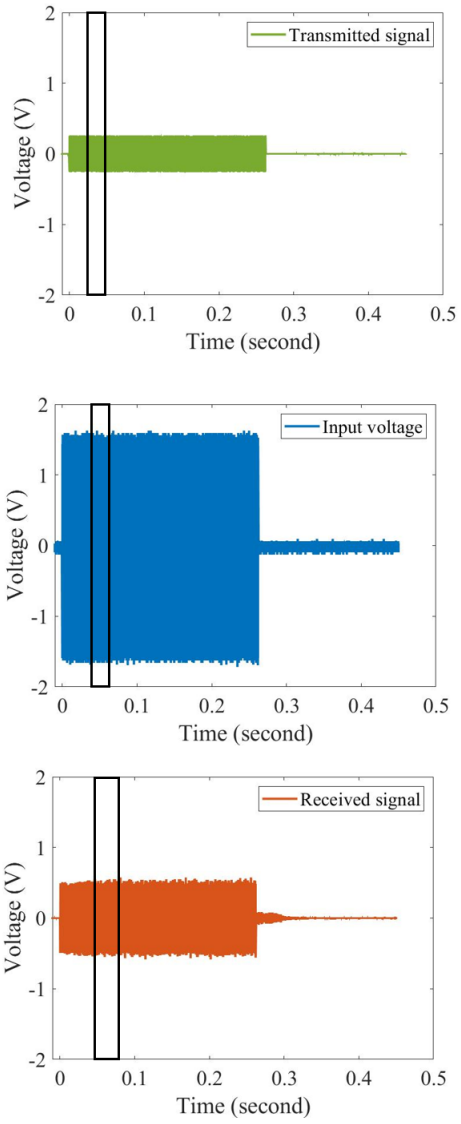

(a) Three cycles of alternate transmission signals

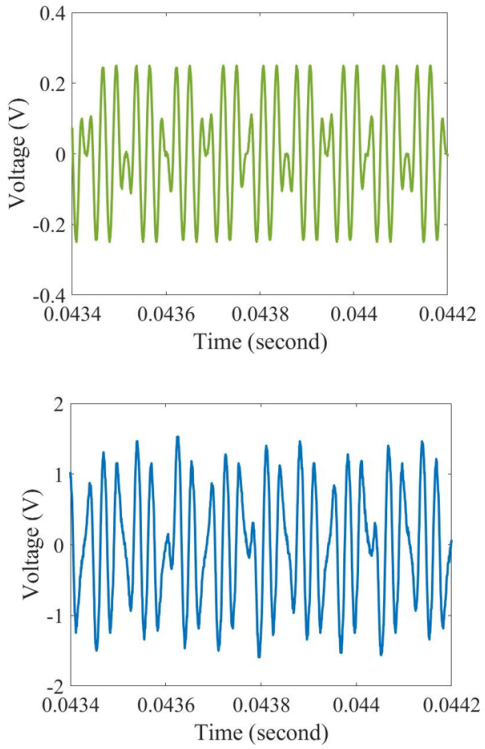

(b) Close-up to indicate character of signals

Figure 5.9: Alternate transmission of integer M-sequence signal in the experiment.

ues in each correlation signal are indicated in Table 5.4. SNR_A in the experiment is a little better than SNR_B about 0.13 dB.

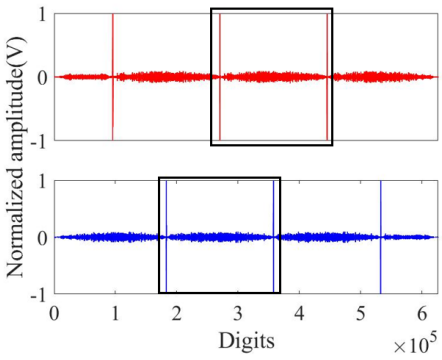

(a) Correlation signal A and B

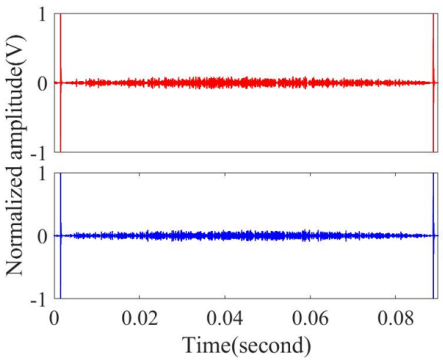

(b) One window of correlation signal A and B

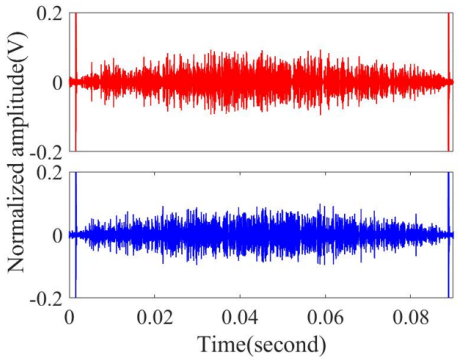

(c) Noise characteristics of correlation signal A and B

Figure 5.10: Obtain cross-correlation function of integer M-sequence signal.

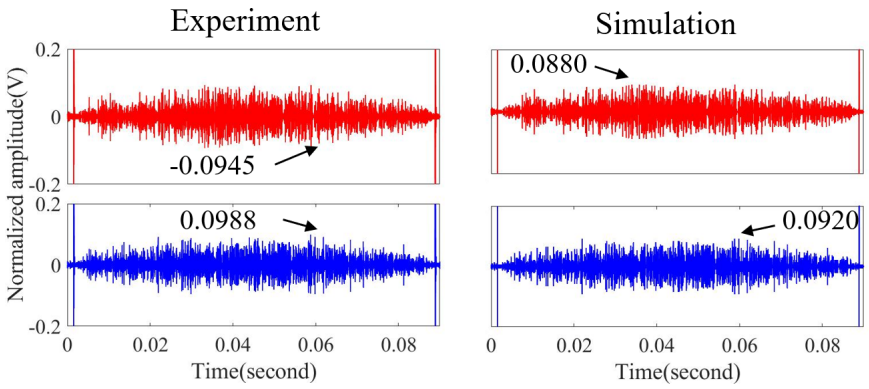

Figure 5.11: Maximum noise amplitude comparison between the experimental result and the simulation result of the integer M-sequence.

Table 5.3: Absolute value of maximum amplitude of noise comparison between the simulation and the experiment in the integer M-sequence signal.

Truncation and truncated interference noise	Simulation			Experiment		
	N_A	N_B	$N_A + N_B$	N_A	N_B	$N_A + N_B$
Maximum amplitudes	0.0880	0.0920	0.1800	0.0945	0.0988	0.1933
Average	0.0186	0.0190	0.0376	0.0218	0.0223	0.0441

Table 5.4: SNRs comparison of integer M-sequence between the simulation and the experiment.

Signals	SNR_A	SNR_B
Experiments	20.49 dB	20.10 dB
Simulations	21.11 dB	20.72 dB

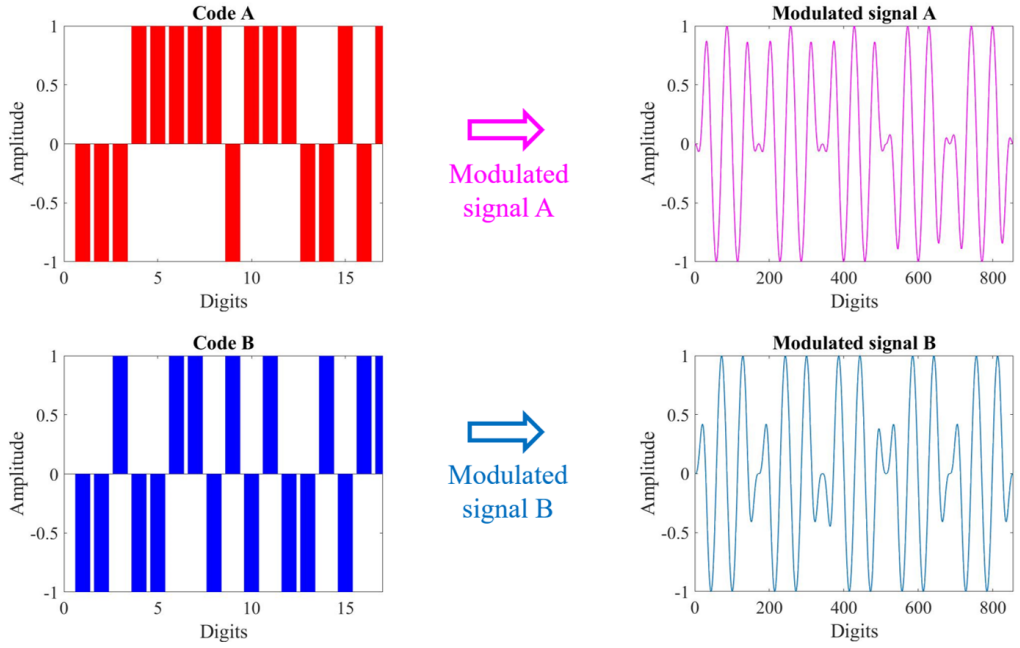

Figure 5.12: Modulated complex M-sequence signal A and B in three cycles for one digit with 0.45 of Tukey window.

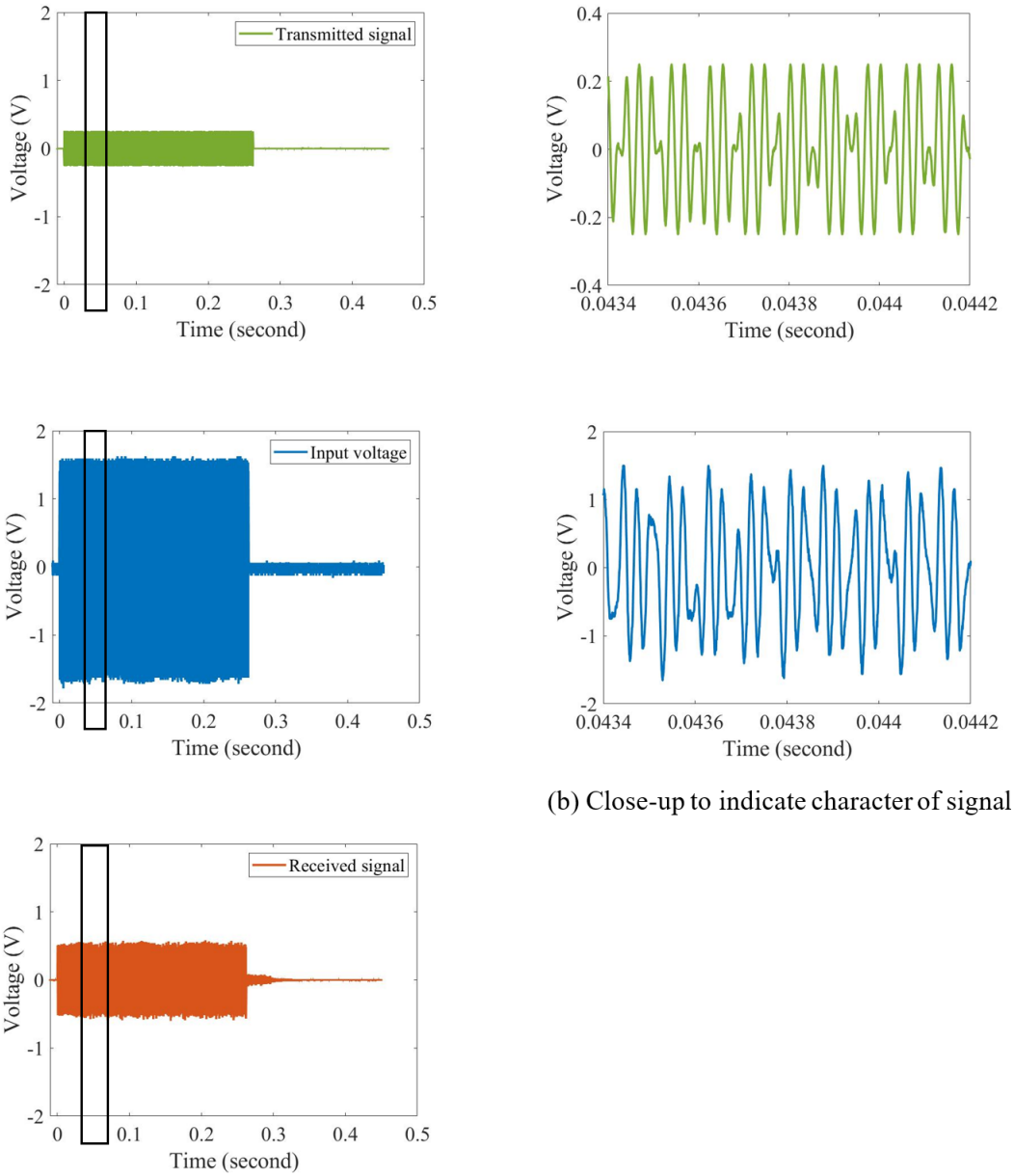

(a) Three cycles of alternate transmission signals

(b) Close-up to indicate character of signal

Figure 5.13: Alternate transmission of complex M-sequences signal in the experiment.

5.3.2 Complex M-sequence signal

In the alternate transmission method of complex M-sequences, $e^{j(\omega t+\theta_L)}$ and $e^{j(\omega t-\theta_L)}$ were assigned to binary characters in the M-sequence A, and $e^{j(\omega t+\theta_L+\frac{\pi}{2})}$

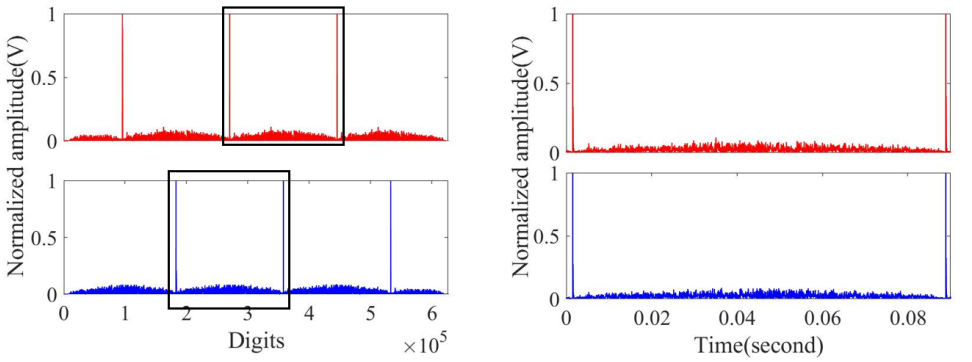

(a) Correlation signal A and B (b) One window of correlation signal A and B

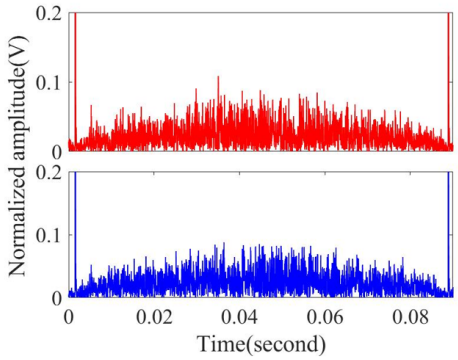

(c) Noise characteristics of correlation signal A and B

Figure 5.14: Obtained absolute cross-correlation functions in the alternate transmission of complex M-sequences.

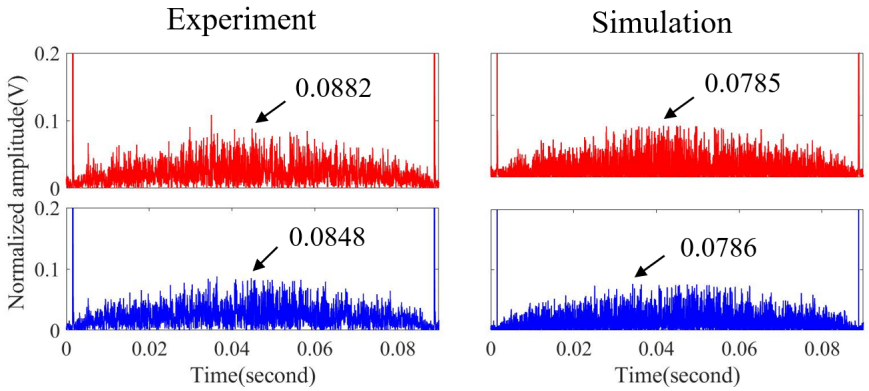

Figure 5.15: Maximum noise amplitude comparison between the experimental result and the simulation result of the complex M-sequence.

and $e^{j(\omega t-\theta_L+\frac{\pi}{2})}$ were assigned to those in the M-sequence B. The integer M-sequences, $e^{j(\omega t)}$ and $e^{j(\omega t+\pi)}$ were assigned to those in M-sequences A and B. The real parts of the M-sequence modulated signals were transmitted. Then, received signals were Hilbert transformed to complex signals. The reference signals were discrete M-sequences, that is $e^{j\omega_L}$ and $e^{-j\omega_L}$, $e^{j(\theta_L+\frac{\pi}{2})}$ and $e^{j(-\theta_L+\frac{\pi}{2})}$, e^0 (=1) and $e^{j\pi}$ (=-1), and with consecutive zeros between them. Subsequently, the transformed received signals were correlated with each reference signal. In the experiment, three cycles for one digit of complex M-sequence signal with r=0.45 of Tukey window is applied to be transmitted signal. A Tukey window is rectangular with the first and last percent of $r/2$ in the sample equal to the part of the cosine. r is a real number between 0 and 1. The sampling point for one sinewave is 57. Carrier frequency is 35 kHz. Modulation signals A and B from M-sequence codes are indicated in Fig. 5.12. Transmitted signal, input voltage signal, and received signal from the experiment are indicated in Fig. 5.13.

The obtained absolute cross-correlation functions in the alternate transmission of complex M-sequences are illustrated in Fig. 5.14. Both noise shapes appear similar, although there is a fluctuation in the correlation values. Maximum peak amplitude is indicated as a reflected echo of the target. There are not peak amplitude of truncation and truncated interference noise. Therefore, a researcher is ignored it to investigate maximum amplitude. In the complex M-sequence, the maximum amplitudes of truncation and truncated interference noises in absolute cross-correlation functions A and B were 0.0882 and 0.0848 as indicated in Table 5.5. Moreover, noise characteristics from the experiment and the simulation are indicated in Fig. 5.15. The SNRs of cross-correlation functions A and B of the 9th order complex M-sequence are presented in Table 5.6. For comparison, the SNRs of integer M-sequences are also indicated. In the experiments, the SNRs degraded by approximately 1.4 dB from the simulations. Moreover, SNR_A is more than SNR_B in the experiment is approximately 0.22 dB. However, the SNRs in the complex M-sequence signal are slightly higher than those in the integer M-sequence signal.

Table 5.5: Absolute value of maximum amplitude of noise comparison between the simulation and the experiment in the complex M-sequence signal.

Truncation and truncated interference noise	Simulation			Experiment		
	N_A	N_B	$N_A + N_B$	N_A	N_B	$N_A + N_B$
Maximum amplitudes	0.0785	0.0786	0.1571	0.0882	0.0848	0.1730
Average	0.0224	0.0215	0.0440	0.0228	0.0232	0.0460

Table 5.6: SNRs comparison of complex M-sequence between the simulation and the experiment.

Signals	SNR_A	SNR_B
Experiments	21.09 dB	21.43 dB
Simulations	22.10 dB	22.09 dB

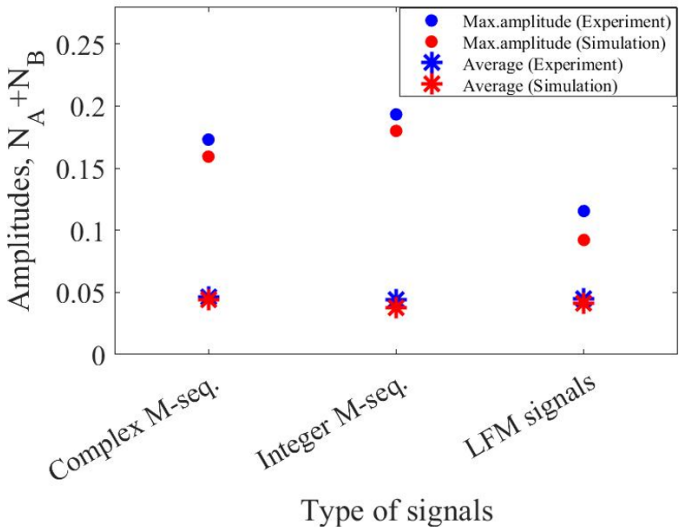

Figure 5.16: Summation, $N_A + N_B$ of maximum noise amplitude and average of each signals between experiments and simulations

5.4 Maximum noise amplitude comparison

This chapter is indicated that the maximum noise amplitude between the simulation and the experiment is different. In the experimental results, the maximum amplitude and average from the experiment are higher than the simulation as

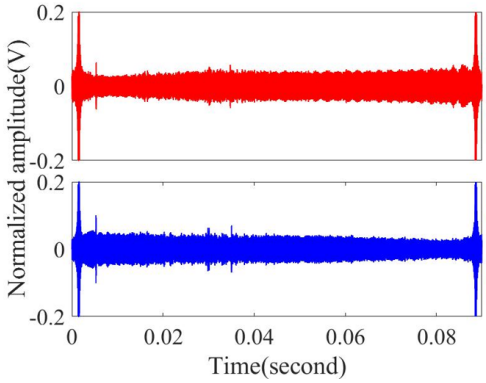

(a) Alternate LFM signal, 30 kHz to 40 kHz and 40 kHz and 30 kHz

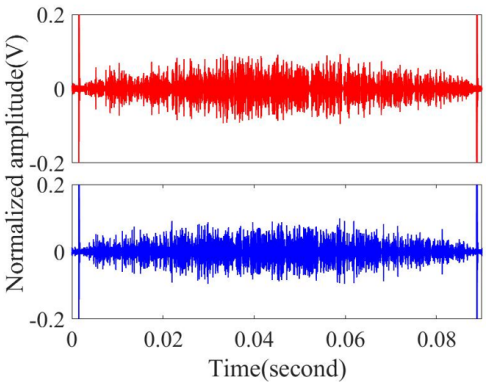

(b) Alternate integer M-sequence signal

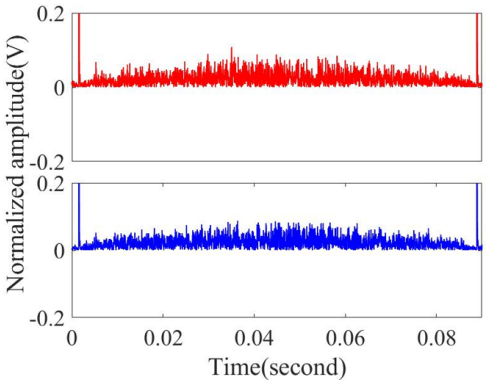

(c) Alternate complex M-sequence signal

Figure 5.17: Noise characteristics comparison between alternate LFM signal and alternate M-sequence signal.

Table 5.7: SNRs in the alternate transmission comparison between the experiments and the simulations

Type of signals	Simulations		Experiments	
	SNR_A	SNR_B	SNR_A	SNR_B
LFM	26.73 dB	26.73 dB	24.75 dB	24.79 dB
Integer M-sequence signals	21.11 dB	20.72 dB	20.49 dB	20.10 dB
Complex M-sequence signals	22.10 dB	22.09 dB	21.09 dB	21.43 dB

indicated in Fig. 5.16. The received signal of the experiment is detected as a reflected echo of some targets, which is not the maximum amplitude of the noise. Therefore, as a result, the maximum amplitude from the experiment is higher than the simulation. Noise characteristic of LFM signal and M-sequence signal is the difference as indicated in Fig. 5.17. The amplitude of these noises is an effect of SNR. Moreover, the comparison of the truncation and truncated interference noises for SNRs of the cross-correlation function A and B in the experiment and the simulation between LFM signal and M-sequence signal is illustrated in Table 5.7. The difference values between the correlation values in the experiment and those in the simulation may have been caused by environmental noise.

5.5 Target detection by alternate transmission of different codes

The alternate transmission of two different M-sequence codes is applied to extend the measurable distance without degradation of the temporal resolution. Then, the received signal is correlated with each M-sequence code. Sharp peaks to determine TOFs alternately occur in each cross- correlation function. Therefore, the measurable distance can double and the temporal resolution is same as the single transmission of each code. This section is indicated the extension of the measurable distance by the alternate M-sequence transmission and the conventional method using airborne ultrasound. In the experiment, the suitable combination of 9th-order M-sequence codes, in which there is the lowest interference, was used

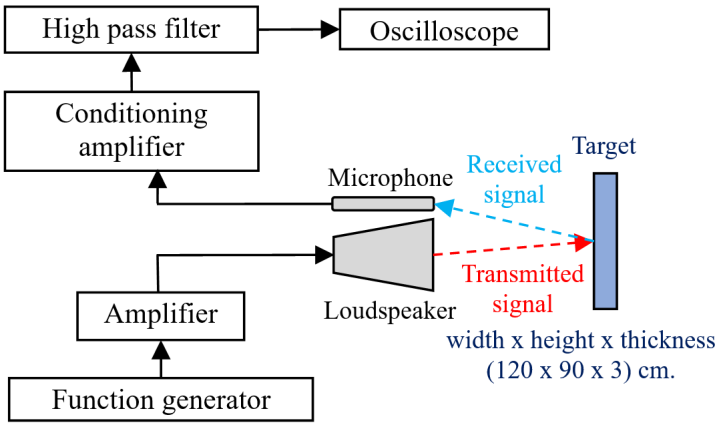

Figure 5.18: Measurement system for the experiment.

to modulate ultrasound. The number of characters in the single 9th-order M-sequence code is 511 digits. Six cycles of M-sequence code A and three sequences of alternate M-sequence code A and B were used as the original and proposed methods, respectively. These signals were generated from the function generator and transmitted from the loudspeaker, as illustrated in Fig. 5.18. Then, the reflected echoes from the target were received by the microphone. The carrier frequency of the transmitted signal was 25 kHz. The cut-off frequency of the HPF and the sampling frequency of the oscilloscope were 1 kHz and 4 MHz.

In the original method, there are 6 peaks in the cross-correlation function. Distances within 3.66 m can be measured by six times. In the proposed method, there are three peaks in each cross-correlation function with code A and B. Distances within 7.32 m can be measured by three times, respectively. By alternatively employing measured distances in the proposed method, the temporal resolution can be kept the same as the original method.

As a result, the cross-correlation functions from the experiment are illustrated in Fig. 5.19[44]. Maximum amplitude of each cross-correlation function is normalized to one. There are three cross-correlation functions in each correlation. Upper functions were achieved when the distance to the target was four meter. Peaks around 0 m indicate directly waves. In Fig. 5.19 (b) and (c), there are

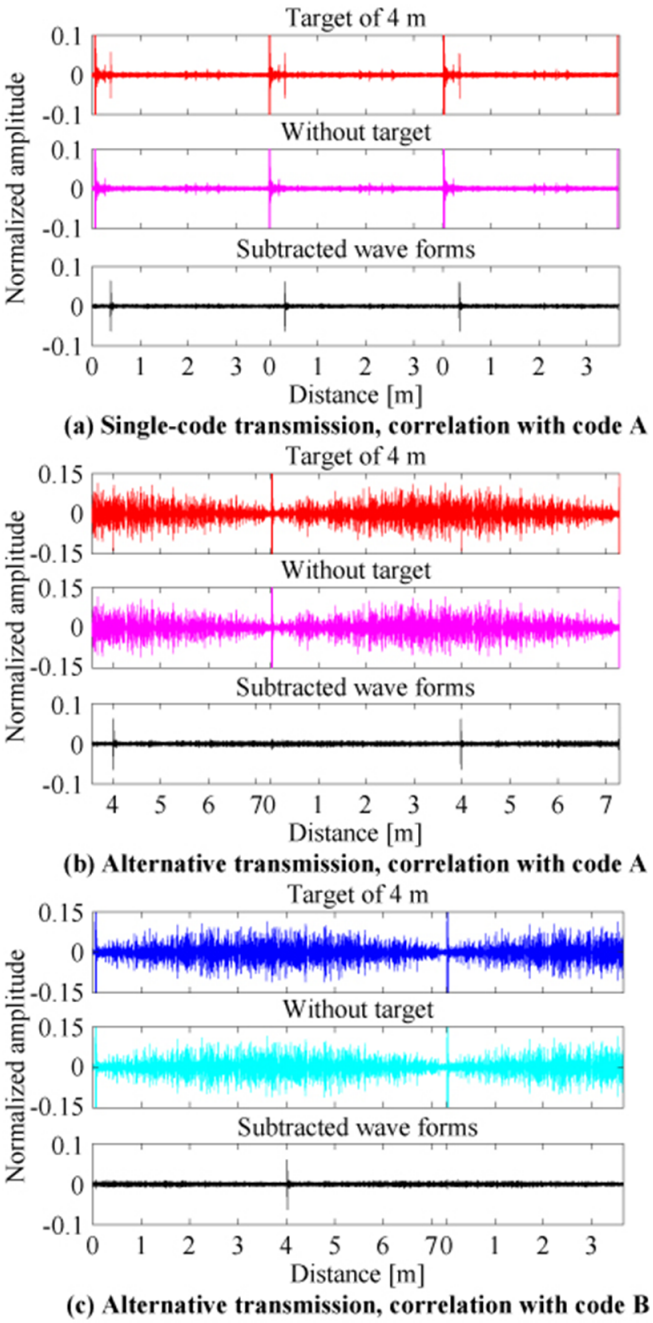

Figure 5.19: Cross-correlation functions of the original (a) and proposed methods (b) and (c) in cases the target distance is 4 m.

large fluctuated signals between peaks. Those signals are interference noise of codes A and B in directly waves. Then, middle functions were achieved without

Table 5.8: SNRs comparison of complex M-sequence between the simulation and the experiment.

Methods	Correlation with reference A	Correlation with reference B
Calculation	0.0881	0.0920
Experiment	0.1156	0.1144

the target. Effects by directly waves can be eliminated by subtraction of middle functions from upper functions, as bottom functions. The measurable distance of the original method is 3.66 m, therefore peaks by the echo signal from the target indicate approximately 0.3 m as the bottom function in Fig. 5.19 (a). On the other hand, peaks of the proposed method indicate approximately four meter in Fig. 5.19 (b) and (c). Thus, the measurable distance of the proposed method could double. Furthermore, the temporal resolution can remain by using of Fig. 5.19 (b) and (c) alternatively for distance measurement. In the subtracted wave from of figure 5.19, SNR of the original and proposed methods is so close. Moreover, maximum amplitudes of interference noises in Fig. 19 (b) and (c) and those calculated by binary codes of A and B are shown in Table 5.8. In the experiment, interference noises seem to be increased by overlapping of the impulse response of the loudspeaker.

Chapter 6

Conclusion and future work

6.1 Conclusion

Pulse-echo method

The pulse-echo method is a typical method of ultrasonic distance measurement based on pulse transmission and time-of-flight (TOF) determination. The pulse width corresponds to the distance resolution. Therefore, a short pulse is applied to obtain the high distance resolution. Moreover, to improve the signal-to-noise ratio (SNR), pulse compression is often employed for the pulse-echo method. In pulse compression, a frequency-swept signal or a pseudo-random modulated signal is transmitted, then, the received signal is correlated with the reference (transmitted) signal. When the received signal and the reference signal match, the high correlation value (compressed pulse) appears in the cross-correlation function.

The temporal resolution of the distance measurement is the time required for a single measurement. The short pulse-repetition time in the pulse-echo method represents the high temporal resolution. In that case, however, the long distance cannot be measured because the pulse-repetition time corresponds to the maximum limit of the measurable TOF (distance). Therefore, there is a trade-o relationship between the temporal resolution and the measurable distance in the pulse-echo method.

Alternate transmission of different coded signals

In this thesis, the alternate transmission of different coded signals in pulse compression is proposed to extend the measurable distance of the pulse-echo method without the degradation of the temporal resolution. In the proposed method, two different coded signals are alternatively and continually transmitted, then, the received signal is correlated with each reference signal to obtain each cross-correlation function. In each cross-correlation function, the compressed pulses alternatively appear, and the interval that corresponds to the pulse-repetition time is extended by double of that in the one-code transmission. Therefore, the measurable distance can be extended with the same temporal resolution as the one-code transmission by the alternate distance measurement from each cross-correlation function.

However, the noise by interference between different coded signals occurs between the compressed pulses. If the noise, which is defined as the noise between peaks (NBP), is larger than the compressed pulses, actual distance cannot be measured. Even if not, the SNR can be degraded by the NBP. Therefore, the combination of different coded signals with low NBP is investigated, and the suitable combinations are determined.

Combination of LFM signals

The combination of linear-frequency-modulated (LFM) signals was studied in this thesis. In the case of the LFM signal, the combination of the up-chirp and the down-chirp can be employed to the alternate transmission. NBPs were estimated on the parameters, the center frequency of 35 kHz, the sweep bands from 10 kHz to 30 kHz, the signal lengths from 3.6 to 43.8 ms.

Combination of M-sequence modulated signals

In the case of M-sequence, the characteristics of NBPs are varied by the combination types of M-sequence. The symmetry pairs and preferred or quasi-preferred pairs could suppress the NBP. NBPs were estimated on the parameters, the orders of M-sequences from 7th to 9th, the frequency of carrier sine wave of 35 kHz, 1 to 3 sine waves assigned to 1 digit in the M-sequence.

In M-sequence pulse compression, sine waves or their inverse waves are assigned to each digit. Furthermore, sine waves whose initial phase is shifted depending on the order of the M-sequence or sine waves whose initial phase is complex conjugate are also assigned. In this thesis, the phases between different coded signals (M-sequence modulated signals) are changed. The characteristics of NBPs are changed by the phase differences. Therefore, the optimal phase differences are searched from complex M-sequence pulse compression. NBPs were estimated on the parameters, the orders of M-sequences from 7th to 9th, the frequency of carrier sine wave of 35 kHz, 1 to 3 sine waves assigned to 1 digit in the M-sequence, the phase differences from 0 to 270 degree.

Comparison of NBP characteristics

Amplitudes of NBPs in LFM and M-sequence pulse compression are compared in particular signal lengths. Maximum amplitudes of NBP are indicated in Table 6.1. In the simulation, one cycle of one digit in the M-sequence signal is modulated. Maximum noise amplitude of NBP in the LFM signal is decreased at long length of signal. However, Maximum amplitude of NBP in the M-sequence signal is decreased in the high order M- sequences. Therefore, the lowest NBP is selected from the proposed modulation in the M-sequence. In the experiment, three cycles of one digit of 35 kHz in the 9th order M-sequence signal are modulated to transmit signal because it helps to reduce the overlapping impulse response of the loudspeaker. Therefore, the signal length is extended from 14.6 to 43.8 ms. In the alternate transmission method, different length of signal is only an effect with NBP of LFM signal. Maximum noise amplitude of NBP in the LFM signal is decreased when the LFM length is increased. Therefore, in this research, the alternate transmission of different codes in the LFM signal for pulse compression should be applied in the proposed method.

The maximum amplitude of the LFM signal and 7th to 9 th order M-sequence is indicated in the figure 6.1. In the alternate transmission of the LFM signal, maximum noise amplitude of long length and high bandwidth is decreased. However, the number of codes for alternate transmission is only two different codes and the distance expansion cannot be increased. On the other hand, the alternate transmission of the M-sequence is modulated one wave for one digit. At the high

Table 6.1: Maximum amplitude of NBP between the LFM signal and the M-sequence signal in the different signal length.

Signal length (Order of M-seq.)	LFM signal	M-sequence	
		Typical modulation	Proposed modulation
3.6 ms (7th order)	0.316	0.315	0.280
7.3 ms (8th order)	0.222	0.243	0.211
14.6 ms (9th order)	0.159	0.180	0.157
43.8 ms (9th order)	0.092	0.180	0.157

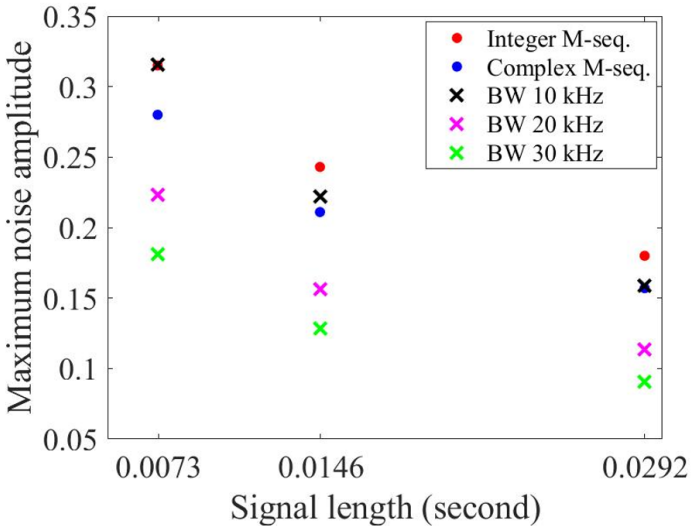

Figure 6.1: Maximum noise amplitude comparison between the LFM and M-sequence signals in the proposed method.

order M-sequence, the maximum amplitude of the noise is the lowest value. The maximum noise amplitude of the complex M-sequence is lower than the maximum amplitude of the integer M-sequence. Moreover, the alternate transmission of M-sequence is many code combinations. It is easy to extend the measurable distance and design the signal. In the real situation, if we have the high performance of the loudspeaker to generate high bandwidth of LFM signal, we should be applied an alternate LFM signal for pulse compression. However, if we have to measure a high measurable distance with high precision, we should be applied an alternate M-sequence signal because the M-sequence signal in the proposed

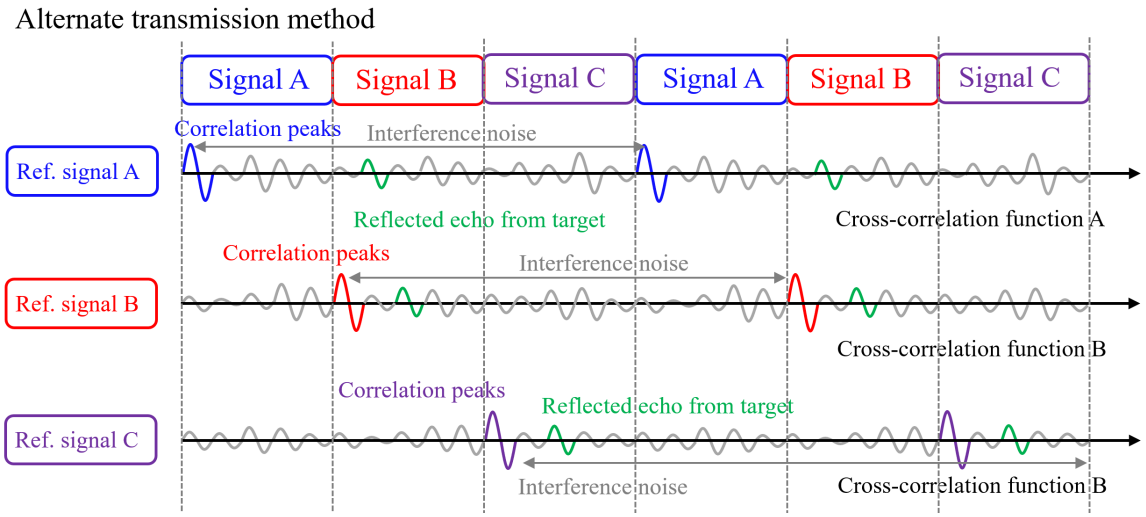

Figure 6.2: Concept for alternate transmission of third different M-sequence codes.

method is extended the measurable distance many times.

6.2 Future work

In this research, the alternate transmission of differentcodes in pulse compression to extend a measurable distance without degraded the temporal resolution is studied. In the alternate M-sequence signal, the measurable distance is extended many times, depends on alternate dierent M-sequence codes. Therefore, the noise characteristic of alternate different M-sequence codes for extending the measurable distance three or more times. The basic concept for guilding alternate transmission of third dofferent M-sequence codes is indicated in Fig. 6.2. There is indicated the correlation function of third different M-sequence codes to extend the measurable distance in third times. However, truncation and truncated interference noise is generated around the correlation peak. Therefore, the noise should be study for search the best pattern of alternate transmission in third or more times.

Bibliography

[1] S.-K. Chow and P. M. Schultheiss. **Delay estimation using narrow-band processes**. IEEE Trans. Acoust., **ASSP-29**(3):478–484, 1981. 1

[2] P. Kleinschmidt and V. Magori. **Ultrasonic remote sensors for noncontact object detection**. In Siemens Forschungs and Entwicklungsberichte, **10**, pages 110–118, 1981. 1

[3] C. Canali, G. D. Cicco, B. Morten, M. I. Prudenziati, and A. Taroni. **A Temperature Compensated Ultrasonic Sensor Operating in Air for Distance and Proximity Measurements**. IEEE Trans. Ind. Electron., **IE-29**(4):336–341, 1982. 1

[4] R. Miyamoto, K. Mizutani, T. Ebihara, and N. Wakatsuki. **Ultrasonic inspection method for billet using time-of-flight deviation of bottom echo and its performance evaluation in numerical simulations**. Jpn. J. Appl. Phy., **56**:07JC09, 2017. 1

[5] R. C. Waag, J. B. Myklebust, W. L. Rhoads, and R. Gramiak. **Instrumentation for non-invasive cardiac chamber flow rate measurement**. IEEE Ultrasonics Symp., (72):74–77, 1972. 2

[6] S. Ohtsuki and M. Okujima. **Ultrasonic Doppler velocity meter by double M-sequence modulation method**. The Second World Congress on Ultrasonics in Medicine, 1973. 2, 15

[7] P. J. Bendick and V.-L. J. Newhouse. **Ultrasonic random-signal flow measurement system**. Acoust. Soc. Am., **56**:860–865, 1974. 2

[8] T. G. Birdsall. **Acoustic telemetry for ocean acoustic tomography**. IEEE J. Ocean. Eng, **OE-9**(4):237–241, 1984. 2

[9] S. Hirata, M. K. Kurosawa, and T. Katagiri. **Accuracy and resolution of ultrasonic distance measurement with high-time resolution cross-correlation function obtained by single-bit signal processing**. Acoust. Sci. Technol., **30**(6):429–438, 2009. 2

[10] S. Hirata and M. K. Kurosawa. **Ultrasonic distance and velocity measurement using a pair of LPM signals for cross-correlation method Improvement of Doppler-shift compensation and examination of Doppler velocity estimation**. Ultrasonics, **52**(7):873–879, 2012. 2

[11] D. V. Sarwate and M. B. Pursley. **Cross-correlation properties of pseudorandom and related sequences**. Proc. IEEE, **68**(5):593–619, 1980. 3

[12] S. Hirata and H. Hachiya. **Truncation-noise characteristics of finite-length M-sequence**. Acoust. Sci. Technol., **36**(3):254–261, 2015. 3

[13] K. Leetang, S. Hirata, and H. Hachiya. **Selection on the combination of M-sequence codes in alternate transmission for extension of measurable distance**. Jpn. J. Appl. Phys., **58**:076503, 2019. 3, 9

[14] W. Nonsakhoo, P. Sirisawat, S. Saiyod, and N. Benjamas. **Ultrasound Indoor Positioning System Based on a Low-Power Wireless Sensor Network Providing Sub-Centimeter Accuracy**. Sensors 2013, **13**:3501–3526, 2013. 7

[15] K. Leetang, S. Hirata, and H. Hachiya. **Improved alternate transmission of dierent codes in M-sequence pulse compression using phase-shifted complex M-sequences**. Jpn. J. Appl. Phys., **59**:086504, 2020. 9

[16] Y. Wang, T. Siginouchi, M. Hashimoto, and H. Hachiya. **Development of Ultrasonic Multiple Access Method Based on M-Sequence Code**. Jpn. J. Appl. Phys., **46**:4490, 2007. 9, 15

[17] S. Hirata, M. K. Kurosawa, and T. Katagiri. **Accuracy and resolution of ultrasonic distance measurement with high-time-resolution cross-correlation function obtained by single-bit signal processing**. Acoust. Sci. Tech., **30**(6):429–438, 2009. 10

[18] H. Panoan. **Research on frequency domain pulse compression of LFM signal**. J. Phys.: Conf. Ser., **1550**:042017, 2020. 11

[19] G. Wang, T. Tang, J. Ye, and Z. F. Zhang. **Research on Sidelobe Suppression Method in LFM Pulse Compression Technique**. Conf. Ser.:Mater. Sci. Eng., **677**:052104, 2019. 11

[20] H. Liu, L. Zhou, L. Wang, and C. Xu. **SNR Estimation Method of LFM Signal Detection**. IEEE computer society, 2009. 11

[21] T. Hayashi, S. Hirata, and H. Hachiya. **A method for the non-contact measurement of two-dimensional displacement of chest surface by breathing and heartbeat uaing an air born ultrasound**. Jpn. J. Appl. Phys., **58**:SGGB10, 2019. 12

[22] H. Matsuo, T. Yamaguchi, and H. Hachiya. **Target Detectability Using Coded Acoustic Signal in Indoor Environments**. Jpn. J. Appl. Phys., **47**(5):4325–4328, 2008. 12, 15

[23] K. Nishihara, T. Yamaguchi, and H. Hachiya. **Position detection of small objects in indoor environments using coded acoustic signal**. Acoust. Sci. Tech., **29**(1):15–20, 2008. 12

[24] K. Yamanaka, S. Hirata, and H. Hachiya. **Evaluation of correlation property of linear-frequency-modulated signals coded by maximum-length sequences**. Jpn. J. Appl. Phys., **55**:07KC09, 2016. 13, 15

[25] H. Zhang, K. Kondo, M. Yamakawa, and T. Shiina. **Simultaneous Multispectral Coded Excitation Using Gold Codes for Photoacoustic Imaging**. Jpn. J. Appl. Phys., **51**(7S):07GF03, 2012. 13

[26] S. W. Golomb. **Shift Register Sequences**. Proc. 4th Inter. Conf., **SETA**(LNCS 4086):1–4, 2006. 15

[27] Y. Takeuchi. **An investigation of a spread energy method for medical ultrasound systems - Part two: proposed system and possible problems**. Ultrasonics, **17**(5):219–224, 1979. 15

[28] Y. Shi and K. E. Hecox. **Nonlinear system identification by m-pulse sequences application to brainstem auditory evoked responses**. IEEE Trans. Biomed. Eng., **38**(9):834–845, 1991. 15

[29] M. ODonnell. **Coded excitation system for improving the penetration of real-time phased-array imaging systems**. IEEE Trans. Ultrason. Ferroelectr. Freq. Control, **39**(3):341–351, 1992. 15

[30] M. A. Benkhelifa, M. Gindre, J. Y. LeHuerou, and W. Urbach. **Echography using correlation techniques choice of coding signal**. IEEE Trans. Ultrason. Ferroelectr. Control, **41**(5):579–587, 1994. 15

[31] J. Shen and E. S. Ebbini. **A new coded-excitation ultrasound imaging system. I. Basic principles**. IEEE Trans. Ultrason. Ferroelectr. Freq. Control, **43**(1):131–140, 1996. 15

[32] Y. Wang, K. Metzger, D. N. Stephens, G. Williams, S. Brownlie, and M. O'Donnell. **Coded EXcitation with spectrum inversion (CEXSI) for ultrasound array imaging**. IEEE Trans. Ultrason. Ferroelectr. Control, **50**(7):805–823, 2003. 15

[33] Y. Wang, T. Siginouchi, M. Hashimoto, and H. Hachiya. **Automatic Interference Elimination Algorithm for Ultrasonic Multiple Access Method**. Jpn. J. Appl. Phys., **47**(5s):4319–4324, 2008. 15

[34] M. Ricci, L. Senni, and P. Burrascano. **Exploiting Pseudorandom Sequences to Enhance Noise Immunity for Air-Coupled Ultrasonic Nondestructive Testing**. IEEE Trans. Instrum. Means., **61**(11):2905–2915, 2012. 15

[35] S. Hirata, L. Haritaipan, K. Hoshiba, H. Hachiya, and N. Nimi. **Non-contact measurement of propagation speed in tissue-mimicking phantom using pass - through airborne ultrasound**. Jpn. J. Appl. Phys., **53**:07KC17, 2014. 15

[36] M. Legg, M. K. Yucel, V. Kappatos, and C. Selcuk. **Increased range of ultrasonic guided wave testing of overhead transmission line cables using dispersion compensation**. Ultrasonics, **62**:35–45, 2015. 15

[37] H. Iwaya, K. Mizutani, T. Ebihara, and N. Wakatsuki. **Acoustical positioning method using transponders with adaptive signal level normalizer**. Jpn. J. Appl. Phys., **56**:07JC07, 2017. 15

[38] H. Iwaya, K. Mizutani, T. Ebihara, and N. Wakatsuki. **Experimental investigation of the eect of signal reflection and coverage area on indoor acoustical positioning using transponders with adaptive signal level normalizer**. Jpn. J. Appl. Phys., **57**:07LC03, 2018. 15

[39] Y. Ikari, S. Hirata, and H. Hachiya. **Ultrasonic position and velocity measurement for a moving object by M-sequence pulse compression using Doppler velocity estimation by spectrum-pattern analysis**. Jpn. J. Appl. Phys., **54**:07HC14, 2015. 15

[40] S. Hirata, Q. Sun, M. Ueda, and H. Hachiya. **Measurement of road surfaces by reflection characteristics of airborne ultrasound**. Acoust. Sci. Tech., **37**(6):322–325, 2016. 15

[41] Z. Nowak, M. J. Zhang, L. Lomonte, M. Wicks, and Z. Wu. **Mixed - modulated linear frequency modulated radar-communications**. IET Radar Sonar Navig., **11**(Iss.2):313–320, 2017. 15

[42] H. Nomura, H. Adachi, and T. Kamakura. **Feasibility of low-frequency ultrasound imaging using pulse compressed parametric ultrasound**. Ultrasonics, **89**(64):64–73, 2018. 15

[43] H. Nomura and R. Nishioka. **Time sidelobe reduction of pulse-compressed parametric ultrasound with maximum-length sequence excitation**. Jpn. J. Appl. Phys., **57**:07LC05, 2018. 15

[44] K. Leetang, S. Hirata, and H. Hachiya. **Target detection using airborne ultrasound alternately modulated by different M-sequence codes for extension of measurable distance**. The 40th Symposium on UltraSonic Electronic, 2019. 74

Publications

List of Publications related to the dissertation

Journal Papers

1. K. Leetang, S. Hirata and H. Hachiya, Improved alternate transmission of dierent codes in M-sequence pulse compression using phase-shifted complex M-sequences, Jpn. J. Appl. Phys., Vol. 59 (2020), pp. 086504. (Accepted for publication)

2. K. Leetang, S. Hirata and H. Hachiya, Selection on the combination of M-sequence codes in alternate transmission for extension of measurable distance, Jpn. J. Appl. Phys., Vol. 58 (2019), pp. 076503. (Accepted for publication)

International Conference Papers

1. K. Leetang, S. Hirata and H. Hachiya, Evaluation of SNR for alternate transmission of different coded ultrasounds to extend the limit of measurable distance in the pulse-echo method, The 42th Symposium on UltraSonic Electronics (USE2021), Shizuoka, Japan, (2021). (Reviewing)

2. K. Leetang, S. Hirata and H. Hachiya, Evaluation of ultrasonic target detection by alternate transmission of different codes in M-sequence pulse compression, IEEE IUS2020, Las Vegas, USA, (2020). (Accepted for publication)

3. K. Leetang, S. Hirata and H. Hachiya, Target detection using airborne ultrasound alternately modulated by different M-sequence codes for extension of measurable distance, The 40th Symposium on UltraSonic Electronics (USE2019), Tokyo, Japan, (2019). (Accepted for publication)

4. K. Leetang, S. Hirata and H. Hachiya, Study about Combination Types of M-sequences in Alternate Transmission of Different Codes for Pulse Compression, The 39th Symposium on UltraSonic Electronics (USE2018), Kyoto, Japan, (2018). (Accepted for publication)

National Conference Papers

1. K. Leetang, S. Hirata and H. Hachiya, Evaluation of codes selection in alternate transmission of difference codes in M-sequence pulse compression for ultrasonic target detection, 2020 Spring Meeting Acoustic Society of Japan (ASJ2020), Saitama, Japan, (2020). (Accepted for publication)

2. K. Leetang, S. Hirata and H. Hachiya, Study on modulation method for alternate transmission of different codes in M-sequence pulse compression, 2019 Spring Meeting Acoustic Society of Japan (ASJ2019),Tokyo, Japan, (2019). (Accepted for publication)